MONTHLY NOTICES

OF THE

ROYAL ASTRONOMICAL SOCIETY

Vol. 114 No. 4 1954

Published and Sold by the
ROYAL ASTRONOMICAL SOCIETY
BURLINGTON HOUSE
LONDON, W.1

Price Thirteen Shillings and Sixpence

NOTICE TO AUTHORS

1. *Communications.*—Papers must be communicated to the Society by a Fellow. They should be accompanied by a summary at the *beginning* of the paper conveying briefly the content of the paper, and drawing attention to important new information and to the main conclusions. The summary should be intelligible in itself, without reference to the paper, to a reader with some knowledge of the subject; it should not normally exceed 200 words in length. **Authors are requested to submit MSS. in duplicate. These should be typed using double spacing and leaving a margin of not less than one inch on the left-hand side. Corrections to the MSS. should be made in the text and not in the margin.** Unless a paper reaches the Secretaries more than seven days before a Council meeting it will not normally be considered at that meeting. By Council decision, MSS. of accepted papers are retained by the Society for one year after publication; unless their return is then requested by the author, they are destroyed.

2. *Presentation.*—Authors are allowed considerable latitude, but they are requested to follow the general style and arrangement of *Monthly Notices*. References to literature should be given in the standard form, including a date, for printing either as footnotes or in a numbered list at the end of the paper. Each reference should give the **name and initials** of the author cited, irrespective of the occurrence of the name in the text (some latitude being permissible, however, in the case of an author referring to his own work). The following examples indicate the style of reference appropriate for a paper and a book, respectively :—

A. Corlin, *Zs. f. Astrophys.*, **15**, 239, 1938.
H. Jeffreys, *Theory of Probability*, 2nd edn., section 5.45, p. 258, Oxford, 1948.

3. *Notation.*—For technical astronomical terms, authors should conform closely to the recommendations of Commission 3 of the International Astronomical Union (*Trans. I.A.U.*, Vol. VI, p. 345, 1938). Council has decided to adopt the I.A.U. 3-letter abbreviations for constellations where contraction is desirable (Vol. IV, p. 221, 1932). In general matters, authors should follow the recommendations in *Symbols, Signs and Abbreviations* (London : Royal Society, 1951) except where these conflict with I.A.U. practice.

4. *Diagrams.*—**These should be designed to appear upright on the page, drawn about twice the size required in print and prepared for direct photographic reproduction except for the lettering, which should be inserted in pencil. Legends should be given in the manuscript indicating where in the text the figure should appear.** Blocks are retained by the Society for 10 years; unless the author requires them before the end of this period they are then destroyed.

5. *Tables.*—**These should be arranged so that they can be printed upright on the page.**

6. *Proofs.*—Costs of alterations exceeding 5 per cent of composition must be borne by the author. Fellows are warned that such costs have risen sharply in recent years, and it is in their own and the Society's interests to seek the maximum conciseness and simplification of symbols and equations consistent with clarity.

7. *Revised Manuscripts.*—When papers are submitted in revised form it is especially requested that they be accompanied by the original MS.

Reading of Papers at Meetings

8. When submitting papers authors are requested to indicate whether they will be willing and able to read the paper at the next or some subsequent meeting, and approximately how long they would like to be allotted for speaking.

9. Postcards giving the programme of each meeting are issued some days before the meeting concerned. Fellows wishing to receive such cards whether for Ordinary Meetings or for the Geophysical Discussions or both should notify the Assistant Secretary.

MONTHLY NOTICES

OF THE

ROYAL ASTRONOMICAL SOCIETY

Vol. 114 No. 4

MEETING OF 1954 MARCH 12

Dr J. Jackson, President, in the Chair

The election by the Council of the following Fellows was duly confirmed:—

Arthur Thomas Goodchild, 3 Murley Road, Winton, Bournemouth, Hampshire (proposed by G. Merton);

Francis James Hooper, Nineteen Steps, Orchard Hill, Bideford, Devonshire (proposed by F. Molesworth);

*Harry Hughes, Ph.D., 27 Yewlands Avenue, Leyland, Preston, Lancashire (proposed by F. Birch);

Charles Lloyd, 11 Benson Avenue, Goldthorn Park, Wolverhampton, Staffordshire (proposed by M. Johnson); and

David Kenneth Northrup, F.R.S.A., 62 Ballater Road, London, S.W.2 (proposed by A. W. Lane Hall).

The election by the Council of the following Junior Members was duly confirmed:—

†Thomas William Morris, 21D Berryland Road, Moreton Wirral, Cheshire (proposed by J. Kershaw); and

Raymond Henry Preston, 4 South Road, West Kirby, Cheshire (proposed by J. Kershaw).

Sixty-six presents were announced as having been received since the last Meeting, including:—

Max Waldmeier, *Radiowellen aus dem Weltram* (presented by the author); and

Wolfgang Gleissberg, *Die Haufigkeit der Sonnenflecken* (presented by the author).

MEETING OF 1954 APRIL 9

Dr J. Jackson, President, in the Chair

The election by the Council of the following Fellows was duly confirmed:—

George Edward William Gosnell, 75 Woodmansterne Road, Coulsdon, Surrey (proposed by F. M. Holborn);

* Transferred from Junior Membership.

† Election later declared to be null and void.

Guillermo Haro, Tonanzintla Observatory, Ap. Postal 216, Puebla, Mexico (proposed by G. Münch);

*Garry Ross Nankivell, 45 Gayhurst Road, Dallington, N.E.1, Christchurch, New Zealand (proposed by A. F. A. L. Jones);

Sibte Nabi Naqvi, Department of Meteorology, Government of Pakistan, (proposed by A. Hunter);

Domingo Taboada, Av. Reforma, 2111, Puebla, Mexico (proposed by G. Münch);

John Graham Whitaker, B.Sc., 26 Woodfield Lane, Ashtead, Surrey (proposed by T. G. Cowling); and

Wilhelm Levi Whittle, Parkstone, 706 Doncaster Road, Foulby, Wakefield, Yorkshire (proposed by G. P. Meredith).

The President announced that the Council had elected the following Associates of the Society:—

Jean Dufay, Professor of Astronomy and Director of the Observatory, Université de Lyon, St Genis-Laval, Rhône, France;

Max Waldmeier, Professor of Astronomy and Director of the Eidgenossische Sternwarte, Zürich, Switzerland; and

Herman Zanstra, Professor of Astronomy in the University of Amsterdam and Director of the Astronomical Institute of the University, Amsterdam, Holland.

One hundred and one presents were announced as having been received since the last Meeting, including:—

American Association for the Advancement of Science, *Astronomical photoelectric photometry* (presented by the American Association for the Advancement of Science);

Astronomische Gesellschaft, *Porträtgallerie*, 1931 (presented by F. Gondalatsch);

Hamburg Observatory, *Bergedorfer Spektraldurchmusterung, Band V;* and *Zweiter Katalog der Astronomischen Gesellschaft, Bande* 5-9 (presented by the Hamburg Observatory);

International Geodetic and Geophysical Union, *La deuxième opération internationale des longitudes, Octobre-Novembre*, 1933 (presented by the International Geodetic and Geophysical Union); and

Bernhard Sticker, *Fünfstellige Tafel der trigonometrischen Funktionen. Ausgabe A* (presented by the author).

* Transferred from Junior Membership.

WHOLE-SKY STATISTICS OF CELESTIAL OBJECTS

C. W. Allen

(Received 1954 February 11)

Summary

The advantages of statistical representations based on only those celestial objects with greatest apparent brightness have been enumerated. The system of observations and results that has been devised can be applied to almost any recognizable category of celestial object. The observable parameters are $m_v(10)$, q, $\overline{M}$, σ_M and $\overline{b}$, representing respectively magnitude of the tenth object, change of number with magnitude, absolute magnitude and its dispersion, and mean galactic latitude. The equations and numerical data are given for conversion of these (in most cases) into the descriptive quantities M_0, σ, D_0 and γ, representing respectively the absolute magnitude and its dispersion, the space density and scale height perpendicular to the galactic plane. Some alternatives to M_0 and D_0 are given which are not so sensitive to the evaluation of σ. The mean absorption coefficient and optical thickness of the galaxy must be known.

The analysis has been exemplified by application to Wolf-Rayet stars, ❶ stars, flare stars, all stars, white dwarfs, globular clusters, open clusters, extra-galactic nebulae, novae and A stars.

---

1. *Introduction.*—The first step towards a systematic study of the many objects found in the sky is to segregate them into various classes, groups, or categories. One can then assume a certain uniformity within each class and proceed to investigate its intrinsic and statistical characteristics. Observations made on individual objects may serve the dual purpose of revealing intrinsic characteristics and also assigning each object to its appropriate class. Once sufficient objects are classified into a particular category one may proceed with statistical studies from which to determine the number density of the objects, their number distribution and their motions. (The statistics in the present paper are concerned with numbers only—not motions.)

The ideal treatment for any particular category would aim at a complete analysis of number density as a function of distance. The data would be obtained by counts of the object per square degree and per magnitude range for a large part of the sky. Such an analysis may be possible for a few well-defined categories, but more usually there is too much difficulty in recognizing the objects to to be counted. Hence the present study is based entirely on the nearer and brighter objects of each category. The objects actually used are the ten or twenty *brightest* objects found anywhere in the sky.

The advantages of basing a statistical analysis on this selection are as follows:

(*a*) There is no arbitrariness in the choice of object since those of lowest apparent magnitude are used exclusively. Results are therefore as general as possible.

(*b*) Those objects used will most probably be the best-recognized members of their class, and the physical measurements are likely to be the most accurate and complete.

(*c*) Working with small numbers involves very little labour and justifies obtaining a result even if high accuracy cannot be expected. The small list of objects may be constantly revised, and the effects of changing values can be readily assessed.

(*d*) The procedure can be applied consistently for all categories of object.

(*e*) Since the objects used are randomly taken from any part of the sky it is legitimate to use a mean value for interstellar absorption.

The whole-sky analysis of celestial objects to be described aims at exploiting these advantages.

2. *Parameters describing the true distribution.*—Since the statistics are to be obtained from a small number of objects (of the order of 10), it is quite evident that one cannot reveal very much statistical detail. Simple assumptions on the form of the distributions must be made, and a small number of parameters introduced to describe them quantitatively.

If the number density of the objects in the neighbourhood of the Sun is D_0, the number per unit magnitude range may be assumed to follow the Gaussian form

$$L(M)=\frac{D_0}{\sigma\sqrt{2\pi}}\,e^{-(M-M_0)^2/2\sigma^2}, \tag{1}$$

where M_0 is the most probable absolute magnitude and σ the dispersion in absolute magnitude. We have thus introduced the three parameters M_0, D_0, σ. Visual magnitudes are employed.

The fall of density with distance z from the galactic plane is approximately exponential (1), and can be represented by the fourth parameter, the scale height γ in

$$D_z=D_0\,e^{-z/\gamma},$$
$$\Delta_z=D_z/D_0=e^{-z/\gamma}. \tag{2}$$

The solar neighbourhood is regarded as being on the galactic plane, and z is measured positively in either direction.

It should be possible to introduce a fifth parameter to represent the rate of density decrease as one moves from the galactic centre through the solar neighbourhood towards the rim of the galaxy. Probably the most satisfactory one-parameter formula to represent the change of density with R, the radial distance from the galactic centre, is

$$D_R=D_0\frac{R_0^2+\epsilon^2}{R^2+\epsilon^2}, \tag{3}$$

where R_0 is the solar distance from the centre. However, no attempt has been made to determine the fifth parameter ϵ in the present paper.

When σ is large or unknown M_0 and D_0 become rather unsatisfactory parameters for describing the distribution. The objects actually used for the analysis, which are those of greatest apparent brightness, tend to be intrinsically brighter than M_0. Hence the evaluation of M_0 (and with it D_0) becomes an extrapolation towards fainter objects. It would be preferable if one could find a system of parameters that are analogous to M_0 and D_0 but which give more weight to intrinsically brighter objects. Unfortunately no system satisfies all purposes,

and it has been found desirable to introduce two further systems represented by M_1 and D_1 and by M_2 and D_2 respectively. The first is somewhat closer to observations, but the second is needed for calculations. They are very similar and it is easy to convert from one to the other.

M_1 is the absolute magnitude of objects giving the greatest emission of visible radiation per cubic parsec, and D_1 is the emission per cubic parsec expressed as the equivalent number of stars of magnitude M_1. M_1 and D_1 therefore have a physical meaning that is just as clear as for M_0 and D_0.

M_2 is the most probable absolute magnitude of objects with a luminosity function (1) and seen to a finite limiting apparent magnitude m_1 when the objects are distributed uniformly in non-absorbing space. The number seen would be D_2 times the volume of the sphere whose radius is given by the modulus $m_1 - M_2$. This serves to define D_2.

The relations with M_0, D_0 and σ are

$$\left.\begin{aligned} M_1 &= M_0 - 0{\cdot}4\ \sigma^2/\log_{10} \mathrm{e}, \\ M_2 &= M_0 - 0{\cdot}6\ \sigma^2/\log_{10} \mathrm{e}, \\ D_1 &= D_0 \exp\{-\tfrac{1}{2}\,(0{\cdot}4\ \sigma/\log_{10} \mathrm{e})^2\}, \\ D_2 &= D_0 \exp\{-\tfrac{1}{2}\,(0{\cdot}6\ \sigma/\log_{10} \mathrm{e})^2\}. \end{aligned}\right\} \qquad (4)$$

These relations may be seen from Fig. 1, where $\log_{10}$ number of, brightness of, or volume occupied by objects is plotted against absolute magnitude. The curve A represents the number of objects per cubic parsec and per unit of M from (1). D_0 is made equal to $\sigma\sqrt{2\pi}$ for convenience.

Curve B represents the luminosity B per object in terms of the luminosity M_0, and hence $d\log_{10} B/dM = -0{\cdot}4$. The curve C, obtained by adding the ordinates of curves A and B, represents the distribution of emitted light expressed as the number of objects of brightness M_0. The dispersion of the curve C is the same as A, and C has a maximum at $M_1 = M_0 - 0{\cdot}4\ \sigma^2/\log_{10} \mathrm{e}$. If the C curve is displaced to represent distribution of emitted light in terms of M_1 instead of M_0 we obtain curve D. The total emission D_1 in terms of M_1 is given by $\log_{10} D_1 = \log_{10} D_0 - 0{\cdot}08\sigma^2/\log_{10} \mathrm{e}$ as in (4).

The argument for M_2 and D_2 is similar. If V is the volume of non-absorbing space within which uniformly distributed objects brighter than apparent magnitude m_1 can be seen, then $d\log_{10} V/dM = -0{\cdot}6$. When $m_1 = M_0$ and the unit of V is a sphere of 10 pc radius, V is represented by curve E. By adding ordinates of A and E we obtain F with a maximum at $M_2 = M_0 - 0{\cdot}6\ \sigma^2/\log_{10} \mathrm{e}$. Displacing the curve F to represent the case of $m_1 = M_2$ instead of $m_1 = M_0$ we obtain curve G, and find D_2 given by $\log D_2 = \log D_0 - 0{\cdot}18\ \sigma^2/\log_{10} \mathrm{e}$ as in (4).

If the slope of the line B or E had been $-q$ it is evident we would obtain a maximum at $M_q = M_0 - q\ \sigma^2/\log_{10} \mathrm{e}$. This is used in Section 4.

3. *Observable parameters.*—It is intended that the observable parameters should be derived from the objects with smallest apparent magnitude. The desirable data for each object are the apparent and absolute visual magnitudes m_v and M_v, and the galactic coordinates l and b. We must reduce these individual observations to suitable mean values that may represent the class of objects and can be analysed to give the parameters of Section 2.

The suggested procedure is to list the brightest objects in order of apparent magnitude. About 20 objects are listed if available. If N is the order number on this list we obtain two parameters by plotting $\log N$ against m_v. It may

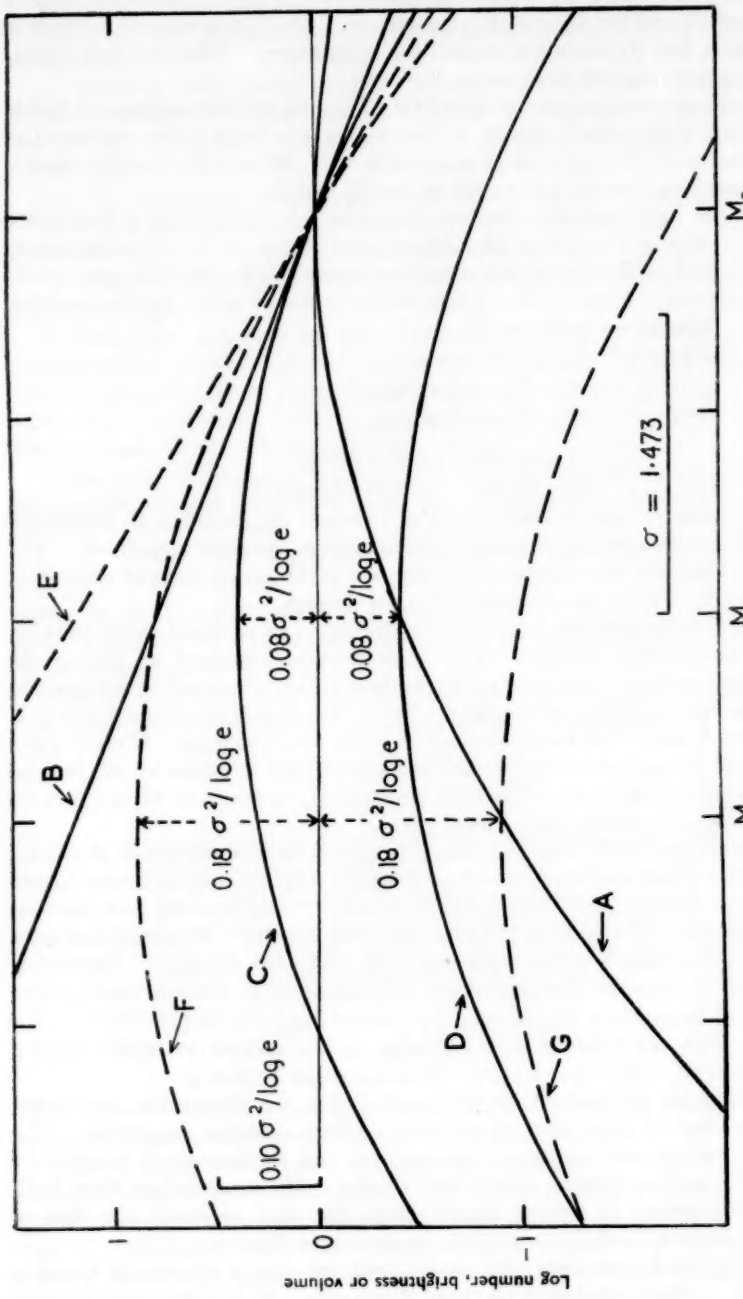

FIG. 1.—*Illustrating relations between* M_0, M_1, M_2, D_0, D_1, D_2 *and* σ.

be assumed that the curve should be linear and that departures from linearity are due to statistical sampling. The two parameters chosen to describe the curve are

(*a*) $m_v(10)$ the brightness of the tenth object (smoothed), i.e. m_v where the curve crosses $\log_{10} N = 1$, and

(*b*) the slope $q = d \log_{10} N/dm_v$.

One sees from the definition of $m_v(10)$ that results are effectively standardized to the tenth object, and that if the list contains more than ten objects the others are used for statistical stability only. The theory of Section 4 however could be applied equally well to any number of objects.

Since so few objects are used it is advisable to study the individual points on the curves and correct irregularities. Least-squares solutions are not suitable. Examples in Section 7 show that q may be influenced by the irregularities but that $m_v(10)$ is a fairly stable measurement.

For determining the appropriate mean of the twenty (say) absolute magnitudes in the list we must consider that the theory to which comparison will be made averages the objects *brighter than* the tenth. We therefore wish to determine mean M_v for the brightest ten, but also to let the results be influenced by the next ten in order to give greater statistical stability. We must decide whether there is, or should be, any systematic trend in mean M_v as N varies. The number of objects seen within the range M to $M+dM$ is proportional to two factors, firstly $L(M)$ the number per unit volume, and secondly the volume V through which objects can be seen to the required limiting apparent magnitude m_1. V is a function of the modulus $(m_1 - M)$, and therefore $d \log_{10} V/dM = -d \log_{10} V/dm_1 = -q$. We saw at the end of Section 2 that such a distribution has a maximum at $M_q = M_0 - q\sigma^2/\log_{10} e$, which is independent of m. Mean M will therefore have no strong tendency to change with N, and we use all available values of M to determine the mean $\bar{M} = M_q$. However, if for any reason certain objects have been discarded when determining $m_v(10)$ and q, it is advisable to omit these objects from the estimation of $\bar{M}$. If the distribution is Gaussian $\bar{M} = M_q = M_0 - q\sigma^2/\log_{10} e$.

The same absolute magnitudes may also be used for the determination of the observed dispersion in M which we call σ_M, but the values so obtained are not very reliable.

The tabulated values of b taken as positive may be used to obtain the mean value $\bar{b}$ and the median value $\bar{\bar{b}}$ of the galactic latitude. In this case there is often a distinct tendency to vary with m_v for which allowance should be made. Suppose that the average is obtained from N objects instead of the standard 10, then the limiting m_v is $m_v(10) + (\log_{10} N - 1)/q$. The correction $\Delta b (= \bar{b}_{10} - \bar{b}_N)$ may be determined from Fig. 2 and is found to depend very little on γ or σ. With sufficient accuracy the correction may be written

$$\Delta b = p[m_v(N) - m_v(10)] = p\ (\log_{10} N - 1)/q, \qquad (5)$$

where p has the values

$\bar{b}$ or $\bar{\bar{b}}$	1°	2°	5°	10°	15°	20°	25°	30°	32°
p	0°·3	0°·6	1°·4	2°·4	2°·8	2°·9	2°·5	1°·5	0°

The most accurate estimates of $\bar{b}$ and $\bar{\bar{b}}$ can be obtained by using all the (non-discarded) objects in the list, and, if necessary, making a small correction from this table.

The most appropriate measure of galactic central concentration is the mean $\bar{l}$ or median $\bar{\bar{l}}$ of $|(l-l_0)|$, where l_0 is the longitude of the galactic centre = 328° and longitude differences $|(l-l_0)|$ are less than 180°. As mentioned earlier there is no analysis for using this observation as yet.

The reason for duplicating the observations $\bar{b}$, $\bar{\bar{b}}$ and $\bar{l}$, $\bar{\bar{l}}$ is that sometimes one figure is more reliable than the other and one should provide the opportunity of using either or both as the occasion demands.

It can be seen that there is a close correspondence between the descriptive and the observable parameters as follows:

Descriptive	M_0, M_1, M_2; D_0, D_1, D_2	γ	σ	ϵ
Observable	$m_v(10)$; q; $\bar{M}$	$\bar{b}, \bar{\bar{b}}$	σ_M	$\bar{l}, \bar{\bar{l}}$

If absolute magnitudes are available there are at least as many observable parameters as independent descriptive ones, and it should be possible to obtain an estimate of the latter. If there is no information at all on absolute magnitude there is, of course, no possibility of determining number density. However, the observations still pave the way to the descriptive solution in the sense that if either M_2 or γ be assumed the other can be determined.

4. *Equations for calculations.*—The problem is to compute the observable parameters of Section 3 from the descriptive parameters of Section 2. To do so one must make an assumption on the form of the interstellar absorption. Following Parenago (**2**) we assume it to be distributed exponentially from the galactic plane. Then the absorption in magnitudes per parsec can be expressed

$$a = a_0 \, e^{-z/\beta},$$

where z is the distance from the galactic plane and β the absorption scale height. The total absorption in magnitudes to a distance r in parsecs is

$$\alpha(r) = a_0\beta(1 - e^{-r \sin b/\beta})/\sin b,$$

where b is the galactic latitude.

As in Seares' method of analysis (**3**) we define r_0 by

$$5 \log_{10} r_0 = 5 \log_{10} r + \alpha(r) = m + 5 - M. \tag{6}$$

The number of stars within solid angle ω and unit apparent magnitude range is (e.g. Smart (**4**))

$$A(m) = \omega \int_0^\infty r_0^2 \, \Delta_0(r_0) L(m + 5 - 5 \log_{10} r_0) dr_0, \tag{7}$$

where $\Delta_0(r_0) = \Delta(r)/G(r)$ expressed in terms of r_0.

$\Delta(r) = D_r/D_0 =$ density of objects at the distance r relative to density of solar neighbourhood.

$$G(r) = \left(1 + \frac{r}{5 \log_{10} e} \frac{d}{dr} \alpha(r)\right) \exp\left(\frac{3\alpha(r)}{5 \log_{10} e}\right).$$

The luminosity function $L(M)$ is given in (1) and it is assumed that the dispersion σ is invariable. Changing the variable in (7) to M by (6) and expressing Δ_0 in terms of the modulus $m - M$ we have

$$A(m) = \frac{\omega}{5 \log_{10} e} 10^3 \, 10^{0.6m} \int_{-\infty}^{+\infty} \Delta_0(m - M) L(M) \, 10^{-0.6M} \, dM.$$

In order to convert to the constants M_2 and D_2 of Section 2 we note from Fig. 1 (curve F) that

$$L(M)10^{-0\cdot6(M-M_0)} = 10^{0\cdot18\sigma^2/\log_{10}e}\frac{D_0}{\sigma\sqrt{2\pi}}\exp[-(M-M_2)^2/2\sigma^2],$$

giving

$$A(m) = \frac{10^3\omega}{5\log_{10}e}10^{0\cdot6(m-M_0)}D_2\int_{-\infty}^{+\infty}\Delta_0(m-M)\frac{1}{\sigma\sqrt{2\pi}}\exp[-(M-M_2)^2/2\sigma^2]dM. \tag{8}$$

The advantages of using M_2 and D_2 are that σ does not appear among the constants outside the integral and that the integral can be easily evaluated with suitable accuracy. Calling the integral Δ_1 the following simple approximation has been used.

$$\Delta_1(m-M_2) = 0\cdot8\Delta_0(m-M_2) + 0\cdot1\Delta_0(m-M_2+2\sigma) + 0\cdot1\Delta_0(m-M_2-2\sigma). \tag{9}$$

The total number of objects brighter than m_1 is

$$N(m_1) = \frac{10^3\omega}{5\log_{10}e}10^{-0\cdot6M_2}D_2\int_{-\infty}^{m_1}\Delta_1(m-M_2)10^{0\cdot6m}\,dm$$

$$= \frac{10^3\omega}{3}10^{0\cdot6(m_1-M_0)}D_2S, \tag{10}$$

where

$$S = \frac{\int_{-\infty}^{m_1}\Delta_1(m-M_2)10^{0\cdot6m}\,dm}{\int_{-\infty}^{m_1}10^{0\cdot6m}\,dm}$$

$$= \text{mean value of } \Delta_1(m-M_2) \text{ weighted by } 10^{0\cdot6m}.$$

Values of S may be determined from these formulae for selected values of b, γ, (m_1-M_2), σ. To determine values for the whole sky S must be expressed as a function of b and integrations carried out. The mean and median values of b, which are denoted $\bar{b}$ and $\bar{\bar{b}}$, are given by

$$\bar{b} = \int_0^{\pi/2} S\,b\cos b\,db \Big/ \int_0^{\pi/2} S\cos b\,db$$

and

$$\int_0^{\bar{\bar{b}}} S\cos b\,db = \int_{\bar{\bar{b}}}^{\pi/2} S\cos b\,db.$$

The number of objects in the whole sky becomes, from (10),

$$N = \frac{10^3}{3}10^{0\cdot6(m_1-M_0)}D_2\int_{-\pi/2}^{+\pi/2}2\pi S\cos b\,db. \tag{11}$$

For the special case of objects uniformly distributed throughout non-absorbing space $S=1$, and we recover the expected result which defined D_2 in Section 2:

$$N = \frac{4\pi}{3}10^3 10^{0\cdot6(m_1-M_2)}D_2. \tag{12}$$

If we write

$$\bar{S} = \frac{1}{4\pi}\int_{-\pi/2}^{+\pi/2}2\pi S\cos b\,db,$$

we obtain the general resulting formula in a convenient form

$$N = \frac{4\pi}{3} 10^3 10^{0.6(m_1 - M_2)} D_2 \bar{S}. \quad (13)$$

Comparison of (12) and (13) shows that $\bar{S}$ can be regarded as the factor by which absorption and change of space density affect the number of visible objects.

Since N is proportional to $10^{0.6m_1}\bar{S}$, the slope q becomes

$$q = d \log_{10} N/dm_1 = 0.6 + d \log_{10} \bar{S}/dm_1.$$

5. *Calculations.*—Before the calculations can proceed it is necessary to choose values for a_0 and β. The values adopted for the main calculations are

$$a_0 = 2.5 \times 10^{-3} \text{ mag/pc (vis.)},$$
$$\beta = 150 \text{ pc},$$

giving an optical half-thickness of the galaxy of $a_0\beta = 0.375$ mag (vis.).

Values usually quoted for mean absorption in the galactic plane are about 0.8×10^{-3} mag/pc (**5**), but van de Hulst has pointed out (**6**) that for absorption by interstellar clouds the amount of absorption along a random sight-line would be two or three times greater than this. It is the larger absorption that is required for our present purpose. The question of interstellar absorption has been studied by Parenago (**2**), who obtained a mean random absorption a_0 of 3.4×10^{-3} mag/pc (pg). These two points of view are in approximate agreement and lead to the adopted value of a_0.

The most useful data for obtaining the optical half-thickness of the galaxy, $a_0\beta$, are counts of extra-galactic nebulae. Hubble's counts (**7**) gave a value of 0.25 mag (pg), but re-analysis of his data by Parenago (**2**) gave 0.34 mag (pg). Other surveys give a greater gradient of nebular number with b and indicate a greater value of $a_0\beta$. The data by Shapley (**8**), Shapley and Ames (**9**), and Neyman, Scott and Shane (**10**) have been plotted against b to obtain the adopted value of $a_0\beta$. Parenago's value of β is 100 pc (**2**).

The values used for other constants were

$$\sin b = 0.0,\ 0.1,\ 0.5,\ 1.0.$$
$$\gamma = 20,\ 50,\ 500,\ \infty \text{ pc}.$$
$$\sigma = 0,\ 1,\ 2 \text{ mag}.$$
$$m - M \text{ from } -5 \text{ to about } +20.$$

For each selection of b the quantities r, $\log_{10} r$, $\exp(-r \sin b/\beta)$, $\alpha(r)$, $G(r)$, $5 \log_{10} r_0$, and $m - M$ were tabulated with intervals of 0.1 in $\log_{10} r$. For each γ and b further tabulations were made of $\exp(-r \sin b/\gamma) = \Delta(r)$, and $\exp(-r \sin b/\gamma)/G(r) = \Delta_0(r)$. By comparison of $\Delta_0(r)$ with $5 \log_{10} r_0$ we obtain $\Delta_0(r_0)$, or $\Delta_0(m - M)$. The argument for further tabulations was $m - M_2$ or $m_1 - M_2$ in intervals of 1 mag. $\Delta_0(m - M)$ was integrated by the approximation (9) to give $\Delta_1(m - M_2)$ for $\sigma = 0$, 1, 2 mag. The integration of (10) to give S was carried out in two parts. For lower values of m the expression $\Delta_1(m - M_2)10^{0.6m}$ was approximately logarithmic and the integration was made numerically; for higher m the form changed and the integration was made graphically. Finally S was plotted against b so that $\bar{S}$, $\bar{b}$ and $\bar{b}$ could be found by graphical methods. Only four values of b were available for this graph and some inaccuracy was introduced when there were rapid changes of S with b. This sometimes occurred for the higher values of $m_1 - M_2$. However, the accuracy throughout appears to be adequate for the application of the analysis.

The results of the calculations for $\sigma = 1$ are given in Figs. 2 and 3 and in Table I. The data for $\gamma = 100$ and 200 pc were obtained by interpolation.

The values for $\sigma = 0$ and 2 magnitudes are not given completely, but the effect of varying σ between 0 and 2 can be seen from Tables II and III in the case of $\gamma = 20$, 50 and 500. The effect is negligible for $\gamma = \infty$.

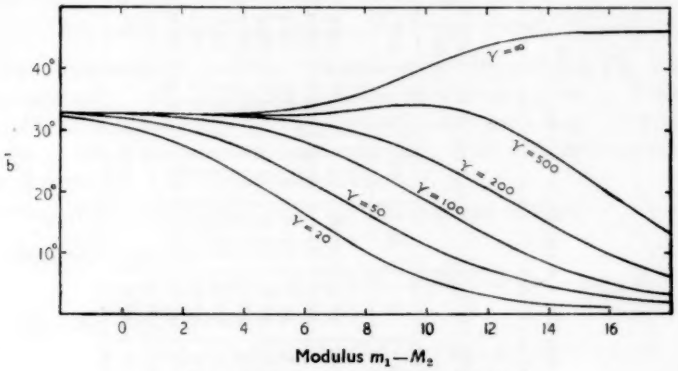

FIG. 2.—*Curves for mean galactic latitude.*

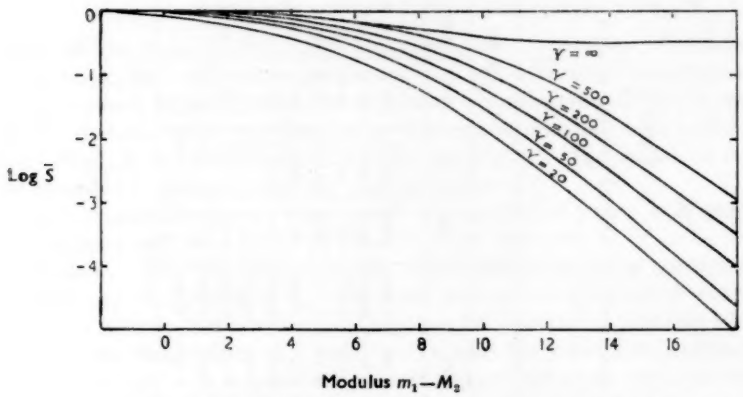

FIG. 3.—*Factor by which absorption and space density change affects the number of visible objects.*

There can be no certainty that the best choice has been made for a_0 and β. The computational labour prevents repetition of the whole calculations for other values but the general trend of a change in the constants can be seen from comparisons within Tables II and III. In the tables the $\gamma = 50$ values have been repeated for (*a*) $a_0 = 1{\cdot}6 \times 10^{-3}$ mag (vis)/pc, $\beta = 150$ pc, and (*b*) $a_0 = 2{\cdot}5 \times 10^{-3}$ mag (vis)/pc, $\beta = 100$ pc. From these calculations it is seen that $\log_{10} \bar{S}$ is not greatly affected by a change in a_0 or β. Reduction of a_0 from 2·5 to 1·6 mag/kpc has the effect of lowering $\bar{b}$ by 2° or 3° when $\bar{b} < 15°$. Reduction of β from 150 pc to 100 pc (to agree with Parenago) has almost negligible effect on $\bar{b}$.

6. *Interpretation.*—The aim of the calculations was to enable one to determine the descriptive parameters from the observable parameters, and we now study Figs. 2 and 3 with this in mind.

TABLE I

Calculations of $\bar{S}$, $\bar{b}$, and $\bar{\bar{b}}$ using the adopted constants $a_0 = 2{\cdot}5 \times 10^{-3}$ mag/pc, $\beta = 150$ pc, $\sigma = 1$ mag

$m_1 - M_2$	$-\log_{10}\bar{S}$						$\bar{b}$						$\bar{\bar{b}}$					
	γ in pc						γ in pc						γ in pc					
	20	50	100	200	500	∞	20	50	100	200	500	∞	20	50	100	200	500	∞
							°	°	°	°	°	°	°	°	°	°	°	°
0	0·10	0·04	0·02	0·00	0·00	0·00	30·4	31·8	32·7	32·7	32·7	32·7	26·6	29·1	29·8	30·0	30·0	30·0
2	0·21	0·12	0·08	0·05	0·03	0·02	27·5	30·5	32·1	32·7	32·7	32·7	23·0	27·3	29·2	29·9	29·9	30·0
4	0·43	0·26	0·20	0·15	0·11	0·08	22·7	27·2	30·8	32·4	32·5	32·8	17·8	23·2	27·7	29·4	29·5	30·0
6	0·76	0·53	0·40	0·32	0·21	0·17	16·4	22·3	28·3	31·4	32·6	33·8	11·9	17·7	24·9	28·5	29·8	31·2
8	1·23	0·95	0·74	0·56	0·40	0·29	10·3	16·5	24·1	29·4	33·6	36·3	6·9	12·2	20·4	26·5	30·9	34·3
10	1·85	1·50	1·22	0·94	0·66	0·40	5·9	11·3	18·7	25·6	34·1	40·2	3·5	7·9	14·5	22·6	31·6	39·4
12	2·55	2·18	1·79	1·45	1·07	0·48	3·0	7·5	13·2	20·5	31·9	43·9	1·8	4·9	9·9	17·1	29·3	43·3
14	3·30	2·94	2·50	2·09	1·64	0·49	1·6	4·6	8·5	14·7	26·7	45·7	1·0	2·9	6·4	12·0	23·3	45·1
16	4·17	3·80	3·24	2·80	2·28	0·49	1·0	3·0		10·0	19·8	46·0		1·9		8·0	16·7	45·5
18	5·06	4·66	4·00	3·52	2·95	0·49		1·9			13·0	46·0		1·4		5·3	11·9	45·5

Suppose in the ideal case that $m_v(10)$, q, $\overline{M}$, σ_M, $\bar{b}$, and $\bar{\bar{b}}$ are all available from measurements and are standardized to the 10th object. We may assume $\sigma = \sigma_M$ (see below). $\overline{M}$ will equal M_q as in Section 3, whence from (4)

$$\left.\begin{aligned} M_0 &= \overline{M} + q\sigma^2/\log_{10} e = \overline{M} + 2{\cdot}3q\sigma^2, \\ M_1 &= \overline{M} + (q-0{\cdot}4)\sigma^2/\log_{10} e = \overline{M} + 2{\cdot}3(q-0{\cdot}4)\sigma^2, \\ M_2 &= \overline{M} + (q-0{\cdot}6)\sigma^2/\log_{10} e = \overline{M} + 2{\cdot}3(q-0{\cdot}6)\sigma^2. \end{aligned}\right\} \quad (14)$$

$\overline{M}$ is always between M_0 and M_2. Using $m_v(10) - M_2$ with $\bar{b}$ in Fig. 2 we obtain an estimate of γ. Fig. 2 may be modified by the data given in Tables I and II if (*a*) $\bar{\bar{b}}$ is used instead of $\bar{b}$, (*b*) σ departs seriously from 1 mag, or (*c*) the adopted constants a_0 and β are not considered suitable. With γ so determined one may obtain $\overline{S}$ from Fig. 3 or Tables I and III.

Putting $N = 10$ in (13) and using (4) and (14) one obtains

$$\left.\begin{aligned} \log_{10} D_0 &= \log_{10} D_2 + 0{\cdot}415\sigma^2 \\ &= -2{\cdot}62 - 0{\cdot}6m_v(10) + 0{\cdot}6\overline{M} + 1{\cdot}38(q-0{\cdot}3)\sigma^2 - \log_{10}\overline{S}, \\ \log_{10} D_1 &= \log_{10} D_2 + 0{\cdot}23\sigma^2 \\ &= -2{\cdot}62 - 0{\cdot}6m_v(10) + 0{\cdot}6\overline{M} + 1{\cdot}38(q-0{\cdot}43)\sigma^2 - \log_{10}\overline{S}, \\ \log_{10} D_2 &= -2{\cdot}62 - 0{\cdot}6(m_v(10) - M_2) - \log_{10}\overline{S} \\ &= -2{\cdot}62 - 0{\cdot}6m_v(10) + 0{\cdot}6\overline{M} + 1{\cdot}38(q-0{\cdot}6)\sigma^2 - \log_{10}\overline{S}. \end{aligned}\right\} \quad (15)$$

Thus all the expected descriptive parameters are obtainable. However, if the modulus $m_v(10) - M_2$ is less than about 3, $\bar{b}$ and $\bar{\bar{b}}$ become insensitive to γ and hence γ cannot be determined. In such cases γ is not needed for the determination of $\overline{S}$. A check on the measured value of q may be obtained since it should equal $0{\cdot}6 + d\log_{10}\overline{S}/dm$, which may be found from Fig. 3. The measured value may be amended if necessary and the analysis repeated.

It is reasonable to put $\sigma = \sigma_M$. Although accidental errors in M would make $\sigma_M > \sigma$ there will be a tendency for individual estimates of M to be somewhat dependent. This will reduce σ_M and may counterbalance the accidental errors. In any case the constants σ_M and σ can seldom be determined with suitable accuracy because the distributions may not be Gaussian. For this reason it is desirable to choose from (14) and (15) the form for which the coefficients of σ^2 are the smallest. It is found for various objects that q can vary over the whole range from 0·0 to 0·6, but it often has intermediate values about 0·3 and 0·4. The representations in M_1 and D_1 are the least sensitive to errors in σ^2, and as their values have also a clear meaning they are regarded as the main results.

For some categories it will not be possible to obtain all of the observable parameters. Some estimate of $m_v(10)$, q and $\bar{b}$ will nearly always be possible if the category is recognizable at all. If σ cannot be estimated it is reasonably safe to assume σ is between 1 and 2. If σ is greater than 2 (as for "all stars") errors introduced can be large. The most serious likely omission from the observables is $\overline{M}$. Fortunately, even though individual values of M for the objects concerned may not be available, it often happens that a general estimate for the category has been made and can be used in place of $\overline{M}$. If M is quite unknown but there are some estimates of γ, a reverse procedure may be used to determine $\overline{M}$.

TABLE II

Calculations of $\bar{b}$ using various values for a_0, β, γ and σ

a_0 in mag_V/kpc	2·5			2·5			2·5			1·6	2·5
β in pc	150			150			150			150	100
γ in pc	20			50			500			50	50
σ in mag_V / m_1-M_2	0	1	2	0	1	2	0	1	2	1	1
	°	°	°	°	°	°	°	°	°	°	°
0	30·6	30·4	29·7	32·0	31·8	31·4	32·7	32·7	32·7	32·2	31·8
2	27·6	27·5	27·0	30·7	30·5	30·0	32·7	32·7	32·7	30·9	30·5
4	22·7	22·7	22·7	27·3	27·2	27·1	32·5	32·5	32·5	27·8	27·2
6	16·3	16·4	16·7	22·2	22·3	22·5	32·6	32·6	32·6	22·4	22·4
8	10·0	10·3	11·0	16·3	16·5	17·0	33·6	33·6	33·6	15·7	16·9
10	5·4	5·9	6·7	11·1	11·3	12·1	33·9	34·1	34·5	8·6	12·2
12	2·6	3·0	4·0	7·0	7·5	8·6	31·3	31·9	33·5	4·6	8·5
14	1·3	1·6	2·3	4·0	4·6	6·1	25·7	26·7	29·5	2·7	5·4
16	0·8	1·0	1·4	2·6	3·0	4·4	18·4	19·8	24·0	1·8	3·3
18				1·6	1·9	2·9	11·5	13·0	17·8		2·0

TABLE III

Calculations of $-\log_{10}\bar{S}$ *using various values for* a_0, β, γ *and* σ

a_0 in mag_V/kpc	2·5			2·5			2·5			1·6	2·5
β in pc	150			150			150			150	100
γ in pc	20			50			500			50	50
σ in mag_V / m_1-M_2	0	1	2	0	1	2	0	1	2	1	1
0	0·10	0·10	0·11	0·04	0·04	0·04	0·00	0·00	0·00	0·04	0·04
2	0·21	0·21	0·22	0·12	0·12	0·13	0·03	0·03	0·03	0·11	0·12
4	0·43	0·43	0·43	0·26	0·26	0·27	0·10	0·11	0·12	0·24	0·26
6	0·78	0·76	0·72	0·54	0·53	0·51	0·21	0·21	0·22	0·47	0·53
8	1·27	1·23	1·12	0·99	0·95	0·85	0·40	0·40	0·39	0·87	0·93
10	1·92	1·85	1·69	1·56	1·50	1·31	0·69	0·66	0·61	1·40	1·44
12	2·63	2·55	2·31	2·25	2·18	1·88	1·15	1·07	0·96	2·04	2·10
14	3·41	3·30	3·00	3·04	2·94	2·56	1·79	1·64	1·44	2·80	2·88
16	4·32	4·17	3·80	3·91	3·80	3·34	2·45	2·28	1·99	3·62	3·77
18		5·06	4·65	4·81	4·66	4·11	3·15	2·95	2·63		

7. *Examples.*—The examples given in this section are intended as preliminary illustrations of the foregoing analysis. Any final studies should be accompanied by complete lists of the objects and values used, but the lists used for the present examples have not been compiled with the accuracy and completeness that would justify their publication. The assortment of objects chosen is varied enough to show up the main features and difficulties of the whole-sky statistics.

Fig. 4 gives the plots of N against m_v (or m_{pg} in two cases) from which $m_v(10)$ and q are obtained. Table IV shows the observable measurements on the left and the resulting descriptive parameters on the right. The calculated value of q ($q_{calc}=0{\cdot}6+d\log_{10}\overline{S}/dm$) is also added.

Wolf-Rayet stars.—Data are mostly from Beals (**11, 12**), but a brighter value of -4 is used for $\overline{M}$ in order to give a more acceptable result for γ. Even with $M=-4$ the value of 25 pc derived for γ is smaller than might be expected.

O stars.—The number of O stars is sensitive to the criteria defining the division between O and B stars. The data in Fig. 4 and Table IV represent O stars from the Henry Draper Catalogue (**13**). The O9·5 stars of the Yerkes Classification (**14**) are mostly Bo on the HD system. Among the bright stars these O9·5 subtypes are more numerous than all other O stars. We might conclude therefore that if they had been included the number density of O stars would have been at least doubled.

Flare stars.—This is an example of a category of which less than ten are known (**15**). Since they are near stars the slope q should be 0·6, and this has been adopted in Fig. 4 and Table IV, although the plotted points would have given a much smaller value. The solution in Fig. 4 is equivalent to making the assumption that very few of the flare stars with $m_v>12$ have been detected but that most of those with $m_v<12$ have been. The two faintest stars on the diagram would not then be among the ten brightest and are discarded for $\overline{M}$, $\bar{b}$ and σ_M. This does not leave enough stars to provide a usable value of $\bar{b}$, which, in any case, could not give a value of γ because $m_v(10)-M_2$ is too small.

All stars.—It could not be expected that a category as heterogeneous as "all stars" could give accurate results by this method. Nevertheless the total star density (0·33 stars/pc^3) and the luminous emission (0·0013 ($M_v=0$ stars)/pc^3) found by this method are not much greater than values from the luminosity function (about 0·18 and 0·0006 respectively). The small value of γ found in this case is probably due to some flattening of the local system of stars and may not represent stars as a whole.

White dwarfs.—When m_v is plotted against N for the brightest known white dwarfs (**16**) one obtains $q=0{\cdot}35$ or less, whereas objects as close as this should have $q=0{\cdot}60$. It may then be noticed that the three brightest stars α CMa B, 40 Eri B and α CMi B are all faint companions which would not be detectable at great distances. The analysis has therefore been made separately for faint-companion white dwarfs and for free ones. For faint companions Fig. 4 shows the slope q to be much less than the theoretical 0·6. The theoretical slope is used in this case and we must conclude that, unless α CMa B and 40 Eri B are chance exceptions, the faint-companion white dwarfs are very numerous. For the free white dwarfs the analysis is straightforward.

Globular clusters.—Data are from Shapley (**17**), Graff (**18**) and Lohmann (**19**). Since the distribution of globular clusters in galactic longitude is asymmetric there should be an analysis of $\bar{l}$, $\overline{l^2}$ to give ϵ before one could assign a clear meaning to D_0, D_1 or D_2.

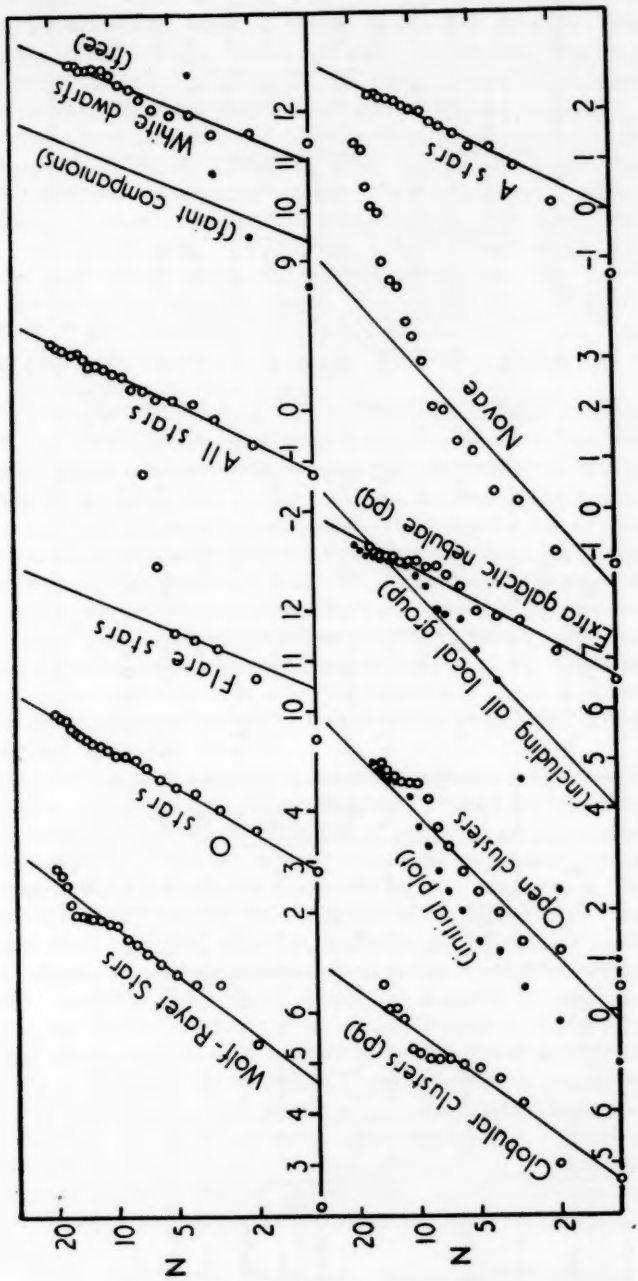

FIG. 4.—*Number of objects plotted against absolute magnitude.*

TABLE IV

Object	$m_V(10)$	q	$\overline{M}$ (vis)	σ_M	$\bar{b}$	$\bar{\bar{b}}$	σ^2	M_0 (visual)	M_1 (visual)	M_2 (visual)	γ	$-\log_{10}\bar{S}$	$\log_{10} D_0$	$\log_{10} D_1$	$\log_{10} D_2$	q(calc)
				mag	°	°					pc		in pc^{-3}	in pc^{-3}	in pc^{-3}	
Wolf-Rayet stars	7·7	0·32	− 4	1·0	3·4	2	1·0	− 3·3	− 4·2	− 4·6	25	2·6	− 7·1	− 7·2	− 7·5	0·23
O stars	5·2	0·41	− 4·5	1	7·8	5·1	1	− 3·6	− 4·5	− 4·9	35	1·8	− 6·5	− 6·7	− 7·0	0·28
Flare stars	12·2	0·6?	+13·1	1·4	21	12	2·0	+15·9	+14·0	+13·1		0·0	− 1·2	− 1·6	− 2·1	0·60
All stars	0·8	0·50	− 0·8	3·2	25	18	10	+10·7	+ 1·5	− 3·1	30?	0·3	− 0·5	− 2·3	− 4·6	0·50
White dwarfs: Faint companions	11·1	0·6	+11·7		22		2	+14·5	+12·6	+11·7		0·0	− 1·4	− 1·8	− 2·3	0·60
White dwarfs: Free	12·7	0·60	+11·8	1·5	33	24	2·3	+15·0	+12·9	+11·8		0·0	− 2·2	− 2·6	− 3·2	0·60
Globular clusters	7·0	0·34	− 8·4	0·9	31	25	0·8	− 7·8	− 8·5	− 8·9	1000	1·8	−10·0	−10·2	−10·4	0·30
Open clusters	3·9	0·24	− 4·3	1·5	16	9	2·2	− 3·1	− 5·1	− 6·1	70	1·4	− 6·3	− 6·7	− 7·3	0·32
Extra-galactic neb.	8·2	0·48	−17·4	1·6	48	44	2·5	−14·6	−16·9	−18·1	∞	0·5	−16·9	−17·3	−17·9	0·60
Normal novae	3·0	0·22	− 7·4	1·5?	11	13	2·3	− 6·2	− 8·4	− 9·4	90	2·0	− 7·2	− 7·6	− 8·1	0·26
A stars	1·9	0·50	− 0·1	2·1	29	17	2·5?	+ 2·8	+ 0·5	− 0·7	50?	0·1	− 3·0	− 3·4	− 4·0	0·53

Open clusters.—Data are from Graff (**18**) and Collinder (**20**). The first four clusters in the list were Sco-Cen, UMa, Hyades and Pleiades. The smallness of q for the initial plot that includes all these suggests that there is a systematic change in the manner of selection with increasing cluster total magnitude. The adopted curve in Fig. 4 is obtained by omitting the first two clusters. The curve then becomes more normal and is probably more representative of open clusters.

Extra-galactic nebulae.—Data are from Holmberg (**21**) and Stebbins and Whitford (**22**) and have been corrected to the new distance scale. Since our own galaxy is a member of the local group (**23**) the nearest nebulae will not be representative of all space. In that case a fairly safe procedure is to start the list at the point where non-local-group galaxies appear. The first five nebulae on the list are Large Mag. Cl., Small Mag. Cl., Andromeda Neb., M 33 and NGC 5128, of which NGC 5128 is the first non-member. The adopted objects for Fig. 4 start one before this at M 33. This has approximately the effect of giving unit weight to the local group.

Normal novae.—Supernovae and recurrent novae have been omitted from the list (**24**). Of the 19 novae listed only 4 occurred outside of the period 1900–1950, hence 50 years might be regarded as the effective observing period. The magnitudes used refer to the intensity maxima. The graph defined by the points in Fig. 4 is more curved and the slope smaller than expected. If this is interpreted as indicating that many $m_v > 3$ novae have been missed we may proceed to obtain the results in Table IV. The density obtained of about 10^{-7} novae pc^{-3} century^{-1} is surprisingly high and amounts to more than one nova per star in 10^9 years. This high evaluation of nova density is due to the assumption that there are many unrecorded novae with $m_{max} > 3$, which assumption is however more likely than that there are more close novae than average. It is possible that the limitations of the galaxy in the direction of the galactic plane have affected this result.

A stars.—The high value of $\sigma_M = 2{\cdot}1$ was influenced by the presence of the supergiant α Cyg in the list. It was reduced to $\sigma = 1{\cdot}6$ for the calculations.

8. *Discussion.*—The whole-sky statistical analysis is general enough and elastic enough to apply to almost any category of celestial object that can be recognized. Its weaknesses are inaccuracies caused by (*a*) the smallness of the number of sample objects used, and (*b*) the simplicity of the assumptions made regarding the distribution of objects, their magnitudes and the absorbing medium.

If 20 objects are used the standard error in D_0, D_1, D_2 from statistical fluctuations will be $20^{-1/2}$ or about 25 per cent, which might be regarded as satisfactory. However, this figure is based on an assumed random distribution, and any clustering of the objects that exists will tend to increase this error. Some indications of the clustering are generally available from large-scale studies of the objects and, furthermore, such effects can be often detected by unevenness in the distribution of b or l and irregularity in the plot of $\log_{10} N$ against m_v. If these data have the predicted symmetry or smoothness it may be assumed that the results are not adversely affected by clustering. On the other hand, if clustering exists one can usually make some allowance for it (e.g. extra-galactic nebulae in Section 7).

The effect of the Gaussian distribution (1) assumed for the luminosity function has already been mentioned in Sections 2 and 6, where it is shown that results expressed in the representation M_1 and D_1 are not very sensitive to departures from the Gaussian form.

The effect of the simplified assumptions on the analysis may be checked eventually by comparison of categories studied by other methods, but very little direct comparison can be made at present. From Section 5 we find that the most recognizable effect of varying a_0 and β is that for a given γ, $\bar{b}$ increases with a_0, or for a measured $\bar{b}$, γ increases with decreasing a_0. The derived γ's for the relevant objects (Wolf-Rayet stars 25 pc; O stars 35 pc; open clusters 70 pc; novae 90 pc) have some tendency to be lower than expected and may indicate that the adopted value of a_0 is too large. The adoption of a lower value of β ($\beta = 100$ pc has been used by Parenago (**2**)) does not improve the situation. More analyses should give clearer indications on these points.

The space densities D_0 obtained for globular clusters, open clusters, all stars and O stars are from 1 to 4 times greater than the corresponding values given by Parenago (**25**). The difference is probably due mainly to the assumption made here that the nearer and brighter objects are representative of all space.

A factor that has considerable effect on the statistics is the fall in percentage recognition of objects with increasing magnitude. In the present method of analysis this effect can often be appreciated by comparing the observed q with q(calc). If the observed q is too small one can assume fainter objects are lost from the list by non-recognition. An allowance for the effect can be made but this may not be entirely impersonal. If, on the other hand, the observed q is larger than q(calc) it may mean that γ has been underestimated, since it can be seen from Fig. 3 that increase of γ (other parameters remaining constant) increases $d \log_{10} \bar{S}/dm_1$ and increases q. In principle γ could be determined from the measured q, but this is less reliable than by using $\bar{b}$ as in Section 6.

The effect on the descriptive parameters introduced by changing any observable parameters may be readily assessed by following through the procedure of Section 6. Small changes do not as a rule produce appreciable variation in q(calc).

Any systematic comparison of absolute magnitudes and number densities of different categories will require a decision as to which of the three systems M_0, D_0; M_1, D_1; or M_2, D_2 should be adopted as standard. The disadvantages of M_0, D_0 have been explained in Section 2, and moreover the usual approximate estimates of density are not generally on this system. For example, the density of white-dwarf stars in the solar neighbourhood quoted as 7×10^5/kpc^3 by Parenago (**26**) does not allow for dispersion in M and might be regarded as an estimate of D_2. It agrees with D_2 in Table IV. The discussion in Section 6 suggests the M_1, D_1 system to be the best compromise.

University of London Observatory,
Mill Hill Park,
London, N.W. 7:
1954 *February.*

References

(1) B. J. Bok and D. A. MacRae, " Fundamental Properties of the Galactic System ", *Ann. N.Y. Acad. Sci.*, **42**, 219, 1941.
(2) P. P. Parenago, *Astron. Zh. U.S.S.R.*, **22**, 129, 1945.
(3) F. H. Seares, *Ap. J.*, **74**, 91, 1931.
(4) W. M. Smart, *Stellar Dynamics*, p. 276, Cambridge, 1938.
(5) R. J. Trumpler and H. F. Weaver, *Statistical Astronomy*, p. 452, California Univ. Press, 1953.

(6) H. C. van de Hulst, *Rech. Astr. Utrecht*, **11**, Part 2, 1949.
(7) E. Hubble, *Ap. J.*, **79**, 8, 1934.
(8) H. Shapley (and R. B. Jones), *Harv. Ann.*, **105**, 137, 1937; **106**, 1, 1938.
(9) H. Shapley and A. Ames, *Harv. Ann.*, **88**, 41, 1932.
(10) J. Neyman, E. L. Scott and C. D. Shane, *Ap. J.*, **117**, 92, 1953.
(11) C. S. Beals, *Publ. Dom. Ap. Obs.*, **4**, 271, 1930.
(12) C. S. Beals, *J.R.A.S. Canada*, **34**, 169, 1940.
(13) A. J. Cannon and E. C. Pickering, *Harv. Ann.*, **91** to **99**, 1918–24.
(14) P. C. Keenan and W. W. Morgan in *Astrophysics*, p. 12, McGraw–Hill, 1951.
(15) H. Shapley, *Harv. Reprint*, No. 344, 1951.
(16) W. J. Luyten, *Ap. J.*, **116**, 283, 1952.
(17) H. Shapley, *Harv. Reprint*, No. 320, 1949.
(18) K. Graff, *Mitt. Wien St.*, **4**, No. 4, 27, 1948.
(19) W. Lohmann, *Zs. f. Ap.*, **30**, 234, 1952.
(20) P. Collinder, *Lund Ann.*, **2**, 1931.
(21) E. Holmberg, *Lund Med.* Ser. II, No. 128, 1950; Ser. I, No. 180, 1952.
(22) J. Stebbins and A. E. Whitford, *Ap. J.*, **115**, 284, 1952.
(23) W. Baade, *Ap. J.*, **100**, 147, 1944.
(24) Ch. Bertaud, *Ann. d'Ap.*, **11**, 1, 1948; **14**, 199, 1951.
(25) P. P. Parenago, *Astron. Zh. U.S.S.R.*, **25**, 123, 1948.
(26) P. P. Parenago, *Astr. Inst. Sternberg*, No. 30, 3, 1949.

THE MAXIMUM EFFECT OF CONVECTION IN STELLAR ATMOSPHERES ON THE OBSERVED PROPERTIES OF STELLAR SPECTRA. II

Antoni Przybylski

(Communicated by the Commonwealth Astronomer)

(Received 1954 April 20)

Summary

Calculations of the equivalent widths of the calcium lines K and g have been carried out for model stellar atmospheres computed in the first part of this investigation (*M.N.*, **113**, 683, 1953).

Diagrams connecting the equivalent widths of calcium lines with the colour gradients are constructed for both radiative and adiabatic models and compared with the same relations established from observational data. This comparison shows that actual stellar atmospheres probably are not far from radiative equilibrium.

1. *Introduction.*—In the first part of the investigations on model stellar atmospheres (*M.N.*, **113**, 683, 1953), which subsequently will be quoted as Paper I, monochromatic fluxes and colour gradients were computed for sixteen model stellar atmospheres. Eight of these models were in radiative equilibrium (radiative models) and the other eight were computed under the assumption that the temperature gradient in the convective zone is adiabatic (adiabatic models). The results of these investigations, arranged in the form of diagrams connecting the colour gradients ϕ with the reciprocal boundary temperature θ_0 for both radiative and adiabatic models, would settle the question as to the amount of energy carried by convection in stellar atmospheres if the boundary temperature were accessible to observation: a simple comparison of observed colour gradients with the computed ones would then show whether the gradients of actual stellar atmospheres approach more to the gradients of the one or the other series of models.

Since, however, the boundary temperature of stars is not known, its replacement by another quantity easily accessible to observation and theoretical computations and, on the other hand, closely related to the boundary temperature must be chosen as an aiternative way to deal with the problem of convection. The equivalent width of the calcium lines K and g seems to be most suitable for that purpose. Absorption lines are formed substantially in low optical depth, where the temperature does not differ greatly from its boundary value; they are therefore closely related to the reciprocal boundary temperature θ_0. On the other hand, the equivalent width of the calcium lines K and g shows a large range of variation for θ_0 varying between 0·6 and 1·0 which enables us to use the equivalent width instead of the reciprocal temperature in spite of the low precision of many equivalent-width determinations.

In the present paper (Section 2) the equivalent widths of the K and g lines are computed for the radiative and adiabatic models published in Paper I.

The logarithms of the equivalent widths are then plotted against the gradients of the corresponding models (Section 3), giving diagrams connecting these (*computed*) quantities for both radiative and adiabatic models; these diagrams are shown in Fig. 1. A similar diagram connecting the *observed* gradients and equivalent widths and based on the investigations of 130 stars (Fig. 2) is then compared with the theoretical relations shown in Fig. 1. This comparison (Section 5) shows that a satisfactory agreement can be achieved between the observed diagram and the theoretical diagram for radiative models. This seems to favour the conclusion that real stellar atmospheres are not far from radiative equilibrium. Finally the possible sources of error are discussed (Sections 6 and 7).

In the way described above the reciprocal boundary temperature θ_0, used as a basic quantity in the computation of stellar models, of their colour gradients and of the equivalent widths of their calcium lines, is eliminated in the final stage of the investigations.

2. *Equivalent width of calcium lines.*—The calculation of line profiles followed closely the method of Strömgren (**1**) as described and illustrated with examples by R. v. d. R. Woolley and D. W. N. Stibbs (**2**). The only change concerns the introduction of partition function in the formula for ionization on account of the fact that the temperatures of some models are higher than the temperature of the model considered by Woolley and Stibbs. This was, however, not possible in the computation of the distribution of calcium atoms in the singly and doubly ionized states (in the absence of L-S coupling for twice ionized atoms); it was assumed here that the ratio of the partition functions is equal to the ratio of the statistical weights in the ground states. An error of about 20 per cent in the computed equivalent widths is therefore possible for hotter models; this is, however, still a tolerable error, changing the logarithm of the equivalent width by only about 0·1.

The assumed abundance of calcium in stellar atmospheres is 0·02 of all metals. The theoretical values of the oscillator strength (2 for neutral and $\frac{2}{3}$ for ionized calcium) were used in the computations. Since the equivalent width is proportional to the square root of the abundance and of the oscillator strength, an error in these quantities has the same effect on the logarithm of the equivalent width of all models and means only as much as an additive constant. This additive constant, however, can be different for the calcium lines *K* and *g*, since the errors in the oscillator strength may be different for the two lines.

Apart from radiation damping, only collision damping by neutral hydrogen was taken into account. The effect of other sources of line broadening is much smaller and probably does not exceed a few per cent of the broadening due to hydrogen and natural radiation damping.

Generally speaking, it may be expected that the logarithms of the equivalent widths of calcium lines can be computed with an error of about 0·10-0·20 for hot models. For cooler models this error is certainly smaller—disregarding of course an additive correction for an error in the assumed abundance of calcium.

The equivalent width of the *K* line was computed for all models and that of the *g* line for six models. The equivalent width of the *g* line for the two hottest models, with $\theta_0 = 0{\cdot}6$, is so small that measurements are no longer reliable and therefore no comparison between computations and observation is possible.

The results of the computations are given in Tables I and II.

The equivalent width of the g line is not affected seriously by convection even in the hottest models for which it was computed; but there is an appreciable luminosity effect—for dwarfs the equivalent width of this line is roughly 1·5 times as great as for giants.

The K line is more sensitive to the possible effect of convection, but only in hot models. In cooler models the effect of convection is small, since the absorption lines are formed substantially above the convective zone. In hot models the instability begins at a small optical depth and therefore the effect of convection is greater; for instance, for $\theta_0=0{\cdot}6$ the equivalent width of the K line is approximately 2·5 times greater for adiabatic than for radiative models. On the other hand, there is little difference between giants and dwarfs.

TABLE I

Equivalent width of the g line in A

Dwarfs ($\log_{10} g=4{\cdot}5$)			Giants ($\log_{10} g=3{\cdot}5$)		
θ_0	Radiative model	Adiabatic model	θ_0	Radiative model	Adiabatic model
0·7	0·073	0·080			
0·8	0·24	0·26	0·8	0·13	0·15
0·9	0·65	0·67			
1·0	1·39	1·40	1·0	0·89	0·90

TABLE II

Equivalent width of the K line in A

Dwarfs ($\log_{10} g=4{\cdot}5$)			Giants ($\log_{10} g=3{\cdot}5$)		
θ_0	Radiative model	Adiabatic model	θ_0	Radiative model	Adiabatic model
0·6	0·26	0·67	0·6	0·22	0·52
0·7	1·89	2·58			
0·8	6·11	6·51	0·8	4·91	5·89
0·9	12·6	12·9			
1·0	18·2	18·4	1·0	18·9	19·2

3. *Relations between computed colour gradient and equivalent width.*—Plotting the logarithmic equivalent widths from Tables I and II against the colour gradients known from Paper I one gets a set of curves shown in Fig. 1. Thus the boundary temperature θ_0 is eliminated from further investigations.

It should be noted that for both the K and g lines there is a fairly large separation between the curves drawn for radiative and adiabatic models, especially for higher temperature. This very fortunate result is due to the fact that convection has a considerable effect on the colour gradient but only a minor effect on the equivalent widths, since the absorption lines are formed substantially above the convective zone.

On the other hand, there is no great difference between giants and dwarfs, the g line for the adiabatic models being the only exception (of minor importance, however, as further investigations show). This is again very fortunate,

since it allows us to disregard any differences in the luminosities of the stars in question.

4. *Relations between observed colour gradient and equivalent width.*—Plotting the logarithms of the observed equivalent widths against the observed colour gradients for a number of stars one gets the observed relations between these two quantities. These relations are shown in Fig. 2 for both calcium lines.

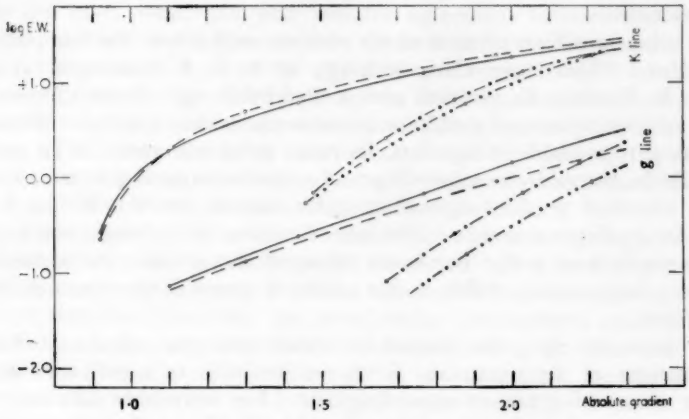

FIG. 1.—*Theoretical gradient–equivalent-width relation.*
Radiative models: ——— *dwarfs* — — — — *giants.*
Adiabatic models: —·—·— *dwarfs* —··—··— *giants.*

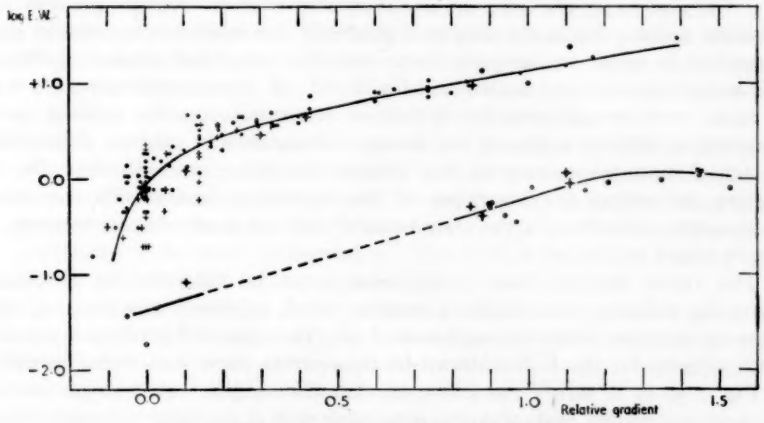

FIG. 2.—*Observed gradient–equivalent-width relation.*
Weight 2 ○ *Weight 1* ● *Weight ½.* + *Peculiar stars.*
Upper curve : K line.
Lower curve : g line.

The equivalent widths were taken from publications listed at the end of this paper (**7–21**). The mean value was used where the equivalent width was determined by many observers; less weight (½) was given to early determinations made with spectrograms of low dispersion. Double stars were included only

if their components were of the same spectral type or if the difference of their luminosities was at least 2 for components of different spectral types. These conditions were not satisfied by two double stars. The *K*-line determinations for six supergiants were rejected, since the gradients of these stars are too high (space reddening). Further, eleven early determinations of the *g* line made by E. G. Williams (**19**) and C. H. Payne (**15**) were rejected, since they seem to be too high (by a factor of about 3) in comparison with recent determinations by other observers.

The colour gradients of most of the stars are available in the lists published by the Royal Observatory, Greenwich (**3**), by S. C. B. Gascoigne (**4**) or by R. v. d. R. Woolley, K. Gottlieb and A. Przybylski (**5**). Since all these lists form a uniform system of gradients, no corrections were applied. Where the gradients were available in two lists, its mean value was used. If no gradient was available, the value corresponding to the spectral type of the star was used.

The observed gradient–equivalent width relation for the *K* line is well defined for gradients over 0·20. The mean deviation of one single star from the mean curve is there 0·08. For lower values of the gradient the scattering of the stars is larger and probably is due mostly to errors in the determination of the gradients.

The curve for the *g* line cannot be drawn with great accuracy. Reliable determinations of the equivalent width are available in a sufficient number only for stars with gradients exceeding 0·80. For early-type stars only three scattered points are available and there is a big gap for gradients between 0·10 and 0·80. A straight line drawn in the diagram must be regarded as a rough approximation to the relation between the gradient and the equivalent width of the *g* line.

5. *Comparison of the observed and computed relations between gradient and equivalent width.*—Since the observed gradients are *relative*, a correction must be applied in order to compare them with the computed *absolute* gradients. This correction has been determined by W. M. H. Greaves (**6**) as $1{\cdot}1 \pm 0{\cdot}1$ for the mean wave-length 5000 A. A further correction must be applied to the computed equivalent width, if the assumed abundance of calcium differs from the actual mean abundance of this element in stellar atmospheres. On the diagram connecting the logarithm of the equivalent width with the colour gradient the correction for the abundance of calcium is an additive constant, as already stated in Section 2.

The curve derived from observations must lie between the theoretical curves for radiative and adiabatic models, which represent two limiting cases of the structure of stellar atmospheres. Using the observed gradient–equivalent width relation for the *K* line drawn on transparent paper and trying to shift it on Fig. 1 so as to satisfy the above condition for higher value of the gradient ($\phi > 2{\cdot}0$), one readily finds that this is possible only if the observed curve follows closely the theoretical curve for radiative models over a wide range. For values of ϕ over 1·4 it is possible to achieve this agreement even if the zero-point correction for the observed gradients is allowed to take values over a fairly large range (between 0·8 and 1·2); for hotter stars, however, this agreement is only possible if the gradient correction does not differ greatly from 1·00 (corrections smaller than 1·00 are, however, impossible, since then the observed curve for hot stars lies outside the allowed area). Actually a very good agreement between the observed relation between gradient and equivalent width

and the theoretical curve for radiative models is possible, if a correction +1·03 is applied to the observed gradients and a correction −0·20 to the logarithm of the computed equivalent width. The agreement of the relations for the *g* line is then also fairly good; the observed curve for the *g* line then lies slightly below the theoretical one, which is perhaps due to the fact that the ionization of calcium in stellar atmospheres may be higher than that computed from Saha's equation.

On the other hand, the best possible agreement between the observed relations for the *K* and *g* lines and the theoretical curves for adiabatic models needs a correction of 1·40 to the observed gradients, which is certainly too high. Even then the agreement between the observed and computed curves is not satisfactory, since there are systematic differences at both ends of the diagram. The observed relation between colour gradient and equivalent width for both *K* and *g* lines would then lie partly below the theoretical curves for adiabatic models; this is physically impossible.

The correction +1·03 for the observed colour gradient, giving a very good agreement between the observed and the theoretical curves for radiative models, lies within the correction range found by Greaves. This is a strong argument in favour of the conclusion that the actual stellar atmospheres are in radiative equilibrium. As far as cooler stars with absolute colour gradient over 1·4 are concerned this conclusion is valid even if the correction for the observed gradient varies within the whole probable range found by Greaves for that correction; for hotter stars, however, a considerable deviation from radiative equilibrium is possible if the correction for observed gradients differs from +1·03. A good determination of this correction would therefore be necessary in order to settle the question as to the amount of energy carried by convection in stellar atmospheres in the way intended in the present investigations.

6. *Possible sources of error.*—The definitive estimation of a possible deviation of stellar atmospheres from radiative equilibrium is at present not possible, since the quantities used in the present investigations are not free from errors. These possible sources of error are briefly mentioned below.

(i) Models are only models and not real stellar atmospheres. The main source of error in the computation of models lies in the mean value of the absorption coefficient, which is unknown as long as the definitive structure of the model is unknown. The effect of a change in the mean absorption coefficient is discussed in Section 7. This difficulty can be solved by computing model stellar atmospheres in higher approximations.

(ii) The equivalent widths, both computed and observed, are known with very low precision, especially for hotter stars. Since, however, the whole range of the variation of the equivalent width is large, even an error of about 50 per cent is here still tolerable.

(iii) Observed gradients of early-type stars may be too high on account of space reddening. The precision of the gradient determination is not very high (mean error about 0·08).

(iv) Calcium abundance in stellar atmospheres is not well known. An additive constant applied to the logarithms of the computed equivalent widths removes this difficulty; this correction can be found fairly easily.

(v) Greaves's correction for the observed relative gradients is not well known. Actually a correction +1·03 for the observed gradients gives good agreement between the observed and computed curves for radiative models,

but the final conclusion as to whether stellar atmospheres are in radiative equilibrium or not will be possible only when the models are constructed in higher approximation and when the correction for the observed gradients is known with higher precision.

In spite of many sources of error it seems to be unlikely that adiabatic models can be better than radiative ones.

7. *Blanketing effect.*—The absorption of radiation in the lines of the Fraunhofer spectrum is an additional source of opacity, which modifies the continuum between the lines. Actually the presence of absorption lines in the spectrum increases the mean value of the absorption coefficient by an amount known as

TABLE III

Model stellar atmosphere: $\theta_0=1\cdot0$, $\log_{10} g=4\cdot5$; *with blanketing effect*

τ	θ	$\log_{10} p$	$\log_{10} p_e$
0·0	1·000		
0·01	0·996	3·88	0·09
0·02	0·993	4·04	0·24
0·03	0·989	4·14	0·32
0·04	0·986	4·21	0·38
0·05	0·982	4·26	0·43
0·06	0·979	4·30	0·48
0·07	0·975	4·34	0·52
0·08	0·972	4·37	0·55
0·09	0·969	4·39	0·58
0·10	0·966	4·42	0·60
0·12	0·959	4·46	0·65
0·14	0·953	4·50	0·69
0·16	0·948	4·53	0·73
0·18	0·942	4·56	0·76
0·20	0·937	4·58	0·80
0·25	0·923	4·63	0·87
0·30	0·911	4·67	0·93
0·35	0·900	4·71	0·99
0·40	0·889	4·74	1·04
0·45	0·879	4·76	1·10
0·50	0·869	4·79	1·16
0·60	0·852	4·82	1·27
0·70	0·836	4·85	1·36
0·80	0·821	4·87	1·46
0·90	0·808	4·89	1·55
1·0	0·795	4·91	1·64
1·2	0·773	4·93	1·79
1·4	0·754	4·95	1·93
1·6	0·736	4·96	2·06
1·8	0·721	4·97	2·17
2·0	0·707	4·98	2·28
2·5	0·677	5·00	2·50
3·0	0·653	5·01	2·69
3·5	0·632	5·02	2·85
4·0	0·615	5·02	2·98
4·5	0·599	5·02	3·10
5·0	0·586	5·03	3·22
6·0	0·562	5·03	3·39
7·0	0·543	5·03	3·54
8·0	0·527	5·04	3·67
9·0	0·512	5·04	3·76
10·0	0·500	5·04	3·86

the blanketing effect. This cannot be disregarded in cool stars; for instance, in the solar atmosphere its contribution to the mean absorption coefficient is estimated to be about 20 per cent of the total absorption; in hotter stars it is less important, since the absorption lines are less numerous in their spectra.

In order to estimate the blanketing effect, a radiative dwarf model, with reciprocal surface temperature $\theta_0 = 1{\cdot}0$ and mean absorption coefficient 1·2 times the value used formerly, was computed. This model is given in Table III. It has a colour gradient of $\phi = 1{\cdot}91$ and the equivalent width of the K line is 17·8 A. The same model without blanketing has a colour gradient 2·00 and the equivalent width is 18·2 A. The change in the equivalent width is negligible, since the lines are formed substantially in the outer layers, whose structure is not greatly influenced by the change in the mean absorption coefficient. The deeper layers, however, which still contribute considerably to the monochromatic fluxes and thus have an effect on the colour gradients, are more sensitive to changes in the mean absorption coefficient. An increase of the mean absorption coefficient substantially means therefore a shift of the model towards lower values of the gradients in Fig. 1, and conversely a decrease means a shift in the opposite direction. This conclusion is of course also valid for a change of the mean absorption coefficient due to other reasons, for instance when higher approximations computed according to the formula

$$\bar{\kappa} = \frac{1}{F} \int_0^\infty k_\nu F_\nu d\nu$$

are used in computations. Since the slope of the theoretical relation between gradient and equivalent width for cool stars is small, inclusion of the blanketing effect has little effect on the curve shown in Fig. 1 and little effect on the general argument of the paper. On the other hand, a change of mean absorption coefficient in the hot stars would require an alteration in our argument about the constant connecting Greaves's relative gradients with absolute gradients.

8. *Acknowledgments.*—The present investigations were carried out at the suggestion and under the supervision of Professor R. v. d. R. Woolley, to whom the author is grateful for many valuable discussions and much advice. The author is indebted to Dr J. L. Greenstein and Mrs A. de Vaucouleurs for their kind permission to use unpublished data on equivalent widths.

Note added in proof.—Recent unpublished determinations of the K line made at the Commonwealth Observatory agree fairly well with the curve drawn in Fig. 2. The same can be said of the determinations of D. Barbier, D. Chalonge and Nina Morguleff (*Ann. d'Ap.*, **4**, 137, 1941), converted tentatively into angstrom units; they were, however, disregarded in this paper, since such conversion, as the authors themselves remarked, is not yet possible with the necessary precision. On the other hand, the determinations of J. A. Hynek, *Ap. J.*, **82**, 338, 1935 (this reference having escaped attention while this paper was being written), disagree considerably with the curves drawn in Fig. 2: the logarithms of his equivalent widths of the K line are systematically lower by about 0·3c, whilst those of the g line are higher by approximately the same amount.

Commonwealth Observatory,
Mount Stromlo,
Canberra, A.C.T.,
Australia:

1954 *April* 15.

References

(1) B. Strömgren, *Ap. J.*, **86**, 1, 1937.
(2) R. v. d. R. Woolley and D. W. N. Stibbs, *The Outer Layers of a Star*, ch. VI, VII, IX, Oxford, 1953.
(3) Royal Observatory, Greenwich, *M.N.*, **100**, 189, 1939.
(4) S. C. B. Gascoigne, *M.N.*, **110**, 15, 1950.
(5) R. v. d. R. Woolley, K. Gottlieb and A. Przybylski, *M.N.*, **112**, 665, 1952.
(6) W. M. H. Greaves, *M.N.*, **108**, 131, 1948.

The equivalent widths of calcium lines were taken from the following sources:

(7) L. H. Aller, *Ap. J.*, **96**, 321, 1942.
(8) L. H. Aller, *Ap. J.*, **106**, 76, 1947.
(9) W. Buscombe, *Ap. J.*, **114**, 73, 1951.
(10) T. Dunham, Jr., *H.B.*, 858, 1928.
(11) J. L. Greenstein, *Ap. J.*, **107**, 151, 1948.
(12) J. L. Greenstein and W. A. Hiltner, *Ap. J.*, **109**, 265, 1949.
(13) A. Pannekoek, *Publ. Dominion Astrophys. Obs.* VIII, No. 5, 1950.
(14) A. Pannekoek and G. B. van Albada, *Publ. Amsterdam*, No. 6, 1939.
(15) C. H. Payne, *H.B.*, 858, 1928.
(16) R. M. Petrie, *Publ. Dominion Astrophys. Obs.* VII, No. 16, 1942.
(17) H. R. Steel, *Ap. J.*, **102**, 43, 1945.
(18) O. Struve and C. D. Higgs, *Ap. J.*, **70**, 131, 1929.
(19) E. G. Williams, *Publ. A.S.P.*, **48**, 113, 1936.
(20) E. T. R. Williams, *H.C.*, 348, 1929.
(21) K. O. Wright, *Publ. Dominion Astrophys. Obs.* VIII, No. 1, 1948.

Unpublished determinations of equivalent widths were supplied by J. L. Greenstein and A. de Vaucouleurs.

THE COLLIMATION ERROR OF THE AIRY TRANSIT CIRCLE

P. J. D. Gething

(Communicated by the Astronomer Royal)

(Received 1954 March 18)

Summary

An analysis of azimuth errors determined from stars " doubled " with the Airy Transit Circle confirms that there is a systematic error in the collimation errors adopted for use with this instrument. The existence of such an error had been suspected for many years because of the discrepancy between clock errors determined with the Transit Circle and with Small Transit " B ". Estimates of the magnitude of the error obtained by four different methods are in fair agreement.

---

1. *Introduction.*—The existence of a systematic error in the collimation errors adopted for the Airy Transit Circle at the Royal Observatory, Greenwich, has been suspected for many years. In October 1926 a small reversible transit instrument, Transit " B ", was brought into use at Greenwich in connection with the international programme of longitude determination. A comparison of the clock errors obtained with the two instruments revealed a discrepancy of about one-tenth of a second, after allowance had been made for the difference of longitude of the two instruments and for the different methods used in reducing the observations. Comparison with the time signals received from other observatories suggested that it was the non-reversible Transit Circle which was at fault; the most probable source of error appeared to be in the determination of collimation error. The clock corrections derived from the Transit Circle observations were not as smooth as those derived from the small transit observations. But the R.A.s of stars determined with the Transit Circle showed better internal agreement when reduced with the determined clock corrections than when reduced with smoothed clock corrections. This is to be expected if the collimation is at fault. There was some evidence that the results with the two instruments would have been more accordant if a constant collimation error had been adopted for the Transit Circle each year, suggesting that the observed changes in the collimation error were not real.

In view of this uncertainty, the Time Service after 1927 July was based on observations made with Transit " B ". The difference between the two instruments, referred to in this paper as TC–B, has persisted at about the same value, with variations that can be attributed partly to the scatter of the observations and partly to the existence of a small annual term. The difference of clock errors, TC–B, has been predominantly positive; clock errors are considered positive when the clock is slow. If the discrepancy is assumed to be due to an error in the determination of collimation error, it can be shown that the true collimation error must be greater than the adopted collimation error by about $0''.3$; collimation error is considered to be positive when a positive correction is required to the times of transit of stars at upper culmination.

The hypothesis that the Transit Circle clock errors are erroneous, and that the error is introduced in the measurement of collimation, is examined and confirmed in this paper. The analysis is based on a method which does not require any comparison between the Transit Circle and another instrument, but only between " fundamental " azimuths as determined from different stars.

The collimation error is measured with the aid of two fixed horizontal collimators placed north and south of the instrument; the process is described in detail in Section 7. The level error is determined by finding the micrometer reading for coincidence of the movable R.A. wire with its own image formed in a pool of mercury. The micrometer reading for coincidence is subtracted from the reading for line of collimation and the resulting difference is the level error expressed in revolutions of the R.A. screw. This can be converted to arc by using the known value in arc of one revolution of the screw. The azimuth error of the instrument can be determined only by observations of stars, but no azimuth marks are available to control possible diurnal changes of azimuth. Circumpolar stars are used for the determination of azimuth, since it is important to be able to observe azimuth stars at transit both above and below the pole. An azimuth star is said to have been " doubled " when it has been observed at two culminations twelve hours apart, and the azimuth error determined from such a pair of observations is here referred to as a " double azimuth ". It has the important advantage of being independent of any error in the star's adopted place.

2. *Method of analysis.*—Suppose that at the first transit the tabular right ascension of the star was T_1, and that the observed time of transit was O_1. Then we have

$$T_1 - O_1 = a_1A_1 + b_1B_1 + c_1C_1 + E_1, \tag{1}$$

where a_1, b_1 and c_1 are the true azimuth, level and collimation errors of the instrument, A_1, B_1 and C_1 are trigonometrical factors depending on the declination δ of the star and the latitude ϕ of the observatory, and E_1 is the true clock error. a_1, b_1 and c_1 are assumed to be expressed in seconds of arc and $(T_1 - O_1)$ and E_1 in seconds of time. This equation is strictly true only if the observations on which it depends are perfect. The effect of diurnal aberration is assumed to be included in c_1 in the usual way. It is assumed that pivot errors are negligible; this point is discussed in more detail in Section 3.

Similarly, at the second transit of the same star, we have

$$T_2 - O_2 = a_2A_2 + b_2B_2 + c_2C_2 + E_2. \tag{2}$$

If we now assume that the azimuth error has not changed in the twelve-hour period between the observations, i.e. that $a_1 = a_2 = a$, the azimuth error can be determined by subtracting (2) from (1). After re-arrangement we have

$$a = \frac{(T_1 - T_2) - (O_1 - O_2) - (b_1B_1 - b_2B_2) - (c_1C_1 - c_2C_2) - (E_1 - E_2)}{(A_1 - A_2)}.$$

The quantity $(T_1 - T_2)$ is known with a high degree of accuracy and is independent of any small error in the assumed R.A. of the star. $(E_1 - E_2)$ is also known with sufficient accuracy, since it depends only on the rate of the clock in a twelve-hour period. The quantities O_1 and O_2, A_1 and A_2 are also known, so that the azimuth error a can be determined.

We shall now suppose that the adopted collimation errors are both subject to the same systematic error Δc, in such a sense that

Δc = True collimation error − Adopted collimation error.

The adopted level errors will also be directly affected by Δc; in fact

Δc = True level error − Adopted level error.

Equations (1) and (2) now become

$$T_1 - O_1 = aA_1 + (b_1 + \Delta c)B_1 + (c_1 + \Delta c)C_1 + E_1, \quad (3)$$

$$T_2 - O_2 = aA_2 + (b_2 + \Delta c)B_2 + (c_2 + \Delta c)C_2 + E_2, \quad (4)$$

where a is still the *true* azimuth error, but b_1, b_2, c_1, c_2 now denote the *adopted* level and collimation errors. Combining equations (3) and (4), we obtain

$$a = \frac{(T_1 - T_2) - (O_1 - O_2) - (b_1B_1 - b_2B_2) - (c_1C_1 - c_2C_2) - (E_1 - E_2)}{(A_1 - A_2)} + \Delta c\left[\frac{(B_2 - B_1) + (C_2 - C_1)}{(A_1 - A_2)}\right]$$

or

$$\text{True azimuth} = \text{Deduced azimuth} + \Delta c\left[\frac{(B_2 - B_1) + (C_2 - C_1)}{(A_1 - A_2)}\right].$$

The formulae for A_1, B_1 and C_1 are as follows:

$$A_1 = \tfrac{1}{15} \sec\delta \sin(\phi - \delta), \quad B_1 = \tfrac{1}{15} \sec\delta \cos(\phi - \delta), \quad C_1 = \tfrac{1}{15} \sec\delta.$$

These three expressions refer to a transit at upper culmination; the corresponding formulae for lower culmination may be obtained by substituting $(180° - \delta)$ for δ.

The quantity $(B_2 - B_1)/(A_1 - A_2)$ is a constant independent of the declination of the star, and is equal to $\tan\phi$, or 1·256 at Greenwich; indeed, this result holds even if two stars at different declinations have been observed. It follows that any systematic error in the determination of level affects all determinations of azimuth equally; they have, as will be seen, no effect on the determination of Δc by the present method.

The quantity $(C_2 - C_1)/(A_1 - A_2)$ is equal to $\sec\phi \operatorname{cosec}\delta$, or 1·606 $\operatorname{cosec}\delta$ at Greenwich. If now several stars are doubled within approximately the same twelve-hour period, the true azimuth will be common to all equations, but the deduced azimuth will vary, apart from the accidental errors of observation, with the star used, through the factor 1·606 $\operatorname{cosec}\delta$. The variation of the deduced azimuths with δ can therefore be used to give an estimate of Δc.

Suppose that two stars have been doubled and that the deduced azimuths are a' and a'' respectively. Then, since the true azimuth is the same for each star, we have

$$(a' - a'') = 1{\cdot}606\ \Delta c\ (\operatorname{cosec}\delta'' - \operatorname{cosec}\delta')$$

or

$$\Delta c = \frac{(a' - a'')}{1{\cdot}606\ (\operatorname{cosec}\delta'' - \operatorname{cosec}\delta')}.$$

For the azimuth stars used at Greenwich the denominator cannot exceed 0·66 even in the most favourable case, and is more likely to be about 0·2. The probable errors of azimuth determinations made with the Airy Transit Circle are about 0″·2 or 0″·3, so that, if ϵ is the probable error of Δc from a single pair of stars,

$$\epsilon > [(0''{\cdot}2)^2 + (0''{\cdot}2)^2]^{1/2}/0{\cdot}66$$

$$> 0''{\cdot}43.$$

In practice, ϵ is probably at least 1″, so that some hundreds of pairs of azimuth stars must be analysed if the existence of a systematic error Δc of the order of 0″·3 is to be demonstrated conclusively.

The impersonal R.A. micrometer was not brought into use until 1915; observations prior to this date are not considered suitable for analysis. From 1915 to 1922 the determinations of azimuth error were based on a list of stars all within $3\frac{1}{2}^\circ$ of the pole. The range of the factor 1·606 cosec δ among these stars is only 0·002, so that this period also must be discarded. A fundamental catalogue was finished in 1938 April, and after that date only a very few double azimuths were obtained. After 1940, regular observations of double azimuths were discontinued and have not been resumed, apart from two short periods in 1953, when a special series of azimuth determinations was made for another purpose. Thus we are left with only the period 1922–1938; however, in this period about a thousand double azimuths are suitable for analysis, so that the data should be adequate.

Between 1922 and 1938 azimuths were determined also by observations of two of the stars in the azimuth star list, one observed above pole and the other below pole; the observations were not usually more than a few hours apart. Azimuths so determined are relatively free from the effects of possible diurnal changes in collimation, but are affected by any errors in the azimuth star places, and they have not been used in the present discussion for this reason.

The method of least squares was used to obtain the best estimate of Δc. An example of the way in which the calculation was set out is given below. Column 1 gives the date, column 2 the name of the star doubled and column 3 the deduced azimuth. This information has been extracted from the annual volumes of *Greenwich Astronomical Results*. The fourth column, x, is the deduced azimuth *minus* the mean of the azimuths in column 3. Column 5 is the factor $f = -1{\cdot}606 \operatorname{cosec} \delta$. Column 6, y, is the factor *minus* the mean factor. Columns 7, 8 and 9 give the products x^2, xy and y^2 respectively, each multiplied by 100 for convenience. The estimate of Δc from these entries alone is

$$\Sigma xy/\Sigma y^2 = +4{\cdot}270/3{\cdot}537 = +1''{\cdot}21.$$

The column showing $100x^2$ is needed for the determination of probable errors.

1 Date	2 Name of star	3 Deduced azimuth	4 x	5 Factor	6 y	7 $100x^2$	8 $100xy$	9 $100y^2$
1922								
Feb. 13	β Cas	+5·52	+·25	−1·878	−·045	+ 6·25	−1·125	+0·202
	α Cas	+4·96	−·31	−1·933	−·100	+ 9·61	+3·100	+1·000
	γ Cas	+5·48	+·21	−1·847	−·014	+ 4·41	−0·294	+0·020
	δ Cas	+5·56	+·29	−1.856	−·023	+ 8·41	−0·667	+0·053
	ε Cas	+4·39	−·88	−1·797	+·036	+77·44	−3·168	+0·130
	50 Cas	+5·71	+·44	−1·687	+·146	+19·36	+6·424	+2·132
Means		+5·27		−1·833				

The columns of $100x^2$, $100xy$ and $100y^2$ have been summed for each month throughout the period under consideration. The results are summarized in Tables I, II and III respectively. Table IV shows the number of double azimuths n, on which each entry in Tables I, II and III depends. Each table consists of two sections, the first for the period 1922–1930 and the second for 1931–1938. The rows and columns in each section of every table have been summed and the results are shown.

TABLE I

Monthly values of $100x^2$

Year	Jan.	Feb.	Mar.	Apr.	May	June	July	Aug.	Sept.	Oct.	Nov.	Dec.	Yearly Sums
1922	...	326	53	116	806	218	...	...	66	335	136	146	2202
1923	92	...	40	7	...	...	...	129	...	214	95	...	577
1924	...	...	98	3	137	...	...	...	442	98	21	52	851
1925	200	49	...	157	276	...	...	3	176	616	434	130	2041
1926	114	10	359	43	11	7	...	...	205	363	0	354	1466
1927	...	114	104	206	25	...	...	52	9	389	215	306	1420
1928	2	395	98	221	350	...	...	221	79	456	222	62	2106
1929	28	...	254	58	1188	...	...	64	186	12	86	190	2066
1930	11	...	26	600	...	173	...	...	...	111	575	...	1496
Sums	447	894	1032	1411	2793	398	...	469	1163	2594	1784	1240	14225
1931	...	58	32	101	75	...	...	48	...	659	63	31	1067
1932	4	19	231	74	17	29	...	...	21	132	56	170	753
1933	...	...	1016	8	60	92	...	...	81	162	87	...	1506
1934	68	88	237	15	161	...	...	...	169	115	104	...	957
1935	8	...	215	4	308	3	...	2	91	935	50	113	1729
1936	15	118	276	223	182	...	...	13	7	20	19	...	873
1937	64	...	...	...	279	...	...	...	...	...	4	...	347
1938	...	...	73	19	...	...	...	...	...	...	...	...	92
Sums	159	283	2080	444	1082	124	...	63	369	2023	383	314	7324

Grand total of monthly values = 21549.

TABLE II

Monthly values of 100*xy*

Year	Jan.	Feb.	Mar.	Apr.	May	June	July	Aug.	Sept.	Oct.	Nov.	Dec.	Yearly Sums
1922	...	+2·3	+11·5	−3·5	−43·0	+15·4	...	...	−7·0	−16·3	−22·1	+3·2	−59·5
1923	−3·9	...	−5·9	−0·7	...	...	...	−11·3	...	+10·0	+5·3	...	−6·5
1924	...	...	−14·2	−3·1	−25·7	...	...	...	−29·6	−22·4	−10·5	+12·7	−92·8
1925	+4·0	+0·1	...	−8·4	+12·3	...	...	−2·2	−4·6	+57·5	+23·6	+5·2	+87·5
1926	+11·3	−0·5	−23·7	+3·8	+2·7	−1·4	...	...	−24·6	+29·9	+0·1	−4·2	−6·6
1927	...	+6·7	+16·2	−15·6	+15·1	...	...	+2·3	−2·5	−17·3	+50·3	−8·5	+46·7
1928	−0·5	+29·5	−3·6	+17·0	+38·2	...	...	+5·6	+3·4	−16·0	+22·9	+8·3	+104·8
1929	+1·0	...	+2·6	+8·4	−19·7	...	...	+4·3	+0·8	+5·3	−12·5	+2·6	−7·2
1930	+1·3	...	+1·4	−4·4	...	−22·8	...	...	...	+21·1	−19·9	...	−23·3
Sums	+13·2	+38·1	−15·7	−6·5	−20·1	−8·8	...	−1·3	−64·1	+51·8	+37·2	+19·3	+43·1
1931	...	+0·3	−1·1	−18·3	−3·3	...	...	−2·2	...	−45·5	−17·7	+2·5	−85·3
1932	−0·3	−2·4	−9·8	+11·6	−8·0	+9·1	...	...	+0·7	+5·5	+9·0	+10·1	+25·5
1933	...	...	+45·3	−1·1	−14·8	+12·7	...	...	+4·6	+10·8	+6·1	...	+63·6
1934	−7·7	+6·1	+17·4	−6·3	−36·4	...	...	...	−0·6	+5·0	+10·8	...	−11·7
1935	+5·3	...	+8·0	+2·4	+16·5	+3·2	...	−3·1	+13·8	+67·5	+4·4	+6·7	+124·7
1936	+3·3	+3·4	−2·9	−1·9	+1·1	...	...	−1·2	+1·9	+0·9	+11·7	...	+16·3
1937	−10·3	...	...	...	−25·7	...	...	...	...	...	+2·0	...	−34·0
1938	...	...	+4·9	+2·4	...	...	...	...	...	...	...	...	+7·3
Sums	−9·7	+7·4	+61·8	−11·2	−70·6	+25·0	...	−6·5	+20·4	+44·2	+26·3	+19·3	+106·4

Grand total of monthly values = +149·5.

TABLE III

Monthly values of $100y^2$

Year	Jan.	Feb.	Mar.	Apr.	May	June	July	Aug.	Sept.	Oct.	Nov.	Dec.	Yearly Sums
1922	...	5·0	2·7	2·3	28·1	2·0	...	...	0·8	27·5	11·1	1·2	80·7
1923	3·9	...	0·9	0·1	...	...	...	3·5	...	24·3	16·6	...	49·3
1924	...	...	9·7	3·1	11·0	...	...	...	2·7	5·1	5·2	5·7	42·5
1925	6·0	0·9	...	6·0	12·2	...	...	1·4	2·1	17·0	44·9	8·6	99·1
1926	4·1	0·1	12·5	0·3	4·4	4·2	...	...	5·2	11·0	0·0	2·5	44·3
1927	...	0·4	3·5	15·5	9·9	...	...	0·1	0·7	21·6	22·9	3·5	78·1
1928	0·2	4·4	2·0	11·5	26·1	...	...	0·3	1·3	34·5	16·2	1·9	98·4
1929	0·0	...	1·0	14·9	57·1	...	...	0·7	3·7	3·4	6·8	5·9	93·5
1930	0·2	...	1·3	27·3	...	24·0	...	...	...	22·2	30·4	...	105·4
Sums	14·4	10·8	33·6	81·0	148·8	30·2	...	6·0	16·5	166·6	154·1	29·3	691·3
1931	...	4·0	1·4	3·3	11·2	...	...	1·0	...	43·6	8·0	0·2	72·7
1932	0·0	0·9	2·1	18·7	3·7	3·6	...	...	1·3	2·0	1·4	8·8	42·5
1933	...	...	26·2	0·2	6·2	6·0	...	...	1·4	21·8	7·8	...	69·6
1934	1·4	1·3	3·3	3·6	25·7	...	...	...	1·2	7·2	8·6	...	52·3
1935	4·8	...	3·7	1·5	47·4	3·9	...	40·8	3·9	46·2	9·3	4·7	166·2
1936	0·8	3·8	1·8	15·6	24·0	...	...	0·1	0·5	19·4	8·0	...	74·0
1937	1·7	...	...	...	23·6	...	...	...	...	...	1·4	...	26·7
1938	...	...	2·2	3·6	...	...	...	...	...	...	...	...	5·8
Sums	8·7	10·0	40·7	46·5	141·8	13·5	...	41·9	8·3	140·2	44·5	13·7	509·8

Grand total of monthly values = 1201·1.

TABLE IV

Monthly values of n

Year	Jan.	Feb.	Mar.	Apr.	May	June	July	Aug.	Sept.	Oct.	Nov.	Dec.	Yearly Sums
1922	0	14	7	8	21	7	0	0	3	25	5	7	97
1923	6	0	2	2	0	0	0	4	0	10	11	0	35
1924	0	0	12	2	9	0	0	0	5	3	2	8	41
1925	10	4	0	4	9	0	0	2	7	24	29	9	98
1926	12	3	14	2	3	3	0	0	4	10	2	17	70
1927	0	2	7	12	6	0	0	2	4	17	14	11	75
1928	2	8	8	9	18	0	0	9	6	22	8	3	93
1929	2	0	19	10	35	0	0	3	11	3	6	14	103
1930	2	0	4	19	0	12	0	0	0	14	21	0	72
Sums	34	31	73	68	101	22	0	20	40	128	98	69	684
1931	0	6	5	3	9	0	0	3	0	26	3	2	57
1932	3	3	8	11	2	4	0	0	5	7	2	12	57
1933	0	0	40	2	4	6	0	0	9	19	4	0	84
1934	4	5	11	3	16	0	0	0	7	11	8	0	65
1935	3	0	11	2	30	2	0	3	10	34	7	5	107
1936	3	13	7	12	22	0	0	2	2	10	3	0	74
1937	2	0	0	0	17	0	0	0	0	0	3	0	22
1938	0	0	11	3	0	0	0	0	0	0	0	0	14
Sums	15	27	93	36	100	12	0	8	33	107	30	19	480

3. *Possible sources of error.*—In this section we examine the assumptions inherent in the double azimuth method and consider whether the approximations involved could have any significant effect on Δc. The following possible sources of error have been considered.

(a) *Pivot errors.*—The effect of errors in the shape of the Transit Circle pivots is to make the telescope trace out in the sky a curve which departs from a true great circle. The effect of a collimation error is to make the telescope describe a small circle instead of a great circle. It follows that the effect of pivot errors can be regarded as a collimation error which varies according to the direction in which the telescope is pointed. Before we can treat Δc as a constant quantity, it is therefore necessary to consider the magnitude of the pivot errors.

The last determination of pivot errors was made in 1924, after new bearings (Y's) had been installed. The Introduction to the 1924 volume of *Greenwich Astronomical Results* gave the results of the investigation in the form of x and y, the horizontal and vertical components respectively of the motion of the western end of the axis relative to the eastern. For the present investigation, smoothed values of x and y have been resolved into a displacement of the telescope in the plane containing its optical and mechanical axes, equivalent to a variable collimation error, and a component which is equivalent to a small rotation of the telescope about its optical axis, which can be ignored. The first component is plotted in Fig. 1, in which a smooth curve has been drawn through points at every 10° of N.P.D. (North Polar Distance). Positive displacements of the curve from the zero-line are equivalent to a positive collimation error.

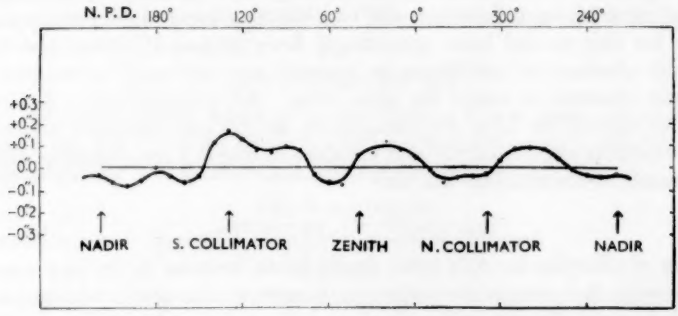

FIG. 1.—*Pivot errors of the Airy Transit Circle.*

From a study of this curve it was found that: (i) if pivot error corrections had been applied to the double azimuths used in the analysis for Δc, the value of Δc would have been increased by $+0''.11$; (ii) if pivot error corrections had been applied to the original observations for collimation error, the adopted collimations would have been decreased by $0''.06$; (iii) if pivot error corrections had been applied to all the original observations of collimation, level and times of transit of clock and azimuth stars, the clock errors derived with the Transit Circle would have been $0^s.018$ greater on average, so that the TC–B difference would have been increased by $0^s.018$.

Pivot error corrections have not been applied in the past to observations made with the Transit Circle, because of their small size and the difficulties

involved in their determination. They have not been applied to the results given in this paper for the same reasons, but the above corrections can easily be applied to results relating to periods after 1924 if desired.

(b) *Variation of azimuth in a period of twelve hours.*—It was assumed in Section 2 that the azimuth error, a, of the telescope was unchanged after a period of twelve hours. Suppose, however, that the true azimuth changes by Δa, i.e. $a_2 = a_1 + \Delta a$. The deduced azimuth is increased by $A_2 \Delta a/(A_2 - A_1)$. One would expect this correction to be sometimes positive and sometimes negative, since it depends both on the sign of Δa and on the order in which the transits were observed. The effect of ignoring the correction would then be to increase the scatter of the double azimuths without affecting Δc.

The assumption that Δa can be ignored is not necessarily correct. The great majority of double azimuths are obtained by observing the above-pole transit in the morning, usually at about 10^h U.T., and the below-pole transit in the evening, at about 22^h U.T. Below-pole transits are much less commonly observed in daylight because of the difficulty of seeing stars in daylight at low altitudes. Hence, if there is an appreciable systematic difference between a_{10}, the true azimuth error at about 10^h U.T., and a_{22}, the error at about 22^h U.T., the estimates of Δc obtained from double azimuths will be in error.

An estimate of the size of $(a_{10} - a_{22})$ can be obtained by comparing an azimuth (not a " double " azimuth) deduced from two stars observed at about 10^h U.T. with an azimuth from two stars observed at about 22^h U.T. on the same day, or the preceding day. Unfortunately, the difference due to Δa cannot, in general, be *easily* separated from that due to Δc, although it is theoretically possible. In the period 1916 to 1921, however, the two effects are easy to separate, and the azimuths for this period have accordingly been analysed. Azimuths in this period were obtained by combining an azimuth star within $3\frac{1}{2}^\circ$ of the pole with a clock star observed at about the same time. All azimuth errors deduced in this way are affected by Δc to the same extent, so that any difference between the deduced azimuths obtained at 10^h and 22^h must be due to a real change of azimuth.

The result of the analysis was that

$$(a_{10} - a_{22}) = -0''{\cdot}04 \pm 0''{\cdot}06.$$

The effect of allowing for this term would be to increase Δc by $+0''{\cdot}04$. For the purpose of the present investigation, it seemed reasonable to suppose that $(a_{10} - a_{22})$ does not differ significantly from zero and that the effect on estimates of Δc is not much greater than $0''{\cdot}04$. The data for the years 1916 to 1921 provide some evidence that the sign of $(a_{10} - a_{22})$ may reverse during the course of a year; if this is true, it may provide an explanation of the large annual term in Δc found in Section 5.

(c) *Neglect of short-period terms of nutation.*—The azimuth errors tabulated in the volumes of *Greenwich Astronomical Results* were calculated without including the short-period terms of nutation in the tabular places T_1 and T_2. Their omission introduces a small scatter into the deduced azimuths which is without any significant effect on Δc.

(d) *Personality.*—With the use of the impersonal micrometer, it is unlikely that the personality differences between different observers, and between observations made by the same observer above and below pole, are sufficiently large to have any appreciable effect on Δc. A following error, in which an observer sets

the wire on a moving image either slightly in front of or slightly behind the true centre, has no effect on double azimuths obtained by that observer. A bisection error, in which the observer sets to the right or left of the true image centre, irrespective of the direction of motion, would affect the determinations of azimuth. It is known that the *differences* of personality among observers are small with the impersonal micrometer, and it must be assumed that the *absolute* personalities are also small. Nevertheless, it was considered advisable to omit from the analysis all stars which transit south of the zenith at upper culmination. This was because there may be a discontinuity in observations at the zenith introduced by changing from the " feet North " position usually adopted in observing azimuth stars to the " feet South " position. For near-zenith stars the observer's position is not always recorded. In practice, those stars with factors f numerically greater than $-2{\cdot}000$ have not been used. A star with a factor of $-2{\cdot}000$ transits nearly 2° north of the zenith, and all the stars used in the analysis would be observed " feet North " in the great majority of cases.

4. *The mean value of Δc; comparison with clock errors.*—If we divide the grand total of Table II by the grand total of Table III, we obtain the mean value of Δc for the period 1922–1938. The result is

$$\Delta c = +0''{\cdot}124 \pm 0''{\cdot}083.$$

This value is of the right sign, but is hardly significant in view of the probable error.

Values of the clock error difference, TC–B, are available from 1927 July onwards. A comparison with Δc from double azimuths is therefore possible for the period 1927 July to 1938 April. The mean value of Δc for this period is (again from Tables II and III)

$$\Delta c = +0''{\cdot}240 \pm 0''{\cdot}096.$$

If the collimation errors adopted for the Transit Circle were increased by Δc seconds of arc, the TC clock errors would be reduced by $0{\cdot}25\Delta c$ seconds of time. Assuming that the TC–B difference is due entirely to Δc, we have

$$\text{TC–B} = +0{\cdot}25\Delta c.$$

This result has been quoted in many of the annual volumes.

The mean value of $\Delta c = +0''{\cdot}24$ means that the average value of TC–B over the period considered should have been about $+0^s{\cdot}060$. A direct comparison with the mean difference of clock errors would be misleading, since the value obtained for Δc is necessarily a *weighted* mean, depending more on observations in the winter months than on the relatively few double azimuth observations in the summer. However, the monthly means of the difference TC–B, which are given in Table V, can be weighted in the same way, by multiplying each monthly mean by the appropriate monthly value of $100y^2$ given in Table III and dividing the sum by $\Sigma 100y^2$. The numbers of determinations of clock error, with both instruments, and their accuracy, are such that the weight depends only on the doubled azimuths. The result is TC–B $= +0^s{\cdot}064$, equivalent to a collimation error $\Delta c = +0''{\cdot}26$.

The agreement between the values of Δc obtained from double azimuths and from the TC–B difference is therefore very good. If the observations are divided into two groups, 1927–1932 and 1933–1938, for example, it may be shown that the close agreement for the whole period is to some extent fortuitous, but

TABLE V

Differences of clock errors, TC–B

Year	Jan.	Feb.	Mar.	Apr.	May	June	July	Aug.	Sept.	Oct.	Nov.	Dec.
	s	s	s	s	s	s	s	s	s	s	s	s
1927	...	...	...	...	...	...	+0·040	+0·031	+0·058	+0·054	+0·114	+0·134
1928	+0·142	+0·100	+0·081	+0·142	+0·052	+0·093	+0·106	+0·067	+0·076	+0·096	+0·107	+0·098
1929	+0·105	+0·101	+0·080	+0·070	+0·003	+0·050	+0·018	+0·036	−0·009	+0·058	+0·066	+0·034
1930	+0·028	+0·007	+0·053	+0·035	+0·059	+0·040	+0·017	+0·001	+0·013	+0·027	+0·037	+0·053
1931	+0·064	+0·034	+0·035	+0·086	+0·041	+0·052	+0·038	+0·053	+0·039	+0·022	+0·066	+0·074
1932	+0·083	+0·081	+0·102	+0·091	+0·067	+0·061	+0·031	−0·011	+0·007	+0·046	+0·062	+0·057
1933	+0·075	+0·084	+0·112	+0·108	+0·088	+0·064	+0·044	+0·031	+0·075	+0·067	+0·069	+0·084
1934	+0·093	+0·040	+0·074	+0·083	+0·080	+0·052	+0·029	+0·024	+0·049	+0·067	+0·042	+0·032
1935	+0·042	+0·049	+0·082	+0·064	+0·076	+0·062	+0·065	+0·098	+0·080	+0·076	+0·104	+0·100
1936	+0·103	+0·114	+0·119	+0·094	+0·106	+0·062	+0·016	−0·023	−0·014	+0·024	+0·078	+0·090
1937	+0·054	+0·088	+0·079	+0·056	+0·008	+0·038	+0·036	−0·001	+0·000	+0·016	+0·061	+0·074
1938	+0·101	+0·113	+0·092	+0·066	...	...	...	...	...	...	...	...
Means	+0·081	+0·074	+0·083	+0·081	+0·058	+0·057	+0·040	+0·028	+0·034	+0·050	+0·073	+0·075

the agreement is still sufficiently good to confirm that the TC–B discrepancy is primarily due to a systematic error in collimation.

The yearly mean values of Δc, as deduced from double azimuths, are tabulated in Table VI. The corresponding weighted estimates of Δc from the clock error difference, TC–B, are also given. The probable errors in column 2 were deduced on the assumption that the probable error of a single determination of azimuth remained at its mean value of about $\pm 0''\cdot 29$ throughout the period considered; they are inversely proportional to $\sqrt{(\Sigma y^2)}$ for each year.

TABLE VI

Yearly means of Δc

Year	Δc from double azimuths	Δc from TC–B
	$''$	$''$
1927 (part)	$+0\cdot 50 \pm 0\cdot 41$	$+0\cdot 35$
1928	$+1\cdot 07 \pm 0\cdot 29$	$+0\cdot 36$
1929	$-0\cdot 08 \pm 0\cdot 30$	$+0\cdot 09$
1930	$-0\cdot 22 \pm 0\cdot 28$	$+0\cdot 14$
1931	$-1\cdot 17 \pm 0\cdot 34$	$+0\cdot 14$
1932	$+0\cdot 60 \pm 0\cdot 44$	$+0\cdot 30$
1933	$+0\cdot 91 \pm 0\cdot 35$	$+0\cdot 34$
1934	$-0\cdot 22 \pm 0\cdot 40$	$+0\cdot 28$
1935	$+0\cdot 75 \pm 0\cdot 22$	$+0\cdot 33$
1936	$+0\cdot 22 \pm 0\cdot 34$	$+0\cdot 31$
1937	$-1\cdot 27 \pm 0\cdot 56$	$+0\cdot 05$
1938 (part)	$+1\cdot 26 \pm 1\cdot 20$	$+0\cdot 30$

It will be seen that the values of Δc given in column 2 show variations from year to year which are much larger than the variations in column 3. In view of the probable errors, however, there is no significant disagreement between the results derived by the two methods. Moreover, the values of Δc in column 2 show a significant correlation coefficient of about $+0\cdot 83$ with the values in column 3.

The correlation between columns 2 and 3 would appear to imply that the variations from year to year are real; it is difficult to understand why the variations in column 2 should be so much larger than the variations in column 3.

5. *The annual term in* Δc.—In Tables II and III the columns have been summed to give totals of $100xy$ and $100y^2$ respectively for each month. These values have been analysed for an annual variation in the value of Δc. The data were divided into two groups, 1922 January–1930 December and 1931 January–1938 April. The inclusion of the data for the period 1922 January–1927 June, which cannot be compared with TC–B differences, appeared to be desirable in order to obtain as much information as possible. The two periods considered coincide with those covered by the *Second Greenwich Catalogue for 1925·0* and the *First Greenwich Catalogue for 1950·0* respectively.

The annual term in Δc was expressed as

$$\Delta c = u_0 + u_1 \cos\theta + v_1 \sin\theta + u_2 \cos 2\theta + v_2 \sin 2\theta,$$

where θ is an arbitrary phase angle equal to 30° in January, 60° in February, 90° in March and so on. A least-squares solution for the coefficients was carried out, taking account of weights. The results for the two periods were as follows:

1922 January–1930 December

$$\Delta c = -0''\cdot035 + 0''\cdot714 \cos\theta + 0''\cdot522 \sin\theta + 0''\cdot251 \cos 2\theta - 0''\cdot090 \sin 2\theta,$$

1931 January–1938 April

$$\Delta c = +0''\cdot389 + 0''\cdot532 \cos\theta + 0''\cdot150 \sin\theta - 0''\cdot214 \cos 2\theta + 0''\cdot275 \sin 2\theta.$$

A comparison of these two results suggests that there is a real variation in Δc with a period of twelve months, but the existence of a six-monthly term is doubtful. The analysis was therefore repeated, with the terms in 2θ omitted. The results were

$$1922\text{–}1930,\ \Delta c = +0''\cdot037 + 0''\cdot689 \cos\theta + 0''\cdot509 \sin\theta,$$

$$1931\text{–}1938,\ \Delta c = +0''\cdot266 + 0''\cdot579 \cos\theta + 0''\cdot133 \sin\theta.$$

A harmonic analysis of the clock error differences given in Table V yielded the series

$$1927\ \text{July–}1938\ \text{April},\ \Delta c = +0''\cdot245 + 0''\cdot049 \cos\theta + 0''\cdot089 \sin\theta.$$

This result does not confirm the existence of an annual term of the amplitude suggested by the double azimuth method.

6. *Other methods of estimating* Δc.—In view of the uncertainty in the determination of Δc it is of interest to consider other methods of obtaining an estimate of its value. Two more methods which have been investigated are discussed below.

(a) *From the R–D discordance in R.A.*—Regular observations of stars by light reflected in a mercury pool were made with the Transit Circle for many years. Observations in both coordinates, R.A. and Declination, were taken until about 1909, when the measurements in R.A. appear to have been discontinued. The results obtained by reflected light, R, showed systematic differences from those made by direct light, D. The R–D discordance in R.A. can be explained as the effect of a systematic error in the adopted level error, since the effect of a level error changes sign at the horizon, whereas the effects of collimation and azimuth errors do not.

An error Δc in the collimation will not give rise to an R–D discordance directly, but, since the line of collimation is used in deducing the level error from nadir readings, it is clear that the R–D difference can be equally well explained in terms of a collimation error or a level error. Since there is no apparent reason why the nadir readings for level error should be systematically wrong, it is reasonable to suppose that the collimation error, Δc, is responsible for the R–D discordance.

In the annual volumes of *Greenwich Astronomical Results* the value of the systematic error, Δb, in level error which could account for the R–D discordance has been tabulated for each star observed by both methods; weighted yearly means for stars transiting north and south of the zenith have been formed. Table VII, giving the values of Δc for the five years 1900–1904, is based on the assumption that $\Delta c = \Delta b$.

The north stars give a mean value of $\Delta c = +0''\cdot376$ for the five years and the south stars give $\Delta c = +0''\cdot397$. The combined mean is $\Delta c = +0''\cdot390$. An analysis of the north stars, which are all azimuth stars, for an annual term gave

$$\Delta c = +0''\cdot438 + 0''\cdot111 \cos\theta + 0''\cdot132 \sin\theta.$$

TABLE VII

Yearly means of Δc from R–D discordance

Year	North stars		South stars	
	Δc	Weight	Δc	Weight
	″		″	
1900	+0·45	103	+0·25	158
1901	+0·44	92	+0·45	224
1902	+0·39	49	+0·47	125
1903	+0·29	73	+0·50	131
1904	+0·20	46	+0·28	96

The observations could only be grouped into hours of R.A. so that it was necessary to assume, in deriving this series, that certain hours of R.A. would always be observed in certain months, e.g. $1^h\ 0^m$ to $2^h\ 59^m$ in November, $3^h\ 0^m$ to $4^h\ 59^m$ in December and so on. This assumption is not entirely satisfactory, since the observations of a particular star are likely to be spread over several months. The coefficients of $\cos\theta$ and $\sin\theta$ in the above expression are probably too small for this reason.

(b) *From an analysis of Greenwich corrections to the FK3.*—The mean effect of Δc on the determined places of clock stars is very small. Nevertheless, there is a differential effect varying with declination. This effect allows us to estimate Δc, provided we can compare the places derived with the Transit Circle with a system of star places which is free from error. Assuming the right ascensions of of the FK3 catalogue to be correct, and the Greenwich observations to be in error only as a result of collimation error, we obtain

$$\text{FK3 place} = \text{TC place} + \Delta c(\gamma - \bar{\gamma}).$$

γ is a factor defined by

$$\gamma = C + B + 3{\cdot}1A$$

and $\bar{\gamma}$ is the mean value of γ for all clock stars. The coefficient 3·1 is the average value of $(1{\cdot}256 + 1{\cdot}606 \operatorname{cosec}\delta)$ for all stars used in deriving the azimuth error.

The above equation allows us to calculate Δc from the tabulated differences of (TC − FK3). The TC places are based on observations made with the Transit Circle in the years 1922–1940. A least-squares solution for Δc yields a mean value of $+0''{\cdot}449$; when the $\cos\theta$ and $\sin\theta$ terms are included, the series for Δc becomes

$$\Delta c = +0''{\cdot}446 - 0''{\cdot}031\cos\theta - 0''{\cdot}000\sin\theta.$$

It was again necessary to identify hours of R.A. with the months in which they were most likely to be observed.

7. *Summary and discussion.*—Four different methods have been used to obtain estimates of Δc. The mean values obtained, and the periods to which they refer, are summarized in Table VIII.

The values of the coefficients u_0, u_1 and v_1 derived by the various methods are shown in Table IX. It must be noted that the coefficients u_1 and v_1 given in Table IX for the R–D and Greenwich corrections methods are probably smaller (numerically) than their true values.

TABLE VIII

Mean values of Δc; summary

Method	Period	Δc
		″
Double azimuths	1922–1938	+0·124
Double azimuths	1927–1938	+0·240
TC–B (weighted)	1927–1938	+0·256
R–D	1900–1904	+0·390
Greenwich corrections	1922–1940	+0·449

It is suggested that two main conclusions can be drawn from a study of Tables VIII and IX:

(i) there is an appreciable systematic error, Δc, in the collimation errors which have been adopted for use with the Airy Transit Circle; Δc is probably between $+0''{\cdot}2$ and $+0''{\cdot}5$, although there have probably been real changes in its value in the present century;

(ii) there is probably a real annual variation in Δc. The coefficients u_1 and v_1 are probably positive, but not so large as suggested by the double azimuth method alone.

TABLE IX

Values of the coefficients u_0, u_1, v_1

Method	Period	u_0	u_1	v_1
		″	″	″
Double azimuths	1922–1930	+0·037	+0·689	+0·509
Double azimuths	1931–1938	+0·266	+0·579	+0·133
TC–B	1927–1938	+0·245	+0·049	+0·089
R–D	1900–1904	+0·438	+0·111	+0·132
Greenwich corrections	1922–1940	+0·446	−0·031	−0·000

The advantage of the double azimuth method, considered in detail in this paper, is that it proves that it is the adopted collimation errors which are at fault. The analysis depends only on observations of times of transit of stars, of collimation and level errors and on the adoption of a clock rate. It is most unlikely that times of transit or adopted clock rates are systematically wrong. It was shown in Section 2 that an error in the adopted level error affects all determinations of azimuth equally, and has no effect on the determination of Δc. Thus, by a process of elimination, we are left with only the collimation error to account for the value of Δc.

The three other methods of estimating Δc provide valuable confirmation of its value, but are not in themselves " fundamental ". The value derived from TC–B clock differences rests on two assumptions, firstly that the tabular places of stars used with the Transit Circle are free from error and secondly that the determinations of clock error with Small Transit " B " are perfect. The R–D discordance gives a determination of $(\Delta c + \Delta b)$, where Δb is a possible systematic error in the nadir readings. We can only equate the value of $(\Delta c + \Delta b)$ with Δc on the reasonable assumption that Δb is insignificant. The analysis of Greenwich

corrections rests on the assumption that the FK3 places of clock stars are entirely free from any error in R.A. which varies with declination. It is to be noted that each estimate of Δc obtained in this paper might be altered if it were possible to allow for the effects of pivot errors.

No satisfactory reason for the existence of a systematic error in the measured collimation can be suggested. The routine of observation for collimation error in the period under review was as follows.

The north collimator was first set on the south collimator, the observation being made through openings in the cube of the Transit Circle. The Transit Circle was then set in turn on the south and north collimators; the mean of the readings obtained was the deduced line of collimation. The setting of the north collimator on the south collimator was then repeated; any discrepancy between the original and final setting was attributed to " motion of the collimators " and an appropriate correction, usually small compared with the scatter of the readings, was applied. The Transit Circle, as designed by Airy and constructed, did not have a pierced cube. To set the north collimator on the south collimator the instrument had to be lifted out of its bearings. After it had been in use for some time, Airy decided to have the cube pierced, so that the setting could be made without raising the instrument, by viewing through the cube with the telescope in a vertical position. The design of the cube, with stiffening webs, was such that it was not possible to cut a circular hole in the cube. It has a number of small apertures, which produce diffraction effects, so that the definition of the south collimator wires, when viewed from the north collimator through the pierced cube, is always extremely poor.

Once a week, on Mondays, the telescope was raised out of its bearings so that an uninterrupted view of the south collimator could be obtained with the north collimator. It was found that the setting of the north collimator with the telescope raised differed systematically from the setting obtained when the south collimator was viewed through the cube. A correction to the deduced line of collimation was therefore always applied, on the assumption that the setting obtained with the telescope raised was the correct one. The values of this so-called " Up minus Down " correction applied from 1900 to 1938 are summarized in Table X. The corrections to the setting of the north collimator wire have been converted to corrections to the deduced collimation errors.

TABLE X

" Up minus Down " correction

Period	Correction to deduced collimation error
	″
1897–1905	+0·41
1906–1914	+0·27
1915–1921	+0·28
1922–1930	+0·31
1931–1940	+0·23

It will be seen that the " Up minus Down " correction is of approximately the same magnitude as Δc; if the correction had not been applied, the adopted collimation errors would have been smaller and the value of Δc approximately doubled.

The illumination used in the measurement of line of collimation was diffused daylight reflected into the collimators. In the absence of artificial illumination, collimation error could not be measured at night when the star observations would normally be obtained. In practice, collimation error was determined about once a day, usually in the morning. The mean of the observations for several days or weeks was taken and was used in reducing all observations in that period. The existence of a diurnal variation of collimation could introduce a systematic error into observations of stars made at night, since the adopted collimation error would differ from the true collimation error at the time of observation. However, when artificial illumination of the collimators was adopted in 1944, it was found that any diurnal term was very small and could certainly not account for a value of Δc of the order of a third of a second.

The collimation error is the difference between the observed line of collimation and the line to which times of transits of stars are referred. It seems most unlikely that the determinations of the latter could be in error by the equivalent of a third of a second of arc.

The star observations are corrected for the effect of diurnal aberration by subtracting $0''{\cdot}19$ from the collimation error.

No significant correlation could be found between monthly values of Δc and monthly means of the measured line of collimation. If any annual term in Δc exists, it is of the opposite sign to the annual term in the measured collimation error itself, and the true collimation error is probably more nearly constant than the measured collimation error. This conclusion has also been suggested in *Greenwich Astronomical Results* for 1927 and 1928, in discussions of the TC–B differences.

The most probable source of error appears to lie in the determination of the setting of the north collimator. The poor definition of the image of the south wire system and the existence of an appreciable " Up minus Down " correction, referred to above, are unsatisfactory features in the determination of collimation error, although it is difficult to see how either could introduce a systematic error.

It is probable that the collimation errors of a reversible transit circle can be freed from systematic error more easily than can the collimation errors of a non-reversible instrument; it is a matter of regret that the Airy Transit Circle cannot be reversed in its bearings.

Royal Observatory,
Greenwich :
1954 *March* 4.

SECOND-ORDER TERMS IN THE FIGURE OF SATURN

Sir Harold Jeffreys, F.R.S.

(Received 1954 April 6)

Summary

The theory of the secular perturbations of Saturn's satellites requires several corrections of the order of the square of the ellipticity, and the result is a substantial increase of the estimate of the parameter l. The data agree fairly well with the model S_2 of Miles and Ramsey. The ratio of the masses of the Sun and Saturn is $3494{\cdot}8 \pm 1{\cdot}1$, but the uncertainty may need to be increased to $2{\cdot}0$ to allow for that of the micrometer screw.

---

1. In my study of the masses of Saturn's satellites and the figure of Saturn* I adopted from H. and G. Struve the expressions for the motions of the apses and nodes to the first order in the constants k and l. Professor D. Brouwer has called my attention to the fact that terms in k^2 have effects larger than the standard errors of some of the observed values. Further, though for the first-order terms the predicted motions of the apses and nodes are equal and opposite, this is not true of the second-order terms.

Brouwer† took the potential due to Saturn in the form

$$U = \frac{\mu}{r}\left\{1 + \frac{k_2}{r^2}(1 - 3\sin^2\beta) + \frac{k_4}{r^4}(1 - 10\sin^2\beta + \tfrac{35}{3}\sin^4\beta)\right\} \tag{1}$$

and derived the expressions

$$\frac{d\varpi}{dt} = n\left(\frac{3k_2}{a^2} - \frac{9}{2}\frac{k_2^2}{a^4} + 10\frac{k_4}{a^4}\right), \tag{2}$$

$$\frac{d\theta}{dt} = -n\left(\frac{3k_2}{a^2} - \frac{27}{2}\frac{k_2^2}{a^4} + 10\frac{k_4}{a^4}\right), \tag{3}$$

where n is the mean motion of the satellite and a is its mean distance; they are connected by

$$n^2a^3 = \mu(1 + 3k_2/a^2). \tag{4}$$

In comparison with the notation of the Struves

$$k_2 = \tfrac{1}{3}k \;;\; k_4 = \tfrac{1}{4}l. \tag{5}$$

Then

$$\frac{d\varpi}{dt} = n\left(\frac{k}{a^2} - \frac{1}{2}\frac{k^2}{a^4} + \frac{5}{2}\frac{l}{a^4}\right), \tag{6}$$

$$\frac{d\theta}{dt} = -n\left(\frac{k}{a^2} - \frac{3}{2}\frac{k^2}{a^4} + \frac{5}{2}\frac{l}{a^4}\right). \tag{7}$$

If it was not for the term in k_2 in (4), the coefficients of k in these formulae would be proportional to $n^{-7/3}$. Those given by the Struves did not satisfy this condition accurately, and I was unable to find out whether they had made

*H. Jeffreys, *M.N.*, **113**, 81–105, 1953.
†D. Brouwer, *A.J.*, **51**, 223–231, 1945.

a correction for k in estimating a, or whether they had used observed values of a. Direct examination of the individual values of a determined by G. Struve* from observation in Hefte 2 and 3 showed systematic differences from his adopted values, and the only safe method was to redetermine the values of a. The k term in (4), if not allowed for, would introduce other errors of order k^2 in the calculated values.

The observed mean distances showed discrepancies definitely larger than the apparent uncertainties would account for, and I took simple means. The results were as in Table I, in seconds of arc.

TABLE I

		D.f.	Adjusted
	″		″
Mimas	26·848 ± 0·011	10	26·843
Enceladus	34·441 ± 0·018	7	34·438
Tethys	42·642 ± 0·013	9	42·633
Dione	54·608 ± 0·014	13	54·602
Rhea	76·260 ± 0·013	16	76·255
Titan	176·716 ± 0·064	3	176·763
Iapetus	515·046 ± 0·086	5	515·125

The Sun reduces the mean motion of Iapetus by $2{\cdot}46 \times 10^{-4}$ deg./1^d, and this must be added to the actual mean motion to give that due to Saturn alone. For other satellites this correction is negligible. Precession is smaller still. Then these data, substituted in (4), give a set of equations for μ and k. On inspection it was clear that they could add nothing of importance to the determination of k, and I took $k/a_0^2 = 0{\cdot}0243$, with $a_0 = 8''{\cdot}75$, and estimated μ.

$$\mu = (28149 \pm 9)10^5(1^\circ/1^d)^2(1'')^3.$$

χ^2 was 2·6 on 6 degrees of freedom. The adjusted values of a are given in Table I.

With these values I recomputed the coefficients of k/a_0^2 and l/a_0^4 in the motions of the apses and nodes. These were as follows :

	Mimas	Enceladus	Tethys	Dione	Rhea	Titan
k/a_0^2	$1{\cdot}48260 \times 10^4$	$6{\cdot}1955 \times 10^3$	$2{\cdot}9342 \times 10^3$	$1{\cdot}2338 \times 10^3$	$3{\cdot}8328 \times 10^2$	$2{\cdot}0207 \times 10$
l/a_0^4	$3{\cdot}939 \times 10^3$	$1{\cdot}0060 \times 10^3$	$3{\cdot}090 \times 10^2$	$7{\cdot}921 \times 10$	12·62	0·1238

The coefficient of k^2/a_0^4 is $-0{\cdot}2$ or $-0{\cdot}6$ of that of l/a_0^4, according as it refers to the apse or the node.

The largest effect of the terms in k^2 is $+1^\circ{\cdot}40/1^y$ for the node of Mimas. I revised the previous solution, taking into account the additional equations on p. 95 for the mass of Titan, and found :

$$\mu_0' = +0{\cdot}13 \pm 1{\cdot}5\,;\ \mu_1' = +1{\cdot}08 \pm 0{\cdot}21\,;\ \mu_2 = +1{\cdot}3 \pm 1{\cdot}5\,;\ \mu_3 = -3{\cdot}54 \pm 0{\cdot}73;$$

$$\frac{k}{a_0^2} = 10^{-2}(2{\cdot}4303 \pm 0{\cdot}0038);\quad \frac{l}{a_0^4} = 10^{-4}(14{\cdot}56 \pm 1{\cdot}47);$$

$$l/k^2 = 2{\cdot}47 \pm 0{\cdot}25\,;$$

$$m_{\mathrm{Rh}} = (3{\cdot}2 \pm 3{\cdot}8)10^{-6};\ m_{\mathrm{Ti}} = (2{\cdot}4115 \pm 0{\cdot}0182)10^{-4};$$

$$1/m_{\mathrm{Ti}} = 4147 \pm 32.$$

$\chi^2 = 9{\cdot}6$ on 7 degrees of freedom.

* G. Struve, *Veröff. Berlin-Babelsberg*, **6**, Hefte 1–5, 1933.

The observed and computed secular motions are as in Table II.

TABLE II

		Calc.	Obs.	O–C
Mimas	apse	365·86	365·60	−0·26 ±0·20
	node	364·93	365·23	+0·30 ±0·20
Enceladus	apse	152·51		
Tethys	node	72·231	72·227	−0·004 ±0·065
Dione	apse	30·72	30·75	+0·03 ±0·42
Rhea	node	10·05	10·20	+0·15 ±0·08
Titan	apse	0·4994	0·5012	+0·0018±0·0070
	node	0·4994	0·492	−0·0074±0·029

0·0008 has been included for Titan to allow for the effect of Iapetus.

2. *The mass of Saturn.*—The above value of μ for Saturn, compared with the value of n^2a^3 for Saturn's orbit, gives a ratio $(2{\cdot}8650 \pm 0{\cdot}0009)10^{-4}$. This needs two corrections. Hill* gives the effect of Jupiter on Saturn's mean distance, for given mean motion, as

$$\delta \log_{10} a' = 0{\cdot}00018522.$$

Other planets raise this to 0·00018538. This must be eliminated by multiplying μ for (Sun + Saturn) by 1·001284 ; then we have for the mass-ratio

$$\text{Sun/Saturn} = 3494{\cdot}04 \pm 1{\cdot}11.$$

This agrees with H. Struve's value 3495·4. Hill† found $3502{\cdot}20 \pm 0{\cdot}53$ from observations of Jupiter, but remarked that the satellites gave a smaller value and therefore continued to use Bessel's 3501·6. Iapetus provides the chief equation in the estimate of μ for Saturn, so that the mass of Titan has effectively been added to that of Saturn. For this reason the above ratio should be increased by about 0·8. Systematic error in the measurements of satellite distances is possible. Newcomb stated that the calibration of a micrometer screw could not be trusted within 1 part in 6000; this alone might give an additional uncertainty of 1·7 in the mass-ratio, which may therefore be taken as $3494{\cdot}8 \pm 2{\cdot}0$. H. G. Hertz‡ has recently given $3497{\cdot}64 \pm 0{\cdot}27$ from perturbations of Jupiter; only an abstract is yet available but it appears that there is now little disagreement between results from Jupiter and the satellites.

3. *Structure of Saturn.*—In attempting to compare with the models given by Miles and Ramsey§ I found an inconsistency. I had taken $m = 0{\cdot}1353$. Their data correspond to $m = 0{\cdot}162$, with an uncertainty of about 3 per cent. This was traced to H. Struve's original solution, which took the period of rotation as 10^h14^m; I had taken 10^h38^m. These are observed periods for two spots in different latitudes, and the difference would affect m by 10 per cent. Struve took the equatorial angular diameter at mean distance as $17''{\cdot}50$, whereas Ramsey followed Russell, Dugan and Stewart, who gave $17''{\cdot}25$. Further, the definition of m is different, since Struve did not allow for the factor $1-e$. For the last reason alone Struve's ellipticity $\frac{1}{9{\cdot}5}$ derived from the perturbations of the satellites should never have been trusted within 10 per cent. But the formula

* G. W. Hill, *Astr. Papers for the American Ephemeris*, **4**, 20, 1890.
† G. W. Hill, *Astr. Papers for the American Ephemeris*, **7**, 17, 1895.
‡ H. G. Hertz, *A.J.*, **58**, 42, 1953.
§ B. Miles and W. H. Ramsey, *M.N.*, **112**, 234–243, 1952.

(16) on p. 241 of Miles and Ramsey's paper depends on de Sitter's definition of m and is inconsistent with the adoption of Struve's ellipticity as a datum.

Having regard to the uncertainties I now take

$$m = 0{\cdot}147 \pm 0{\cdot}006.$$

If a_0 is the equatorial radius,

$$Ja_0^2 = k;\ Da_0^4 = \tfrac{35}{12}\, l.$$

The present determinations of k/a_0^2 and l/a_0^4 refer to $a_0 = 8''{\cdot}75$, whence, with $a_0 = 8''{\cdot}625$,

$$J = 0{\cdot}0250,\ D = 0{\cdot}00449 \pm 0{\cdot}00045.$$

We have also

$$J = e - \tfrac{1}{2}\, m + e(-\tfrac{1}{2}\, e + \tfrac{1}{7}\, m),\ D = \tfrac{7}{2}\, e^2 - \tfrac{5}{2}\, m\, e + 4\kappa,$$

whence $e = 0{\cdot}101 \pm 0{\cdot}003$, $\kappa = 0{\cdot}00149 \pm 0{\cdot}00025$.

Since e and m are fairly well determined, the most convenient way of comparing with the models seems to be to use Miles and Ramsey's equation (16) to determine η_s, which depends very directly on the model. This gives

$$\eta_s = 1{\cdot}657 \pm 0{\cdot}042.$$

Their model S_2 gives $\eta_s = 1{\cdot}67$, so that the value of J corresponds to a body at least as strongly condensed to the centre as S_2 (17 per cent of the mass in the central particle). They preferred S_3 ($\eta_s = 1{\cdot}34$); for convenience of computation I used S_4 ($\eta_s = 1{\cdot}04$), but it is clear that S_2 is better than either.

I computed κ for S_2 and S_3; the surface values were 0·00185 for S_2, 0·00134 for S_3. This favours S_3 slightly, but the evidence from η_s is stronger. η_s could be used to give an estimate of the central condensation and hence of κ; but since a large part of the uncertainty of the relation between l and κ comes from that of m, little would be gained by using the calculated value of κ to re-estimate l.

All the models used by Miles and Ramsey, except J_4 and S_4, have a massive particle at the centre. It is worth while to notice that for such models direct study of Clairaut's equation makes e behave like r^3 for r small, so that $\eta \to 3$. But the Radau approximation would make $\eta \to 2{\cdot}5$.

160 *Huntingdon Road,*
Cambridge:
1954 *April* 5.

THE INFLUENCE OF STELLAR RADIATION ON THE RATE OF ACCRETION

L. Mestel

(Received 1954 March 31)

Summary

Bondi's discussion of spherically symmetric accretion (**1**) is extended to take account of the heating of the cloud by ultra-violet radiation from the star. It is shown that if the accretion rate is to be high, the radius of the H II zone must not be more than about one thousand stellar radii. The absorbing power of a cloud is enormously increased by the high densities near the star, so that a cloud of moderately high density at infinity is able to keep the H II zone small enough for rapid accretion to take place. For a star of given type, there is a lower limit to the cloud density that will keep the H II zone small; when a star, accreting from a cloud of given density, reaches a critical mass, the H II zone increases rapidly to Strömgren's value, and accretion effectively ceases. The conditions under which the state of rapid accretion can be set up are investigated: it is shown, for example, that this state can be reached with the cloud of density 10^3 particles/cm^3 and temperature 100 deg. K, provided the star entering the cloud is of mass less than $1{\cdot}75\,\odot$.

1. *Introduction.*—The first discussions of accretion treated the problem purely dynamically, it being assumed that radiation losses would keep the thermal energy low enough for pressure to be negligible. The rate of accretion was found to be limited by the velocity V of the star through the undisturbed cloud (**2**):

$$\frac{dM}{dt} = 2\pi\alpha\,(GM)^2\,V^{-3}\rho_\infty, \tag{1}$$

where M is the mass of the star, t the time, ρ_∞ the density of the cloud at infinity, G the gravitational constant and α a constant of order unity.

More recently Bondi (**1**) has discussed the limiting case of spherically symmetric accretion, in which a star is considered at rest in an infinite cloud. In this case the rate of accretion is controlled by the thermal energy of the gas:

$$\frac{dM}{dt} = 4\pi\lambda\,(GM)^2\,c_\infty^{-3}\,\rho_\infty, \tag{2}$$

where c_∞ is the velocity of sound at infinity and λ a constant. The maximum value of λ (λ_c) depends on the amount of heating by compression suffered by the gas as it flows in. If the gas contains powerful radiators, or if γ, the ratio of the specific heats at constant pressure and constant volume, is near unity, the flow will be nearly isothermal, and $\lambda_c = 1{\cdot}12$. In adiabatic flow of a gas with the greatest possible value of γ ($\frac{5}{3}$), $\lambda_c = 0{\cdot}25$.

By comparing (1) and (2), Bondi was led to conjecture for the intermediate case, when c_∞ and V are of comparable magnitude, an accretion rate of order

$$\frac{dM}{dt} \simeq 2\pi\,(GM)^2\,(V^2 + c_\infty^2)^{-3/2}\,\rho_\infty. \tag{3}$$

This has been confirmed by Dodd (**3**) for the case of supersonic isothermal flow.

McCrea (**4**) has applied (1), (2) and (3) to a specific cosmogonical problem: the origin of O and B type stars. The lifetime of these stars as determined by their rate of hydrogen consumption is much shorter than the galactic lifetime, so they must be the result either of late condensation or of growth by accretion of stars of moderate mass born earlier. If the explanation by accretion is correct, McCrea points out that the mechanism cannot be purely dynamical, as summarized by (1). In order that accretion should be of importance, V cannot be much greater than 1 km/sec; with larger velocities, the increase of stellar mass from (1) would not affect the star's evolution unless the gas clouds were much denser or much more extensive than those observed. But the velocity of sound in ordinary neutral interstellar clouds $\simeq$ 1 km/sec (corresponding to a temperature $\simeq$ 100 deg. K (**5**)), so that the accretion rate must be governed by formulae (2) and (3). McCrea shows further that a star entering a cool dense cloud of reasonable extent (density $\simeq 10^3$ particles/cm^3, temperature $\simeq$ 100 deg. K, radius $\simeq$ 10 parsecs) with a velocity of about 1 km/sec will be reduced effectively to rest by the retarding force of the gas before it has penetrated through the cloud, so that ultimately the accretion process will be spherically symmetric. This result removes the necessity for clouds of great dimensions. Finally, McCrea remarks that the small number of stars with velocities as low as 1 km/sec is not necessarily a disadvantage to the theory, as the proportion of O and B type stars is in any case very small.

Since this work, the case of spherically symmetric accretion can no longer be regarded as a mathematical problem of little astronomical interest, but may itself turn out to be the most important accretion mechanism. It therefore deserves closer study.

Bondi's results show that as long as the variations in temperature in the gas cloud are due solely to compression of the inflowing gas, the effect on the accretion rate is not larger than a factor of about 4. However, since the work of Strömgren (**6**), it is known that a bright star is surrounded by a zone of almost completely ionized hydrogen (an "H II zone") at a temperature nearly the same as that of the star's surface, and it has been asserted (**7**) that this heating of the gas near the star will inevitably cut down the accretion rate to a negligible value. This possibility is examined quantitatively in the present paper. In Section 2 the maximum accretion rate is found as a function of the radius $\bar{r}$ of the H II zone. The ionization of hydrogen ceases once the bulk of the ultra-violet light (of frequency greater than the threshold frequency for hydrogen ionization) has been absorbed. Thus the value of $\bar{r}$ depends on the properties of the star (principally its surface temperature) and on the densities in the cloud. In Section 3 the absorption of ultra-violet light is analysed, and in Section 4 the relation is found between the maximum rate of accretion by a star of given temperature and the density at infinity of the cloud in which it is embedded.

2. *The variation of the accretion rate with the radius of the H II zone*

2.1. *The equations of flow.*—The problem is idealized as follows: a star of mass M and radius R is at rest in an infinite spherically symmetric cloud, consisting mainly of hydrogen, which is at rest at infinity. A sphere of radius $\bar{r}$ (zone II) is almost completely ionized, and is at a constant temperature of 10^4 deg. K, while the rest of the cloud (zone I) is un-ionized and at 10^2 deg. K. Once again c_∞ and ρ_∞ represent the velocity of sound and density at infinity, while p, ρ, v, all functions

of the radial coordinate r only, are the pressure, density and inward velocity. A steady state is assumed to have been reached. Further discussion and justification of these assumptions is postponed until later.

The treatment follows closely that in Bondi's paper (1). The equation of continuity for steady spherically symmetric flow is

$$A = 4\pi r^2 \rho v, \tag{4}$$

where the constant A is just the accretion rate.

For each zone the equation of motion integrates to give Bernoulli's equation

$$\tfrac{1}{2}v^2 + \int \frac{dp}{\rho} - \frac{GM}{r} = \text{constant}. \tag{5}$$

As each zone is isothermal, we have

$$\left.\begin{aligned} p &= K_1 \rho, \\ p &= K_2 \rho, \end{aligned}\right\} \tag{6}$$

in zones I and II respectively, where $K_1 = 10^2 \mathscr{R}$, $K_2 = 2 \times 10^4 \mathscr{R}$ and $\mathscr{R}$ is the gas constant. The factor 2 in K_2 arises from the contribution to p from the free electrons in zone II. The velocity of sound is constant in each zone because of the assumed constancy of temperature, and equals $\sqrt{K_1}$ in zone I and $\sqrt{K_2}$ in zone II.

For zone I, (5) reduces to

$$\tfrac{1}{2}v^2 + K_1 \ln \frac{\rho}{\rho_\infty} - \frac{GM}{r} = 0 \tag{7}$$

on using the condition of zero velocity at infinity. In zone II we have

$$\tfrac{1}{2}v^2 + K_2 \ln \rho - \frac{GM}{r} = \tfrac{1}{2}\bar{v}_2^2 + K_2 \ln \bar{\rho}_2 - \frac{GM}{\bar{r}}, \tag{8}$$

where bars refer to conditions at the interface and suffixes to zones I and II respectively.

At the interface the conditions of fit are

$$\bar{\rho}_1 \bar{v}_1 = \bar{\rho}_2 \bar{v}_2 \tag{9}$$

and

$$\bar{p}_1 + \bar{\rho}_1 \bar{v}_1^2 = \bar{p}_2 + \bar{\rho}_2 \bar{v}_2^2. \tag{10}$$

Equation (9) expresses the conservation of mass and (10) equates the change of momentum per second across one square centimetre of the interface to the difference of the pressures acting.

The following transformations are made:

$$r = \left(\frac{GM}{c_\infty^2}\right) x, \quad v = \left(c_\infty \frac{K_i}{K_1}\right) y, \quad \rho = \left(\frac{K_1}{K_i}\rho_\infty\right) z, \tag{11}$$

where the suffix i takes the values 1, 2 in zones I and II respectively. Then (4) reduces to

$$x^2 y z = \lambda, \tag{12}$$

where

$$A = 4\pi\lambda (GM)^2 c_\infty^{-3} \rho_\infty, \tag{13}$$

identical with Bondi's equation (2). Equations (7) and (8) become

$$\tfrac{1}{2}y^2 + \ln z - \frac{1}{x} = 0, \tag{14}$$

$$\tfrac{1}{2}y^2 + \frac{K_1}{K_2}\ln z - \frac{1}{x}\left(\frac{K_1}{K_2}\right)^2 = \tfrac{1}{2}\bar{y}_2^2 + \frac{K_1}{K_2}\ln \bar{z}_2 - \frac{1}{\bar{x}}\left(\frac{K_1}{K_2}\right)^2. \tag{15}$$

The interface conditions (9) and (10) reduce to

$$\bar{y}_1\bar{z}_1=\bar{y}_2\bar{z}_2, \tag{16}$$

$$\bar{z}_1(1+\bar{y}_1^2)=\bar{z}_2\left(1+\frac{K_2}{K_1}\bar{y}_2^2\right), \tag{17}$$

which combine to give

$$\frac{1+\bar{y}_1^2}{\bar{y}_1}=\frac{1+\bar{y}_2^2(K_2/K_1)}{\bar{y}_2}=2\eta, \tag{18}$$

say.

2.2. *Conditions at the interface.*—In order that $\bar{y}_1$ and $\bar{y}_2$ should exist to satisfy (18) for given η, the condition $\eta^2\geqslant K_2/K_1\,(>1)$ must hold. When this is satisfied, it appears that there should exist two possible values of $\bar{y}_1$ for given $\bar{y}_2$, and similarly two values of $\bar{y}_2$ for given $\bar{y}_1$. However, the choice is in fact restricted to values giving either subsonic or supersonic flow on both sides of the interface.* In the narrow zone in which the temperature rises steeply from 10^2 deg. K to 10^4 deg. K the velocity of sound increases monotonically. The condition (10) holds over this region (neglecting the small variation of gravity) so that

$$p+\rho v^2=\rho\,(c^2+v^2)=\text{const.} \tag{19}$$

Combined with the equation of mass conservation

$$\rho v=\text{const.}, \tag{20}$$

this gives

$$c\left(\frac{c}{v}+\frac{v}{c}\right)=\text{const.} \tag{21}$$

where c is the velocity of sound. Thus from the graph of v/c against c it is seen that in a region of monotonically increasing c the velocity must be either subsonic or supersonic over the whole range. In our notation, $\bar{v}_1=c_1$ is given by $\bar{y}_1=1$ and $\bar{v}_2=c_2$ by $\bar{y}_2=\sqrt{K_1/K_2}$. Hence if $\bar{y}_1<1$, $\bar{y}_2\leqslant\sqrt{K_1/K_2}$, and if $\bar{y}_1>1$, $\bar{y}_2\geqslant\sqrt{K_1/K_2}$.

From (18)

$$\bar{y}_2\Big/\sqrt{\frac{K_1}{K_2}}=\left\{\eta\pm\sqrt{\left(\eta^2-\frac{K_2}{K_1}\right)}\right\}\Big/\sqrt{\frac{K_2}{K_1}}, \tag{22}$$

and

$$\bar{y}_1=\eta\pm\sqrt{(\eta^2-1)}. \tag{23}$$

Thus either the positive or the negative sign must be chosen on both sides of the interface.

2.3. *Conditions in zone II.*—From (12) and (15),

$$\left(\tfrac{1}{2}y^2-\frac{K_1}{K_2}\ln y\right)=\frac{K_1}{K_2}\left(2\ln x+\frac{K_1}{K_2}\frac{1}{x}\right)+\alpha, \tag{24}$$

where α is a constant.

The expression $(2\ln x+(K_1/K_2)1/x)$ has a minimum at $x_c=\frac{1}{2}(K_1/K_2)$, and if $\bar{x}\geqslant x_c$, this minimum will be attained. Also, $(\frac{1}{2}y^2-(K_1/K_2)\ln y)$ has a minimum for $y^2=K_1/K_2$. Hence, if $\bar{x}\geqslant x_c$, the constant α cannot be less than

$$\frac{1}{2}\frac{K_1}{K_2}\left(1+\ln\frac{K_2}{K_1}\right)-\frac{K_1}{K_2}\left(2+2\ln\frac{K_1}{2K_2}\right). \tag{25}$$

For $K_2/K_1=2\times10^2$, this gives

$$(\tfrac{1}{2}y^2-5\times10^{-3}\ln y)-\left(10^{-2}\ln x+\frac{2{\cdot}5\times10^{-5}}{x}\right)\geqslant6{\cdot}57\times10^{-2} \tag{26}$$

* The writer is indebted to Professor Cowling for drawing his attention to this limitation.

for all y in the range $x(\text{star}) < x < \bar{x}$. In particular, at $\bar{x}$ equation (26) provides a new restriction on the allowed values of $\bar{y}_2$: either

$$\bar{y}_2 \geqslant Y_\alpha > \sqrt{\frac{K_1}{K_2}} \tag{27}$$

or

$$\bar{y}_2 \leqslant Y_\beta < \sqrt{\frac{K_1}{K_2}}. \tag{28}$$

The different possibilities are summarized in Fig. 1.

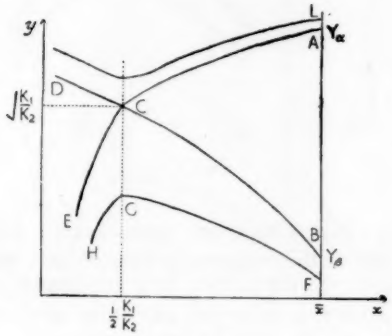

FIG. 1.

It is seen that for $\bar{y}_2 = Y_\alpha$ or $\bar{y}_2 = Y_\beta$, the solutions pass through the point C for which the gas velocity equals the velocity of sound. The initially supersonic solution from A may either pass smoothly into subsonic flow or, by means of a finite jump in the acceleration at C, remain supersonic up to the surface of the star; similarly, the initially subsonic solution from B may either become supersonic or remain subsonic after passing through C. All other solutions, such as those starting from F and L, remain either supersonic or subsonic for all x in the range.

If $\bar{x} \leqslant x_c$, there is no limitation on the range of $\bar{y}_2$; $(2 \ln x + (K_1/K_2)1/x)$ attains its minimum at $\bar{x}$, and the smallest possible value of α is given on substituting $\bar{x}$ for x and $\sqrt{(K_1/K_2)}$ for y in (24). Solutions that are either supersonic or subsonic at $\bar{x}$ remain so up to the surface of the star; for $\bar{x} = x_c$, there are two solutions branching from the point $\bar{y}_2 = \sqrt{(K_1/K_2)}$, one into the subsonic and the other into the supersonic region.

2.4. *Conditions in zone I.*—The solution in zone I must satisfy the condition of zero velocity at infinity. From (12) and (14) we have

$$\ln \lambda = \left(\frac{1}{x} 2 + \ln x \right) - (\tfrac{1}{2} y^2 - \ln y) \tag{29}$$

for all x from $\bar{x}$ to infinity. Suppose first that $\bar{x} < 0{\cdot}5$. Then at $x = 0{\cdot}5$, $(1/x + 2 \ln x)$ attains its minimum; $(\frac{1}{2}y^2 - \ln y)$ has a minimum value for $y = 1$. If for $x = 0{\cdot}5$, $y < 1$, then y remains less than 1 for all x in zone I, and similarly, if $y(0{\cdot}5) > 1$, then $y > 1$ throughout the range; thus only the subsonic sets satisfy the condition $y = 0$ at infinity. If $y(0{\cdot}5) = 1$, then again there is a branching of solutions, and the flow that is subsonic from $x = \infty$ to $x = 0{\cdot}5$ may, by a discontinuous jump in acceleration, remain subsonic, or may pass smoothly into

supersonic flow for $\bar{x}<x<0{\cdot}5$. For this critical case $\ln\lambda$ attains its maximum value 0·1138, while the other solutions correspond to smaller values of λ. The run of the solutions is shown in Fig. 2.

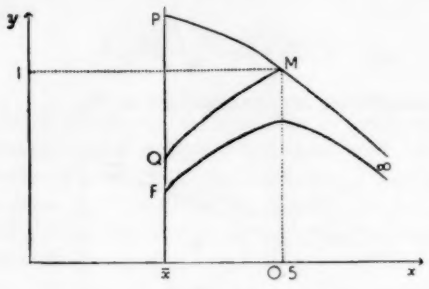

FIG. 2.

When $\bar{x}\geqslant 0{\cdot}5$, $(1/x+2\ln x)$ increases monotonically outwards, and so there is no possibility of a flow with a supersonic velocity at $\bar{x}$ becoming subsonic and so vanishing at infinity. Thus if $\bar{x}>0{\cdot}5$, $\bar{y}_1$ is necessarily $\leqslant 1$.

To sum up: for $\bar{x}\geqslant 0{\cdot}5$, $\bar{y}_1$ may take any value up to unity. For $\bar{x}<0{\cdot}5$, it is allowed just one supersonic value, namely the value at P, the point where the smooth solution through M meets $x=\bar{x}$ (see Fig. 2). The subsonic values allowed must all be less than the value at Q, where the other branch of the maximal solution cuts $x=\bar{x}$. The value of $\ln\lambda$, and hence the accretion rate, is fixed by (29) when $\bar{y}_1$ is known.

2.5. *Solutions for the complete range.*—The results of the last three sections must now be combined so as to determine what solutions satisfy all the conditions at the interface, in zones I and II, and at infinity. The following cases arise:

(*a*) $\bar{x}\geqslant 0{\cdot}5$

By (27) and (28) either

$$\bar{y}_2\geqslant Y_\alpha>\sqrt{\frac{K_1}{K_2}}$$

or

$$\bar{y}_2\leqslant Y_\beta<\sqrt{\frac{K_1}{K_2}}.$$

The supersonic cases may be rejected at once, as the corresponding values of $\bar{y}_1$ must also be supersonic, by the condition of fit, and so cannot, as shown in 2.3, lie on a solution satisfying the condition at infinity.

Any solution with $\bar{y}_2\leqslant Y_\beta$ satisfies all the conditions. The corresponding value of $\bar{y}_1$ is found from (18) to be $\simeq\bar{y}_2$, as the velocities are so much below the velocity of sound that (10) reduces effectively to equality of pressure at the interface. The solutions behave as in Fig. 3. The largest value of λ, λ_c, corresponds to either of the two solutions ∞BCD and ∞BCE, while smaller values characterize solutions such as ∞FGH. A set of values is given in Table I, assuming $K_2/K_1=2\times 10^2$. These should be compared with $\ln\lambda_c=0{\cdot}1138$, Bondi's maximum. In the limiting case $\bar{x}=\infty$, when the whole cloud is at a temperature

10^4 deg. K, λ_c is reduced by $(K_1/K_2)^{5/2}$, due to $(K_1/K_2)^{3/2}$ from the increase in c_∞^3, and (K_1/K_2) from the decrease in density. It is readily verified that (2) gives precisely the accretion rate in Table I, when c_∞^3 and ρ_∞ have these new values substituted.

TABLE I

$\bar{x}$	$\ln \lambda_c$
0·5	−11·15
1	−12·15
∞	−13·14

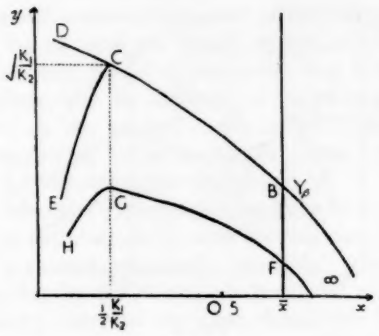

FIG. 3.

(*b*) $0{\cdot}075 \leqslant \bar{x} \leqslant 0{\cdot}5$

For this range the solutions behave similarly to the set (*a*). Again there are solutions in zone II for $\bar{y}_2 \leqslant Y_\beta$, with corresponding values for $\ln\lambda$. For $\bar{y}_2 = Y_\beta$, there are two solutions, ∞BCD and ∞BCE (*cf.* Fig. 4), the first being supersonic, the second subsonic near the star; for $\bar{y}_2 < Y_\beta$ the solutions are everywhere subsonic. The condition of fit at $\bar{x}$ again reduces effectively to continuity of pressure, so that $\bar{y}_1 \simeq \bar{y}_2$. It is found that within this range of $\bar{x}$, the point P (corresponding to a supersonic velocity) gives values of η not satisfying the condition $\eta^2 \geqslant K_2/K_1$ of Section 2.2, so that only solutions subsonic in zone I exist. As zone I now includes the point $x = 0{\cdot}5$, the solutions in zone I all have a maximum. The lower limit to this range of $\bar{x}$ is fixed by the coincidence of the points Q and B, giving for $\ln\lambda_c$ the value 0·1138, Bondi's maximum. With our chosen value of $K_2/K_1 = 2 \times 10^2$, this limit is 0·075, as in the heading. For different values of K_2/K_1, the limit varies slightly; e.g. for $K_2/K_1 = 10^2$, 4×10^2, it is 0·087, 0·067 respectively. Typical values of $\ln\lambda_c$ are as follows:

TABLE II

$\bar{x}$	$\ln \lambda_c$
0·5	−11·15
0·1	− 3·125
0·075	0·1138

(*c*) $2{\cdot}45 \times 10^{-3} < \bar{x} \leqslant 0{\cdot}075$

The diagram for this range is similar to Fig. 4, except that Q falls below B. Thus all the solutions remain subsonic right up to the star. Again there are no solutions passing through P. The maximum allowed value of $\ln\lambda$ is again 0·1138, corresponding to the curve ∞MQ(star).

(*d*) $\bar{x} \leqslant 2{\cdot}45 \times 10^{-3}$

The subsonic solutions are similar to those in case (*c*), but in addition there is now a solution ∞MPR(star), as the value of η corresponding to P satisfies the condition $\eta^2 \geqslant K_2/K_1$ (*cf.* Fig. 5). Again, the upper limit $\bar{x} = 2{\cdot}45 \times 10^{-3}$ is the value corresponding to $K_2/K_1 = 2 \times 10^2$; for all K_2/K_1, this upper limit is slightly less than $x_c = \frac{1}{2}K_1/K_2$, so that all the zone II solutions are monotonic (*cf.* Section 2.3). For ∞MPR(star) and ∞MQ(star), $\ln\lambda$ is again 0·1138, with correspondingly smaller values for all the other subsonic solutions.

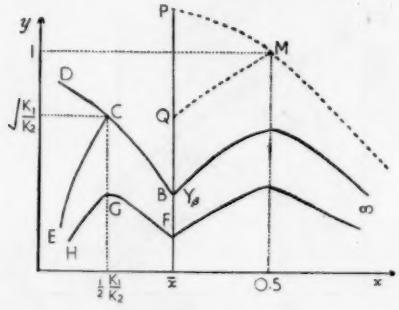

FIG. 4.

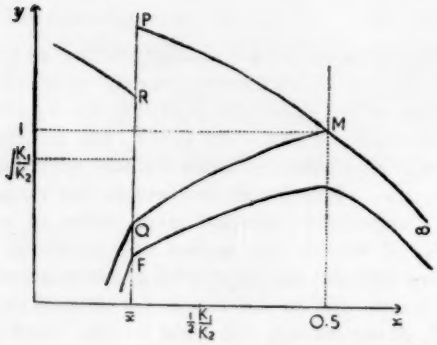

FIG. 5.

3. *The theory of radiation heating*

3.1. *Physical discussion.*—It was Eddington who first drew attention to the heating effect of stellar radiation on the interstellar gas (**8**). Ultra-violet radiation of frequency greater than the photoelectric threshold for hydrogen will liberate electrons from the hydrogen atoms in the cloud, the mean kinetic energy of the expelled electrons corresponding to a kinetic temperature about two-thirds the temperature of the exciting radiation (assumed to be given by a black-body distribution). The electrons suffer many Coulomb collisions with each other and with the heavy particles in a time short compared with the time for recombinations to occur, so that the particles take up a Maxwellian velocity distribution with a definite kinetic temperature at each epoch. The slower electrons are

much more easily re-captured than the faster, so that an initially cool cloud is gradually heated up by the net transfer of ultra-violet light from the central star into kinetic energy.

Neglecting all reactions but the photoelectric ionization of hydrogen and the recombination of electrons and protons, the ultimate steady state will be determined by conditions of statistical but non-thermodynamic equilibrium. The thermal radiation from the star liberates electrons at a rate depending primarily on the temperature of the radiation and its dilution; recombinations occur to both the ground and excited states of the hydrogen atom, removing electrons from the gas and transforming some of the kinetic energy into photons. The temperature of the gas and the degree of ionization are determined by a balance between gains and losses of electrons and kinetic energy. As the radiation field is so dilute, and the lifetimes of the excited states of hydrogen so short, the population of the excited states is low enough for photoelectric ionizations from these states to be negligible; also, stimulated emission is negligible compared with spontaneous emission.

If all the proton–electron recombinations were to the ground state, there would be no reason, in the absence of other cooling mechanisms, for the sphere of hot hydrogen not to extend continually outwards. The dilution of the stellar radiation reduces the density of ionizing photons, and so also the proportion of free electrons in a steady state, but does not change the high mean energy with which the electrons are expelled; the process outlined above might therefore be expected to continue indefinitely, the extent of the hot region being limited simply by the longer time that diluted radiation takes to heat up the gas, and so ultimately by the lifetime of the star. However, in the presence of diluted thermal radiation the hydrogen atom fluoresces, emitting fewer high-energy photons than it absorbs, the balance being made up by emission in the Balmer, Paschen, etc. series (**9**). Thus there is a net extinction of ionizing photons. Strömgren has shown (**6**) that this leads to a sharp division between a sphere of almost completely ionized hydrogen (H II zone) and the outer H I zone of almost completely un-ionized hydrogen. Spitzer and Savedoff (**5**) have performed detailed estimates of the temperatures of static H I and H II regions, taking into account all the heating and cooling mechanisms occurring; they give 10^2 deg. K as a good average for the H I zones, while H II zones take up temperatures of the same order as the exciting stars.

3.2. *Mathematical discussion.*—The energy density of radiation of frequency ν at distance r from the star is given by

$$\rho_\nu d\nu = \frac{8\pi h\nu^3}{c^3} \frac{d\nu}{(e^{h\nu/kT}-1)} We^{-\tau_\nu}, \tag{30}$$

where W is the distance dilution factor $R^2/4r^2$ and $e^{-\tau_\nu}$ is the extinction factor in frequency ν, defined later. Let N_H, N_p, N_e be the number densities of hydrogen atoms, protons and electrons respectively, and let $N_1, N_2, \ldots N_s$ be the densities of H atoms in the ground, 2nd, ... sth quantum state, so that $N_H = \Sigma N_s$.

From Gaunt's work on continuous absorption by hydrogen-like atoms (**10**), the absorption cross-section from the sth quantum state is given by

$$\sigma_\nu^s = \frac{2^6\pi^4 m e^{10}}{3\sqrt{3}ch^6} \frac{1}{s^5} \frac{1}{\nu^3} = \frac{\sigma_0}{s^5\nu^3}, \tag{31}$$

with the Gaunt factor put equal to unity; m and e are the electronic mass and charge respectively, c the velocity of light and h Planck's constant. The application of detailed balancing (9) leads to the formula

$$\beta_\nu^s = \frac{2h^2\nu^2}{m^2c^2v^2}s^2\sigma_\nu^s = \frac{2h^2\sigma_0}{m^2c^2}\frac{1}{v^2}\frac{1}{s^3\nu} \tag{32}$$

for the recombination probability to state s for unit current of electrons with velocity v. The factor s^2 arises from the degeneracy of the sth energy level.

The binding energy of the sth level is χ_1/s^2, where $\chi_1 = 2{\cdot}15 \times 10^{-11}$ erg. The frequency of the radiation emitted or absorbed is related to the electron velocity by

$$h\nu = \tfrac{1}{2}mv^2 + \chi_s. \tag{33}$$

From (32), and an assumed Maxwell distribution for the electron gas

$$n_e(v)\,dv = \frac{N_e\,4\pi\,m^3}{(2\pi mkT_0)^{3/2}}v^2\,dv\,e^{-mv^2/2kT_0} \tag{34}$$

(T_0 being the electron temperature), we have for the rate per cm^3 of recombination to the sth state:

$$R_s = \frac{8\pi h^3\sigma_0}{c^2}\frac{N_eN_p}{(2\pi m)^{3/2}}\frac{1}{\chi_1}\frac{1}{(kT_0)^{1/2}}\frac{1}{s}\left(u_se^{u_s}\int_{u_s}^{\infty}\frac{e^{-x}\,dx}{x}\right), \tag{35}$$

where

$$u_s = \frac{\chi_s}{kT_0} = \frac{\chi_1}{s^2kT_0}.$$

The total loss of electrons from the gas is then just ΣR_s. Thus must be balanced, in statistical equilibrium, by the rate per unit volume of photo-ionization from the ground state:

$$Q = N_Hc\int_{\nu=\chi_1/h}^{\infty}\frac{\rho_\nu\sigma_\nu^1\,d\nu}{h\nu}, \tag{36}$$

where ρ_ν and σ_ν^1 are given by (30) and (31), and N_H has been written for N_1, owing to the low occupation of excited states (*cf.* Section 3.3). Expression (36) reduces to

$$Q = N_H\frac{8\pi}{c^2}\sigma_0W\int_{\chi_1/kT}^{\infty}\frac{e^{-\tau_\nu}}{x(e^x-1)}\,dx. \tag{37}$$

The rate of photoelectric absorption of energy per cm^3 is given by multiplying the integrand in (36) by $h\nu$ before integrating:

$$N_H\frac{8\pi}{c^2}\sigma_0WkT\int_{\chi_1/kT}^{\infty}\frac{e^{-\tau_\nu}}{(e^x-1)}\,dx. \tag{38}$$

Hence the mean kinetic energy of the expelled electrons is

$$\frac{kT\displaystyle\int_{\chi_1/kT}^{\infty}\frac{e^{-\tau_\nu}}{(e^x-1)}\,dx}{\displaystyle\int_{\chi_1/kT}^{\infty}\frac{e^{-\tau_\nu}\,dx}{x(e^x-1)}} - \chi_1. \tag{39}$$

If the extinction factor $e^{-\tau_\nu}$ is put equal to unity, this expression reduces to kT, Eddington's result.

Similarly, from (32) and (34), the rate of emission of radiant energy by the electron gas by recombinations to ground and excited states is given by

$$\frac{8\pi h^3\sigma_0}{(2\pi m)^{3/2}c^2}\frac{1}{(kT_0)^{1/2}}N_eN_p\left(\sum_{s=1}^{\infty}\frac{1}{s^3}\right), \tag{40}$$

and the rate of loss of kinetic energy by the gas is given by subtracting from (40) the expression

$$\sum_{s=1}^{\infty}\chi_sR_s=\frac{8\pi h^3\sigma_0}{(2\pi m)^{3/2}c^2}\frac{1}{(kT_0)^{1/2}}N_eN_p\sum_{s=1}^{\infty}\left(\frac{1}{s^3}u_se^{u_s}\int_{u_s}^{\infty}\frac{e^{-x}\,dx}{x}\right). \tag{41}$$

Hence the mean loss of kinetic energy per recombination is

$$\frac{\chi_1\sum_{s=1}^{\infty}\frac{1}{s^3}\left(1-u_se^{u_s}\int_{u_s}^{\infty}\frac{e^{-x}\,dx}{x}\right)}{\sum_{s=1}^{\infty}\frac{1}{s}u_se^{u_s}\int_{u_s}^{\infty}\frac{e^{-x}\,dx}{x}}. \tag{42}$$

If a steady state has been reached, the electron gas will have warmed up the heavy particles to its own temperature by Coulomb collisions, so that on balance no energy is transferred from the electron gas by collisions. In the absence of any other heating or cooling mechanisms, the condition of thermal equilibrium is satisfied by equating (39) to (42); anticipating that $e^{-\tau_\nu}$ differs sensibly from unity only at the edge of the H II zone, it is then found, on using tables of the integral $\int_u^{\infty}e^{-y}\,dy/y$ (11), that $T_0\simeq T$. In fact, there are in general other cooling mechanisms active (5); in particular, it is shown in Section 3.3 that collisional ionization will prevent the temperature of the gas from rising much above 10^4 deg. K. Thus the precise temperature of the gas is determined by a much more complicated equation of thermal balance, but the results of Spitzer and Savedoff (5), and of Section 3.3, show that the assumption of a standard value of 10^4 deg. K for T_0 is a good approximation.

From tables (11), it is found that

$$\sum_{s=1}^{\infty}\frac{1}{s}u_se^{u_s}\int_{u_s}^{\infty}\frac{e^{-x}\,dx}{x}\simeq 2{\cdot}5, \tag{43}$$

where T_0 has been put equal to 10^4 deg. K. As the term for $s=1$ has the value unity very nearly, it follows that three-fifths of the photons absorbed are re-emitted in low, non-ionizing frequencies. The degree of ionization γ, defined by

$$N_e=N_p=\gamma(N_p+N_H)=\gamma N, \tag{44}$$

is given as a function of r by equating the recombination rate $\sum_{s=1}^{\infty}R_s$ to the rate of ionization (37), and making use of (43); the result is found to be

$$\frac{\gamma^2N}{(1-\gamma)}=\frac{2}{5}\frac{(2\pi mkT)^{3/2}}{h^3}\left(\frac{T_0}{T}\right)^{1/2}\frac{\chi_1}{kT}W\int_{\chi_1/kT}^{\infty}\frac{e^{-\tau_\nu}\,dx}{x(e^x-1)}, \tag{45}$$

where N is now the density at r of the heavy particles (protons and H-atoms).

The extinction factor $e^{-\tau_\nu}$ is given by the equation

$$d\tau_\nu=N(1-\gamma)(\alpha(\nu)\sigma_\nu^1)(3{\cdot}08\times 10^{18})\,dr, \tag{46}$$

where $(3{\cdot}08\times 10^{18})$ has been inserted so that r is measured in parsecs. The factor $\alpha(\nu)$ is the proportion of the absorbed photons of frequency ν that are

re-emitted in low frequencies. The emission from the gas is isotropic, and not just in the outward directions; the use of $\alpha(\nu)$ in (46) will therefore tend to under-rate the extinction slightly, and the correct factor should be between $\alpha(\nu)$ and 1. However, it is easily seen that the error involved is not large, and the value $\frac{3}{5}$ found from (43) for the integrated extinction factor will be used. τ_ν as defined is the analogue of the optical depth, but the distinction is clearly drawn between absorption and re-emission in ionizing frequencies, and re-emission in lower frequencies.

From (37) it is seen that the bulk of the photoelectric absorption occurs very near the absorption edge; also, the high-frequency photons emitted by the gas are from (35) and (41) nearly all of energy near the ionization energy of hydrogen. It is therefore a legitimate approximation (**6**) to give $e^{-\tau_\nu}$ in (45) its value ω at the absorption edge, so that (45) becomes

$$\frac{\gamma^2 N}{(1-\gamma)} = \frac{2}{5}\frac{(2\pi mkT)^{3/2}}{h^3}\left(\frac{T_0}{T}\right)^{1/2} W\omega e^{-\chi_1/kT}. \tag{47}$$

We now introduce the variables x and z of Section 2, i.e.

$$\left.\begin{aligned} r &= (5{\cdot}19\times 10^{-3} M/\odot)x, \\ N/N_\infty &= (5\times 10^{-3})z. \end{aligned}\right\} \tag{48}$$

Then (46) and (47) reduce to

$$\frac{d\omega}{dx} = -BN_\infty{}^2(\gamma^2 x^2 z^2), \tag{49}$$

$$\frac{(1-\gamma)}{\gamma^2} = CN_\infty\left(\frac{zx^2}{\omega}\right), \tag{50}$$

where

$$\log_{10} C = 2\log_{10} M' - 2\log_{10} R' - \log_{10} T' + \bar{1}2{\cdot}34 + 13{\cdot}53/T', \tag{51}$$

and

$$\log_{10} B = \bar{4}{\cdot}595 + \log_{10} C + \log_{10} M'. \tag{52}$$

The value $T_0 = 10^4$ has been used here. Quantities with primes have been expressed in solar units. Equations (49) and (50) differ from Strömgren's through the presence of z, measuring the density variation.

Integrating (49), we have

$$\omega - 1 = -BN_\infty{}^2 \int_{x_0}^{x} \gamma^2 x^2 z^2\, dx, \tag{53}$$

where use has been made of the boundary condition that τ_ν vanishes when x has the value x_0 corresponding to the surface of the star. Hence ionizing radiation is completely extinct at a distance $\bar{x}$ given by

$$1 = BN_\infty{}^2 \int_{x_0}^{\bar{x}} \gamma^2 x^2 z^2\, dx, \tag{54}$$

where γ is given by (50). As Strömgren remarks (**6**), the value $\gamma = 1$ may be used in (54) as γ differs sensibly from unity only within a narrow region near $\bar{x}$: as soon as the proportion of neutral hydrogen becomes important, the absorption of photons increases rapidly, and the extinction of the ionizing frequencies is soon complete.

Substituting $z=\lambda/x^2y$ from (12) into (54), and putting $\gamma=1$, we have an equation for (λN_∞), proportional to the rate of accretion, in terms of $\bar{x}$:

$$1=B(\lambda N_\infty)^2\int_{x_0}^{\bar{x}} dx/x^2y^2. \tag{55}$$

From Section 2 the allowed values of λ as a function of $\bar{x}$ are known; (55) therefore fixes the density at infinity so that all the ionizing radiation may be extinguished within the sphere $\bar{x}$.

3.3. *Discussion of the approximations made.*—The following assumptions are implicit in the theory so far:

(*a*) In computing the degree of ionization, the contribution from absorption of energy by excited states of hydrogen has been neglected.

(*b*) No modification has been made to take account of the motion of the gas. If the time taken to reach ionization equilibrium were comparable with the time of flow of matter through the H II zone, then the results found from (55) would seriously overestimate the required value of N_∞ for extinction, as the proportion of neutral hydrogen at any point would be significantly greater than that given by (50).

(*c*) The flow is taken as isothermal in both zones; i.e. it is assumed that the heat generated by compression is rapidly absorbed and radiated away. In the H II zone, collisional ionization becomes active as a cooling mechanism once the temperature rises much above 10^4 deg. K. It has to be shown that the consequent drop in the proportion of neutral hydrogen does not diminish seriously the absorbing power of the gas.

(*d*) The diminution of gravity due to the pressure of absorbed radiation has been neglected.

These effects are now discussed in turn.

(*a*) The equation of balance for transitions to and from the sth energy level for $s>1$ is

$$R_s-N_sc\int_{\chi_s/h}^{\infty}\frac{\rho_\nu\sigma_\nu^s}{h\nu}\,d\nu=N_s\sum_{r=1}^{s-1}P_{sr}+\sum_{r=s+1}^{\infty}N_rP_{rs}, \tag{56}$$

where P_{ik} is the spontaneous transition probability from state i to state k. (The dilution of the radiation justifies the neglect of both line absorption and stimulated emission.) From (30) and (31),

$$c\int_{\chi_s/h}^{\infty}\frac{\rho_\nu\sigma_\nu^s}{h\nu}\,d\nu=\frac{8\pi\sigma_0W\omega}{c^2s^5}\int_{\chi_s/kT}^{\infty}\frac{dx}{x(e^x-1)}. \tag{57}$$

It is known that the lifetimes of the excited states of hydrogen are of order 10^{-8} sec, and so the probabilities P_{ik} are of order 10^8/sec. On substituting numerical values, it follows that for W appreciably below unity the value of (57) $\ll 10^8$. Thus equation (56) reduces effectively to one of balance between photoelectric recombination and spontaneous transitions, and in the generalized equation of balance for the electron gas

$$\sum_{s=1}^{\infty}N_sc\int_{\chi_s/h}^{\infty}\frac{\rho_\nu\sigma_\nu^s}{h\nu}\,d\nu=\sum_{s=1}^{\infty}R_s, \tag{58}$$

only the first term on the left-hand side makes a significant contribution.

(*b*) Consider an element of matter with its degree of ionization γ considerably lower than the equilibrium value as given by (50). Then by (37), the rate of decrease of $(1-\gamma)$ is given by

$$-\frac{d}{dt}(1-\gamma)=\frac{8\pi}{c^2}\sigma_0 W\omega\frac{kT}{\chi_1}e^{-\chi_1/kT}(1-\gamma). \tag{59}$$

From (47) the space-variation of $(1-\gamma)$ in matter in ionization equilibrium satisfies

$$-\frac{d(1-\gamma)}{(1-\gamma)}=\frac{2dr}{r}. \tag{60}$$

Thus matter ionized to a degree $\gamma(r)$ given by (50) will attain the value $\gamma(r-dr)$ in a time of order

$$\frac{2c^2}{8\pi}\frac{1}{\sigma_0 W\omega}e^{\chi_1/kT}\frac{\chi_1}{kT}\frac{dr}{r}, \tag{61}$$

while the time for matter to flow through dr is dr/v, where v is the local value of the velocity. Insertion of numerical values shows that for all r

$$v\ll\frac{8\pi\sigma_0 W\omega}{c^2}e^{-\chi_1/kT}\frac{kT}{\chi_1}\frac{r}{2}, \tag{62}$$

so long as T is greater than about 10^3 deg. K. As the present theory is irrelevant to such low temperatures, it follows that in all cases of interest deviations from ionization equilibrium are negligible.

Similarly, it can be shown that matter flowing into the H II zone is heated up to about 10^4 deg. K and ionized rapidly enough for the approximation of assuming a sharp discontinuity between the two zones to be adequate.

(*c*) Consider first the H II zone. The work done in compressing unit mass of the inflowing gas is

$$\frac{p}{\rho^2}\frac{D\rho}{Dt}=-\frac{p}{\rho^2}v\frac{d\rho}{dr}. \tag{63}$$

On substituting (11) of Section 2.1, and using the standard values 10^4 and 10^2 for the temperatures of the H II and H I zones respectively, (63) reduces to

$$-\frac{1\cdot88\times10^3}{M'}\left(\frac{y(dz/dx)}{z}\right). \tag{64}$$

If there are no other cooling mechanisms active, this energy must be absorbed by collisional ionization, if the zone is to remain isothermal. The probability per second of collisional ionization of a hydrogen atom by an electron is taken (**12**) as

$$S_{12}=\frac{12\pi e^4 b}{(2\pi mkT_0)^{1/2}}\frac{kT_0}{\chi_1}e^{-\chi_1/kT_0}, \tag{65}$$

where T_0 is the temperature of the gas and b a factor of order unity. At each ionization the kinetic energy of the electron gas is decreased by χ_1 erg; the rate of loss of energy per second per gram of gas is therefore

$$\frac{S_{12}\chi_1 N_e N_H}{Nm_H}=7\times10^{21}bT_0^{1/2}\exp(-1\cdot57\times10^5/T_0)\gamma(1-\gamma)N. \tag{66}$$

Some of this energy will be returned to the gas by the reverse process of collisional recombination, while the rest will be transformed into both high and low frequency radiation by photoelectric recombination. As photons of energy less than χ_1 are lost to the gas, collisional ionization is a powerful cooling mechanism. In

a gas at rest, the temperature is automatically cut down to a value at which collisions are negligible. In the present problem the temperature of the gas at any point is given by including in the equation of energy both (64) and (66); as, however, the other terms in the energy equation (*cf.* (39) and (42)) are insensitive to changes in T_0, it is adequate to equate (64) to (66).

The value of γ is given by the generalized equation of ionization equilibrium

$$\sum_{s=1}^{\infty} R_s + \gamma^3 N^3 S_{21} = Q + \gamma(1-\gamma) N^2 S_{12}, \tag{67}$$

where Q and R_s are defined in (36) and (35) respectively and S_{21} is the probability per second of collisional recombination.

Provisionally, both S_{12} and S_{21} in (67) are neglected, so that the equation for γ reduces to (50). The heat of compression is absorbed by collisions when

$$-\frac{1{\cdot}88\times 10^3}{M'}\left(\frac{\gamma(dz/dx)}{z}\right) = \frac{S_{12}\chi_1 N_e N_H}{N m_H}$$
$$= 7\times 10^{21} b T_0^{1/2} \exp(-1{\cdot}57\times 10^5/T_0)\gamma(1-\gamma)N. \tag{68}$$

From (68), (35) and (43), $\gamma(1-\gamma)N^2 S_{12} \Big/ \sum_{s=1}^{\infty} R^s$ is found to be

$$5{\cdot}6\times 10^4 \left(-\frac{yz'}{z^2}\right)\Big/ M' N_\infty,$$

which has a maximum value $3{\cdot}75/M'N_\infty$. Thus for any value of N_∞ large enough for the accretion rate to be significant, neglect of the S_{12} term in (67) is a good approximation. The S_{21} term is negligible *a fortiori*. From the principle of detailed balancing (12), S_{21} is given by

$$S_{21} = \left(\frac{1-\gamma}{\gamma^2 N}\right)_T S_{12}, \tag{69}$$

where the suffix T refers to conditions of thermodynamical equilibrium. In the presence of diluted thermal radiation, the value of $\gamma^2 N/(1-\gamma)$ is from (47) very nearly $W(\gamma^2 N/(1-\gamma))_T$, and so collisional recombination is much less probable than collisional ionization, which is itself negligible. Hence γ is given accurately by (47), and values of N_∞ calculated from (55) will be trustworthy. From (68) it is seen that the temperature of the gas is not allowed to rise above about $1{\cdot}5\times 10^4$ deg. K, so that the temperature variation through the H II zone is very slight. To sum up: collisional ionization is able to preserve nearly isothermal conditions without seriously increasing the degree of ionization over the value given by (47).

If radiative processes are not strong enough to prevent some compressional heating of the H I zone, the maximum allowed accretion rate will be reduced, and the values of N_∞ as computed from (55) will be increased somewhat. The results of this paper therefore refer to the best possible conditions for accretion.

(*d*) As emission from the gas is isotropic (stimulated emission being negligible) the rate of absorption of momentum per cm^3 of the gas from the radiative stream is from (38)

$$\frac{8\pi\sigma_0}{c^3} WkT\omega e^{-\chi_1/kT} N(1-\gamma), \tag{70}$$

or from (47)

$$\frac{8\pi\sigma_0 k}{c^3}\frac{h^3}{(2\pi m k)^{3/2}}\frac{1}{T_0^{1/2}}\frac{5}{2} N^2. \tag{71}$$

Hence the ratio to gravitation of the force due to radiation absorption is

$$\frac{8\pi\sigma_0 k}{c^3}\frac{h^3}{(2\pi mk)^{3/2}}\frac{1}{T_0^{1/2}}\frac{5}{2}N^2\Big/\frac{GMNm_H}{r^2}=2{\cdot}14\times10^{-6}M'N_\infty zx^2, \tag{72}$$

where z and x are given by (11) of Section 2.1.

We confine attention to the cases of maximal accretion (sequence (b) solutions of Section 4.1). The product $zx^2=(1{\cdot}12)/y$, and this attains its maximum value at $x=\bar{x}$; hence for a given H II sphere, neglect of radiation pressure is justified for all $x\leqslant\bar{x}$ if

$$\beta=2{\cdot}39\times10^{-6}M'N_\infty/\bar{y}_2\ll1. \tag{73}$$

From (24) and (55) it follows that β decreases with increasing N_∞ until $\bar{x}$ reaches the value ex_0; for larger N_∞ and correspondingly smaller $\bar{x}$, β increases to infinity with N_∞.

From Tables III and V, we have the following results: with $\bar{x}=2{\cdot}45\times10^{-3}$, β has the values 0·33, 1·68, 8·98 for Bo, O8, O5 type stars respectively, while with $\bar{x}=10^{-5}$, the corresponding values are 0·04, 0·25, 1·34. Thus for stars earlier than type Bo radiation pressure from photoelectric absorption is not small even for moderate values of N_∞. The reduction in gravity will lead near the star to smaller velocities and hence higher densities than those given by the present theory. The consequent increase in the absorptive power of the gas reduces the radius of the H II zone for a given value of N_∞. For bright enough stars the radiation pressure will exceed gravity; we must therefore impose an extra condition that the material entering the H II zone has enough momentum to reach the star in spite of the deceleration within the zone. It is hoped to extend the theory so as to take account of both this effect and also of radiation pressure on dust particles in the cloud.

4. *The combination of accretion theory with the theory of radiation heating*

4.1. *Numerical results.*—On applying the ionization theory to the accretion problem it is at once seen that the results obtained depend critically on the behaviour of the flow near the star. In solutions which are subsonic near the star the velocity decreases to a small value as the surface is approached, and the finite accretion rate is maintained by the density becoming large. From (12) and (24), y and z behave near the star like

$$-\ln y=\frac{5\times10^{-3}}{x}, \tag{74}$$

$$z=\frac{\lambda}{x^2}e^{\frac{5\times10^{-3}}{x}}, \tag{75}$$

respectively. Substituting this expression for y in (55), the integral becomes so large that only very small values of N_∞ are required for extinction of ionizing radiation to be complete just outside the star's surface. Hence for "subsonic" type solutions the edge of the H II zone will in all cases of interest lie very close to the star, so that Bondi's theory effectively governs the accretion rate. But the densities near the star given by (75) are so enormous as to be quite unplausible —with $x=10^{-5}$, z turns out to be 10^{225}, corresponding to a mass-density of order 10^{200} g. While it is difficult to rule out rigorously these "subsonic" solutions, it is unlikely that the potential energy of an element of gas in the field of the star

should all be ultimately converted by compression into thermal energy (subsequently radiated away) and none into kinetic energy. In the non-spherical problem of accretion by a star embedded in a cloud possessing angular momentum, it is conceivable that a very high density could be built up near the star by the joint action of gravitation and centrifugal force; but this effect could not be combined with a large accretion, as the centrifugal force would prevent flow into the star. It seems likely that the "subsonic" solutions arise from the artificial assumption of a steady state, and a rigorous discussion of the time-dependent equations of flow would eliminate them by showing that the natural tendency of a spherically symmetric system is to approach a state in which matter falls freely on to the surface. The "subsonic" type solutions can thus be eliminated by an extra boundary condition demanding that the star's gravitational field should lead to rapid inflow, and not build up an enormous pressure gradient. In the rest of the paper only "supersonic" type solutions will be discussed.

The following stellar types are considered, with the Sun for comparison (**6, 15**):

TABLE III

Spectral type	$M/\odot$	$R/R_\odot$	$T_\odot/T$	$10^6 \times x_0$	$\log_{10} B$
O5	60	30	0·063	2·19	$\bar{14}$·965
O8	19	12	0·126	2·765	$\bar{13}$·42
Bo	14	8	0·2	2·503	$\bar{12}$·57
B2	10	6·5	0·245	2·85	$\bar{12}$·82
Ao	2·84	2·27	0·470	3·5	$\bar{9}$·61
Sun	1	1	1	4·38	$\bar{2}$·46

The problem is then the determination of N_∞ from (55) for the two sequences of "supersonic" type solutions discussed in Section 2.

(*a*) *Sequence with* $\bar{x} \geqslant 7{\cdot}5 \times 10^{-2}$.—In order to estimate numerically the integrals in (55), a curve of $1/x^2y^2$ against x is plotted, y being given by (26) with the inequality sign replaced by equality. The following integrals are estimated numerically:

$$\int_{x_0}^{7{\cdot}5\times10^{-2}} dx/x^2y^2 = 4{\cdot}65 \times 10^7; \quad \int_{x_0}^{0{\cdot}1} dx/x^2y^2 = 1{\cdot}03 \times 10^8. \tag{76}$$

The slight variation of x_0 with spectral type is of no consequence. If $\bar{x} > 0{\cdot}1$, then

$$\int_{0{\cdot}1}^{\bar{x}} dx/x^2y^2 = 8{\cdot}67 \times 10^{10}(\bar{x}^3 - 10^{-3}) \tag{77}$$

to a good approximation; use has here been made of

$$-\ln y = 13{\cdot}14 + \ln x^2, \tag{78}$$

to which (26) reduces for large x. The results are as shown in Table IV with computed values of N_∞ and λN_∞ for a typical case, a B2 star.

A remarkable feature of this sequence is the peak in the computed values of N_∞ at $\bar{x} = \frac{2}{3}$. As $\bar{x}$ increases beyond 0·075, the accretion rate drops off sharply; the increase in the volume of the H II sphere is therefore at first more than off-set by the drop in the densities near the star, so that the value of N_∞ necessary for the ultra-violet extinction to be complete within $\bar{x}$ increases with $\bar{x}$. After $\bar{x} = \frac{2}{3}$, $\ln\lambda$ is so near its asymptotic value $-13{\cdot}14$ that with increasing x the extra volume of the absorbing sphere more than balances the slight drop in

density, and so the computed values of N_∞ decrease with increasing $\bar{x}$. For large $\bar{x}$, the density through the bulk of the H II zone is nearly constant, and the theory reduces effectively to Strömgren's.

TABLE IV

$\bar{x}$	$\int_{x_0}^{\bar{x}} \frac{dx}{x^2y^2}$	$\ln\lambda$	$N_\infty\sqrt{B}$	N_∞	λN_∞
0·075	$4{\cdot}65 \times 10^{7}$	0·1138	$1{\cdot}309\times10^{-4}$	51	57
0·1	$10{\cdot}3 \times 10^{7}$	− 3·125	$2{\cdot}24 \times 10^{-3}$	$8{\cdot}7 \times 10^{2}$	38
0·2	$7{\cdot}1 \times 10^{8}$	− 8·17	$1{\cdot}33 \times 10^{-1}$	$5{\cdot}1 \times 10^{4}$	14
0·5	$1{\cdot}08 \times 10^{10}$	−11·15	$6{\cdot}69 \times 10^{-1}$	$2{\cdot}6 \times 10^{5}$	3·7
0·667	$2{\cdot}57 \times 10^{10}$	−11·64	$7{\cdot}09 \times 10^{-1}$	$2{\cdot}75\times10^{5}$	2·4
1	$8{\cdot}68 \times 10^{10}$	− 12·15	$6{\cdot}48 \times 10^{-1}$	$2{\cdot}5 \times 10^{5}$	1·3
118	$1{\cdot}425\times10^{17}$	− 13·14	$1{\cdot}35 \times 10^{-3}$	$5{\cdot}25\times10^{2}$	$1{\cdot}03\times10^{-3}$

The accretion rate, proportional to λN_∞, decreases monotonically with increasing $\bar{x}$. Even in the most favourable case, $\bar{x}=0{\cdot}075$, λN_∞ is too small for accretion to be an important factor in the star's evolution. It is further shown in Section 4.3 that the solutions between $\bar{x}=0{\cdot}075$ and $\bar{x}=\frac{2}{3}$ are unstable.

(*b*) *Sequence of solutions with* $\bar{x}\leqslant 2{\cdot}45\times10^{-3}$.—All solutions in this sequence have the same parameter $\ln\lambda=0{\cdot}1138$. The solutions for y and z in the H II zone vary as x varies, though they all have similar asymptotic behaviour for $x\to0$. Two values of $\bar{x}$ have been chosen: the limiting case $\bar{x}=2{\cdot}45\times10^{-3}$ and, for comparison, the case $\bar{x}=10^{-5}$. The results are summarized in Table V.

TABLE V

Spectral type	$\int_{x_0}^{2\cdot45\times10^{-3}} \frac{\lambda^2\,dx}{x^2y^2}$	$N_\infty\sqrt{B}$ ($\bar{x}=2{\cdot}45\times10^{-3}$)	N_∞ ($\bar{x}=2{\cdot}45\times10^{-3}$)	$\int_{x_0}^{10^{-5}} \frac{\lambda^2\,dx}{x^2y^2}$	$N_\infty\sqrt{B}$ ($\bar{x}=10^{-5}$)	N_∞ ($\bar{x}=10^{-5}$)
A0	$2{\cdot}65\times10^{5}$	$1{\cdot}35\times10^{-3}$	21	$2{\cdot}64\times10^{4}$	$6{\cdot}16\times10^{-3}$	96
B2	$2{\cdot}65\times10^{5}$	$1{\cdot}35\times10^{-3}$	$5{\cdot}25\times10^{2}$	$3{\cdot}15\times10^{4}$	$5{\cdot}16\times10^{-3}$	2×10^{3}
O8	$2{\cdot}65\times10^{5}$	$1{\cdot}35\times10^{-3}$	$2{\cdot}6\times10^{3}$	$3{\cdot}23\times10^{4}$	$5{\cdot}16\times10^{-3}$	10^{4}
O5	$2{\cdot}65\times10^{5}$	$1{\cdot}35\times10^{-3}$	$4{\cdot}4\times10^{3}$	$3{\cdot}82\times10^{4}$	$5{\cdot}12\times10^{-3}$	$1{\cdot}7\times10^{4}$

The results in the fourth column are the most important, as they give the minimum density necessary for a star of given spectral type to be able to accrete at a significant rate. Although somewhat high, the estimates are certainly not unreasonable for cool dense clouds (**13**). For the accretion rate to be high, the cloud must be dense, and the H II zone must be limited to a small sphere surrounding the star; densities of order 10^3 particles/cm^3 perform both functions.

It is to be noted that the satisfactory results of Table V are due directly to the shielding effect of the high densities near the star, caused by the star's gravitational field. This is shown strikingly by computing N_∞ from (54) with z put equal to unity, as assumed by Strömgren (**6**): the minimum values of N_∞ that will keep $\bar{x}\leqslant2{\cdot}45\times10^{-3}$ are then 10^7 times those given in the fourth column of Table V, while densities of order 10^3 particles/cm^3 give values for $\bar{x}\simeq100$, with correspondingly negligible accretion rates. Even for a star with the same temperature as the Sun, neglect of the density variations near the star leads to a minimum value for N_∞ as high as 8×10^4 particles/cm^3 in order that the H II zone be kept small enough for rapid accretion to take place. The density gradient is therefore crucial for the theory, and the conditions under which we may expect the mechanism to work will require careful discussion. This is postponed until Section 4.3.

4.2. *The heating effect of the accreted material.*—The effect of accretion on the atmosphere of a star is studied in the Hoyle–Lyttleton–Bondi theory of the solar corona (**14**). The incoming material is stopped by collisions with the heavy particles in the solar atmosphere, and the kinetic energy of inflow is converted into heat. A system of convection currents is set up, transporting downwards the energy accreted. In a star of surface temperature below about 10^4 deg. K, all the ionized hydrogen will become neutral by the time it reaches the photosphere, the bulk of the emission taking place at temperatures near 10^4 deg. K. In a star of surface hotter than 10^4 deg. K, the photospheric layers consist of largely ionized hydrogen, but Hoyle's results show that there will still be an appreciable ultra-violet emission as the convection currents approach the photosphere. An upper limit to the effect of this emission on the accretion theory can be obtained by assuming in all cases that all the hydrogen becomes neutral before finally being swallowed by the star.

If A is the accretion rate, the number of ultra-violet quanta emitted outwards per second per cm^2 of the star's surface is

$$\frac{1}{2}\left(\frac{2}{5}\frac{A}{m_H}\right)\Big/4\pi R^2, \tag{79}$$

the factor $\frac{2}{5}$ being roughly the proportion of recombinations to the ground state.

At distance r from the star, the number density of ionizing quanta is

$$\frac{4}{5}\frac{A}{m_H}\frac{1}{4\pi R^2}\frac{Ww}{c}, \tag{80}$$

where W and w are defined in Section 3.2. The rate of photo-ionization in the cloud by the quanta (80) is therefore

$$\frac{4}{5}\frac{A}{m_H}\frac{1}{4\pi R^2}Ww(1-\gamma)N\frac{\sigma_0 h^3}{{\chi_1}^3}, \tag{81}$$

where the value of the absorption coefficient at the absorption edge has again been used. As most of the quanta will be emitted when the matter is near the photospheric temperature T, the temperature of the liberated electrons will be of order T.

This "accretion heating" becomes important if (80) is comparable with the number of ionizing quanta in the star's natural radiation, i.e. if

$$A \simeq 40\pi^2 R^2 \frac{m_H {\chi_1}^2}{h^3 c^2} kT e^{-\chi_1/kT}. \tag{82}$$

From (13), the maximum accretion rate is given by

$$A = 5{\cdot}25 \times 10^{15} M'^2 N_\infty. \tag{83}$$

Then (82) and (83) give, for a star of temperature T, the density at which accretion heating becomes comparable with natural heating. The results found must be compared with those of Table V, which give as a function of T the minimum values of N_∞ which allow maximal accretion.

For an A0 star, N_∞ is found from (82) to be about 10^3, which from Table V is larger by a factor 50 than the lower limit for maximal accretion. For brighter stars the accretion heating is, for the case $\bar{x} = 2{\cdot}45 \times 10^{-3}$, an even smaller fraction of natural heating, so the lower limits given in Table V are trustworthy. If the

star is accreting rapidly from a cloud of much greater density than the critical value, the calculation of the actual radius of the H II zone from (55) would need to be modified by the inclusion of the accretion heating; thus the radius of the H II zone would be rather bigger than that given by Table V, but still less than the critical value $2{\cdot}45 \times 10^{-3}$, so that maximal accretion can occur. The important result is that the lower limits from Table V do not require modification.

For stars a little less massive than those of type Ao, accretion heating necessarily predominates—the density given by (82) is much less than the lower limit found from (55) for maximal accretion. A new equation of ionization equilibrium can be calculated from (35) and (81) to replace (45), and the result substituted in (46). The temperature of the H II zone will again be nearly the same as the surface temperature of the star, so that K_2/K_1 of Section 2.1 will be $2T/10^2$. On substitution of numerical values the analogue of (55) is

$$1 = 3{\cdot}5 \times 10^{-6} \frac{M'}{T'^{5/2}} N_\infty \int_{x_0}^{\bar{x}} z^2 x^2 dx. \tag{84}$$

N_∞ appears linearly, as the accretion rate A is itself proportional to N_∞. The value of the integral is taken from Tables IV and V (the modification of the theory due to the temperature of the H II zone being lower than 10^4 deg. K is negligible). The minimum values of N_∞ are given by (84) with $\bar{x} = 2{\cdot}45 \times 10^{-3}$, and are all found to be quite small; e.g. for the Sun, $N_\infty = 1$, as compared with 0·011 given by (55). Thus for values of N_∞ high enough for accretion to be significant, (84) determines the radius of the H II zone, and the values found are necessarily less than the critical radius $2{\cdot}45 \times 10^{-3}$.

4.3. *Interpretation of results.*—Consider a star embedded in a cloud of density greater than the lower limit for maximal accretion. The star will then increase its mass substantially in a time short compared with its time of exhaustion of energy sources; but the increased mass leads to an increase in luminosity and surface temperature, and so to a greater emission of ultra-violet light. Hence the radius of the H II zone must gradually move outwards. Provided the supply of matter in the cloud does not run out, sooner or later the critical radius $\bar{x} = 2{\cdot}45 \times 10^{-3}$ must be reached. Further increase in ultra-violet emission will expand the H II zone beyond this limit; but, as shown in Section 2.5, the pressure is then unable to drive cool material into the hot zone, so that a steady state cannot be set up. Thus the ultra-violet light is not extinguished, but heats up a still larger zone.

At first, it might appear plausible that a new steady state is reached, with the radius of the H II zone $\bar{x} \simeq 0{\cdot}1$; for it is known from Table IV that with this value of $\bar{x}$ there exists a steady-state solution belonging to Sequence (*a*), with the density at infinity precisely that corresponding to the limiting solution of Sequence (*b*). The value of λ for this solution is about $\frac{1}{25}$ of the maximal value, so that the accretion rate would be considerably lower than in the previous state, but we should still have the H II zone limited—because of the high densities near the star—to a much smaller sphere than that predicted by Strömgren. However, it is easy to show that such a state is essentially unstable. A slight increase in ultra-violet emission, due either to a perturbation or to a secular increase in mass, immediately expands the H II sphere; but, in striking contrast to the behaviour of Sequence (*b*) solutions, and those of Sequence (*a*) beyond the peak found for $\bar{x} = \frac{2}{3}$, increase in $\bar{x}$ *lessens* the absorptive power of the H II zone, as shown by the increase of the computed values of N_∞ with increasing $\bar{x}$ (*cf.* Table IV). Thus a slight excess of

ultra-violet light over the value for equilibrium immediately leads to a state in which the gas is still more unable to absorb it, so that the expansion must continue. If the cloud is of moderate mass, the large increase in the thermal energy of a large fraction of the mass may destroy the gravitational stability of the cloud and scatter it, with interesting dynamical consequences. A more massive cloud will be able to preserve its stability; the ultimate steady state reached will be the one in Sequence (*a*) with $\bar{x} \simeq 118$, since a sphere of this radius corresponds to the same density at infinity as does the limiting Sequence (*b*) solution. The accretion rate is quite negligible, and the system is effectively as described by Strömgren.

The next problem concerns the way in which the initial state of accretion is reached. It must again be emphasized that the moderate densities given in Table V are due to the shielding effect of the star's gravitational field. A star condensing from a dense cloud, and continuing to accrete further matter from its birth, satisfies the shielding condition from the start, so that the use of the density function z in the integral in (55) is justified. On the other hand, a star which moves into a cloud from outside will *initially* ionize a zone of roughly uniform density. If the cloud is massive enough to withstand the heating of part of itself up to 10^4 deg. K, then an initial state of equilibrium will be approached as expansion of the cloud and consequent decrease in density lead to equality of pressure. The radius of the H II zone will be that given by Strömgren's theory, with $\frac{1}{3}\bar{x}^3$ substituted for $\int_{x_0}^{\bar{x}} x^2 z^2 \, dx$ in (55). However, once the expansion has effectively ceased, infall of matter on to the star must commence, and the consequent increase of densities near the star must lead to greater ultra-violet absorption and a shrinking of the H II zone.

The ultimate state reached depends critically on whether the quantity $N_\infty \sqrt{B}$ is less than or greater than the maximum value 0·71 found in Table IV for $\bar{x} = \frac{2}{3}$. If N_∞ is so small that $N_\infty \sqrt{B} < 0{\cdot}71$, then the contracting H II zone must reach a new stable equilibrium radius $\bar{x} > \frac{2}{3}$, with a resulting accretion rate that is quite negligible. The fact that the lower limit to the densities for maximal accretion is less than $0{\cdot}71/\sqrt{B}$ (*cf.* Tables IV and V) is of no avail, as the system cannot reach a state with $\bar{x} \leqslant 2{\cdot}45 \times 10^{-3}$.

If $N_\infty \sqrt{B} > 0{\cdot}71$, the situation is quite different. The initial value of $\bar{x}$, found from Strömgren's equation

$$BN_\infty^2 \frac{\bar{x}^3}{3} = 1, \tag{85}$$

may be greater than or less than $\frac{2}{3}$, depending on the value of N_∞; but even if it is greater than $\frac{2}{3}$, the subsequent contraction of the H II zone cannot be halted at a smaller radius, $\bar{x} > \frac{2}{3}$, as by hypothesis the cloud density is too great. Neglecting for a moment the increasing influence of accretion heating, the contraction must continue until a Sequence (*b*) state is reached, so that rapid accretion can take place.

As an example, consider a cloud of density $N_\infty = 10^3$. Then the critical stellar parameter B is, from

$$N_\infty \sqrt{B} = 0{\cdot}71, \tag{86}$$

given by $\log_{10} B = \bar{7}{\cdot}7$. Assuming $T' \propto M'$, $L' \propto M'^{5{\cdot}2}$, (51) and (52) give $M' = 1{\cdot}75$. From (48) and (85) the initial radius of the H II zone is about 0·016 parsec. From (86), a B2 star will need to move into a cloud of density greater than $2{\cdot}75 \times 10^5$ if it is to be able subsequently to accrete; the corresponding value for an A0 star

is $N_\infty = 1{\cdot}1 \times 10^4$. For stellar types earlier than B2, it is seen from (73) that radiation pressure at the edge of the H II zone defined by (85) is no longer negligible, but in any case the densities required to satisfy (86) for such stars are larger than any observed. Thus radiation pressure may become important only when the system in any case cannot reach a state of rapid accretion.

It remains to be shown that accretion heating is not important in this context. Consider a system in which only accretion heating is operative; then the equation analogous to (55) is

$$3{\cdot}9 \times 10^{-6} \frac{M'}{T'^{5/2}} (\lambda N_\infty) \int_{x_0}^{\bar{x}} \frac{dx}{x^2 y^2} = 1. \tag{87}$$

This reduces to (84) when λ is put equal to 1·12. Then for varying $\bar{x}$, this equation will behave similarly to (55); in particular, the computed values of N_∞ will possess a maximum, which from (77) and (78) is found to be near $\bar{x} = \frac{1}{3}$. Then (87) reduces to

$$N_\infty \frac{M'}{T'^{5/2}} = 2. \tag{88}$$

In order that, with N_∞ given by (86), accretion heating should not prevent contraction to a Sequence (*b*) state, by providing a steady state solution with $\bar{x} > \frac{1}{3}$, the value of N_∞ from (86) should be greater than that from (88). By inspection this is shown to be the case for the three values of B just discussed. For very much smaller stars, N_∞ from (88) will exceed that computed from (86), but the density given by (88) is then far too small for accretion to be significant: any cloud of reasonable density must automatically be denser than both the critical values from (86) and (88). We may therefore conclude that in all cases of interest, if a star of parameter B entering a cloud of density N_∞ is to reach a state of maximal accretion, the condition $N_\infty \sqrt{B} > 0{\cdot}71$ is sufficient (as far as the considerations of this paper are concerned). Accretion heating is never able to prevent the H II zone from contracting to the required size, although as shown in Section 4.2, it may very well dominate over natural heating in the ultimate steady state.

It must of course be remarked that this paper deals with only one aspect of the accretion problem, and the results found must necessarily be combined with those found by other workers in the field. Thus McCrea's conclusions on the velocity with which a star enters the cloud (**4**) are of crucial importance, as higher-velocity stars will never be reduced to rest, and what accretion does take place will be described by Hoyle and Lyttleton's formula (**1**). Departures from symmetry due to the presence of a magnetic field, or angular momentum in the cloud, are likely to play an important part in the theory, but discussion of these problems is beyond the scope of this paper.

Acknowledgments.—The writer is indebted to Professor T. G. Cowling for helpful discussions and for his criticisms of the manuscript, and to the University of Leeds for the award of an I.C.I. Research Fellowship.

Note added in proof.—Since this work was completed, the author has learned that Dr E. Schatzman has arrived independently at similar conclusions, to be published in the Proceedings of the *Second Symposium on Gas Dynamics of Interstellar Clouds*, Cambridge, 1953. Dr Schatzman has priority by this publication.

Dept. of Mathematics,
The University,
Leeds, 2:
1954 *March.*

References

(1) H. Bondi, *M.N.*, **112,** 195, 1952.
(2) H. Bondi and F. Hoyle, *M.N.*, **104,** 273, 1944.
(3) K. N. Dodd, *Proc. Camb. Phil. Soc.*, **49,** 486, 1953.
(4) W. H. McCrea, *M.N.*, **113,** 162, 1953.
(5) L. Spitzer, Jr. and M. P. Savedoff, *Ap. J.*, **111,** 593, 1950.
(6) B. Strömgren, *Ap. J.*, **89,** 526, 1939.
(7) L. Biermann and A. Schlüter, paper submitted to Second Symposium on Gas Dynamics of Interstellar Clouds, Cambridge, 1953.
(8) A. S. Eddington, Bakerian Lecture, *Proc. Roy. Soc.* A, **111,** 424, 1926.
(9) S. Rosseland, *Theoretical Astrophysics*, Chap. X, Oxford, 1936.
(10) S. Chandrasekhar, *Introduction to the Study of Stellar Structure*, Chap. VII, Chicago, 1939.
(11) New York W.P.A. 1940, *Tables of sine, cosine and exponential integrals*, New York, Federal Works Agency.
(12) R. v. d. R. Woolley and D. W. N. Stibbs, *The Outer Layers of a Star*, Chap. XI, Oxford, 1953.
(13) J. H. Oort, private communication.
(14) F. Hoyle, *Some Recent Researches in Solar Physics*, Cambridge, 1949.
(15) W. Becker, *Sterne und Sternsysteme*, Chap. I, p. 66, Steinkopff, 1950.

STAR-STREAMING FROM THE STARS OF SPECTRAL TYPE B

T. R. Tannahill

(Communicated by the Director, University Observatory, Glasgow)

(Received 1954 March 30)

Summary

The proper motions of 1536 stars of spectral types O and B in the Boss *General Catalogue* have been analysed, according to the two-streams hypothesis, by Eddington's method. It is found that the phenomenon of star-streaming is clearly shown. The galactic coordinates of the vertex of star-streaming are ($343°{\cdot}3$, $-1°{\cdot}6$), and the equatorial coordinates of the solar apex ($260°{\cdot}7$, $+37°{\cdot}3$). The stars in the regions containing the Scorpio–Centaurus group exhibit anomalous behaviour.

---

1. The B-type stars have always been regarded as an anomalous group as regards the phenomenon of star-streaming. Eddington (**1**), in a review of the existing knowledge of star-streaming in 1914, summed up the position as follows: " A more minute investigation of this phenomenon shows that it is complicated by differences in the behaviour of stars according to their spectral type. An analysis which treats the heterogeneous mass of the stars as a whole without any separation of the different types will fail to give a complete insight into the phenomenon. But, until a great deal more material is accumulated, this interrelation of stream motions and spectral type cannot be worked out very satisfactorily. The outstanding feature, however, is that the stars of the Orion Type (Type B) seem not to share to any appreciable extent in the star-streaming tendency. Their individual motions, which are always very small, are nearly haphazard, though the apparent motions are, of course, affected by the solar motion. They thus form a third system, having the motions of neither of the two great streams, but nearly at rest relatively to the mean of the stars." Later, the position as regards the B-type stars is again unequivocally stated: " . . . the stream-motion appears with remarkable suddenness. Throughout Type B, even up to B8 and B9, the two star-streams are unperceived ; but in the next type A, the phenomenon is seen in its clearest and most pronounced form."

Opinion has not changed since then. There are many reasons why investigations of the B-type stars from this particular point of view tend to be discouraged. They are not very numerous, and investigations on star-streaming generally require a fair number of stars grouped in limited areas of the sky. Their proper motions are generally small; Eddington, indeed, removed them (**2**) from the material of the Boss *Preliminary General Catalogue* before investigating star-streaming with the data of this catalogue, for this very reason. Their radial velocities are affected by two principal uncertainties: the high proportion of spectroscopic binaries and a large K-term. Their distribution in the sky is far

from uniform; apart from their concentration near the galactic equator (which is not in itself a disadvantage) the distribution within this zone is very irregular, and a considerable number of the stars appear to form small groups or clusters.

2. The present paper is an attempt to exploit the accurate proper motions of the Boss *General Catalogue* (**3**) in order to investigate the problem anew. There are in this catalogue 1625 O- and B-type stars, of which seven belonging to the Pleiades and all those outside the zone $\pm 30°$ galactic latitude have been omitted in this investigation. There remain 1536 for discussion—a number which is just sufficient to populate ten galactic regions adequately. Consideration of the treatment to be given to the " clusters " delayed the start of this investigation for some time. In the end, the treatment accorded was the simplest possible—the clustering tendency was ignored.

The material was grouped into ten regions, each consisting of a " square " of north galactic latitude combined with the diametrically opposite region of south galactic latitude. Details of these regions are given in Table I. The

TABLE I

Region	Limits of galactic longitude		Centre l	Centre b	Number of stars	Analysis of drift-curves: Drift I hV_1	Drift I N_1	Drift I θ_1	Drift II hV_2	Drift II N_2	Drift II θ_2
1	0°→	30°	21°	+ 8°·5	144	0·75	55	115°	0·65	60½	260°
2	30	60	47	+ 7	240	1·2	79½	135	0·45	121	210
3	60	90	77	+ 6	212	1·1	100	120	0·6	79	210
4	90	130	111	+ 7	134	1·05	61	100	0·4	40½	170
5	130	160	142	+ 6	131	1·1	43	70	0·7	59½	150
6	160	210	185	+ 7	105	0·4	48	170	0·8	43	120
7	210	260	240	+ 7	171	1·3	67	225	0·4	72½	170
8	260	290	275	+ 8	126	2·2	77	242½	0·5	32	170
9	290	330	308	+ 8	145	2·3	95	257½	0·9	33½	200
10	330	360	350	+13	128	0·5	67	280	0·45	51	230

coordinates adopted for the centre of a region have been chosen after consideration of the distribution of stars in the region. The centre is a median position with respect to galactic latitude and longitude. Systematic corrections to the catalogue proper motions were applied as in a previous paper on the later-type stars (**4**). The position angles of the proper motions were then obtained. It was deemed advisable to convert these to galactic position angles, and this was done using galactic parallactic angles obtained from charts which were constructed from the Lund Tables (**5**). This procedure avoided any need for applying corrections for convergency of meridians. The system of weighting adopted was the same as in the previous paper (**4**), namely, a star is assigned half-weight if the probable errors of the centennial proper motion in right ascension and in declination both exceed $0''·075$, or if either exceeds $0''·085$. Counts of the numbers of stars, in each region, moving in galactic position angles between $\theta - 5°$ and $\theta + 5°$ (θ being a multiple of 10°) were then made, the figures being smoothed by taking the running means of three adjacent sectors. These observed frequency curves are indicated by the full lines in Figs. 1 and 2, which also show the " theoretical " drift-curves for each region which follow from the analysis by Eddington's " trial-and-error " method (**2**). The constants hV, θ and N—

the projection of the space-velocity of the drift on the tangent-plane at the centre of the region, the position angle of the direction to the drift apex, and the weight of stars belonging to the drift—are given, for each drift, in Table I.

3. It is clear from an examination of Table I and the drift-curves of Figs. 1 and 2 that the proper motions of the B-type stars are not sufficiently represented by a single drift. In each region it has been necessary, in order to secure a satisfactory fit, to assign a considerable proportion of the stars to a second drift, the number in some cases exceeding that allotted to Drift I. In two regions (8 and 9) there is a great preponderance of Drift I stars, accompanied by values of hV_1

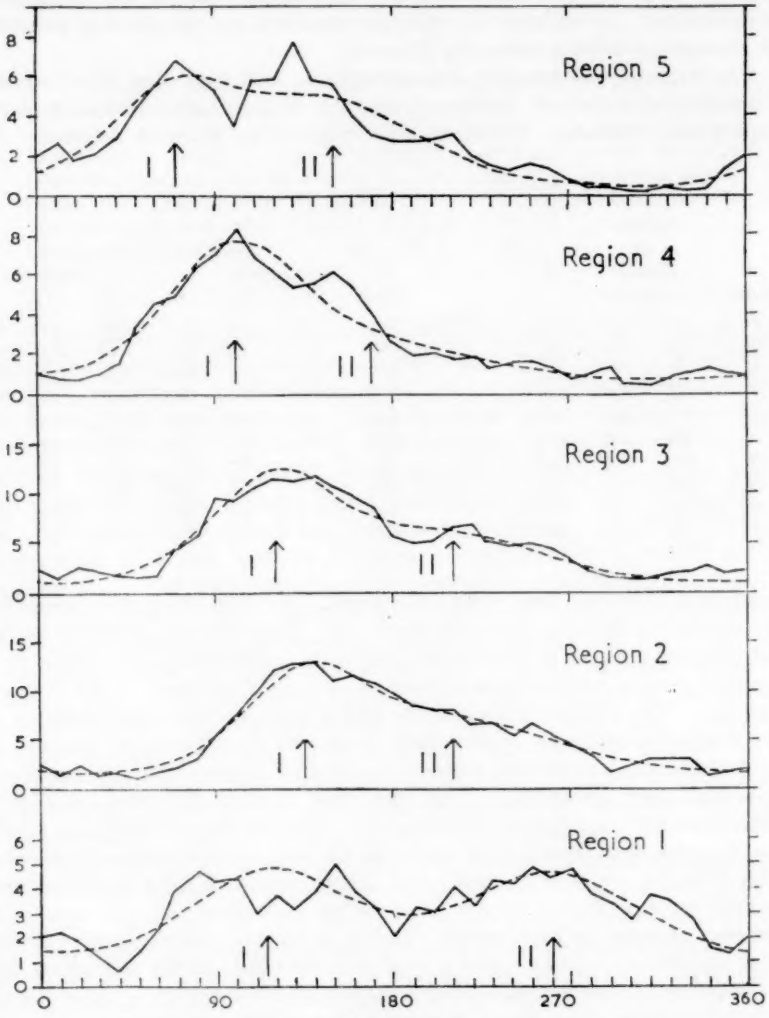

FIG. 1.—*Frequency curves with galactic position angle, regions 1–5.*
——— *observed values, running means of three adjacent sectors.*
– – – – *theoretical drift-curves from Eddington's analysis.*

which are exceptionally high. The divergences in these regions are so considerable that the regions concerned have been omitted in arriving at the final solutions; but it should be noted that the divergences relate to Drift I, the existence of which is not in question. It is probable that in these regions an alien population exists whose characteristics approximate in some respects to those of Drift I—this would account for the large number of stars assigned to Drift I, and for the high value of hV_1. Divergences in this region of the sky were not indeed unexpected: this is the area containing the troublesome Scorpio–Centaurus group, which cannot, evidently, be ignored.

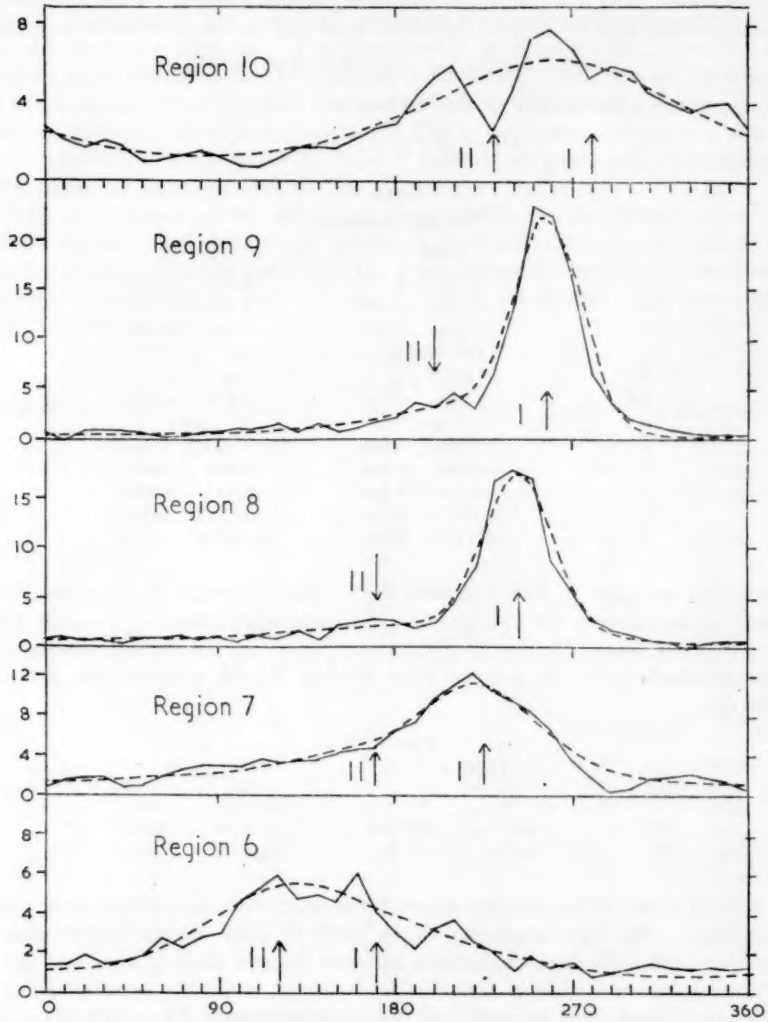

FIG. 2.—*Frequency curves with galactic position angle, regions 6–10.*
——— *observed values, running means of three adjacent sectors.*
- - - - *theoretical drift-curves from Eddington's analysis.*

4. From the analysis given in Table I (omitting regions 8 and 9) two equations of condition are obtained for each region:

$$x \sin l - y \cos l = -hV \sin \theta.$$

$$x \cos l \sin b + y \sin l \cos b - z \cos b = -hV \cos \theta.$$

Here x, y, z are the linear components of the space-velocity of a drift relative to the Sun, referred to the usual axes associated with the galactic equator (**5**), l and b the galactic longitude and latitude of the centre of the region as given in Table I. In forming the normal equations equal weight was given to each of the eight regions used. The solution of the normal equations gives x, y, z from which the galactic coordinates L and B of each drift apex may be found from the equations

$$\tan L = y/x, \qquad \tan B = z/(x^2+y^2)^{1/2},$$

and the space-velocities hW of the drifts from

$$hW = (x^2+y^2+z^2)^{1/2}.$$

TABLE II

The drift constants

	Drift I	Drift II
x	$-1{\cdot}165 \pm 0{\cdot}126$	$+0{\cdot}028 \pm 0{\cdot}058$
y	$-0{\cdot}132 \quad 0{\cdot}116$	$-0{\cdot}490 \quad 0{\cdot}054$
z	$-0{\cdot}375 \quad 0{\cdot}087$	$-0{\cdot}409 \quad 0{\cdot}041$
L	$186^\circ{\cdot}5 \quad 5^\circ{\cdot}6$	$273^\circ{\cdot}3 \quad 6^\circ{\cdot}8$
B	$-17^\circ{\cdot}7 \quad 4^\circ{\cdot}3$	$-39^\circ{\cdot}8 \quad 4^\circ{\cdot}2$
hW	$1{\cdot}231 \quad 0{\cdot}123$	$0{\cdot}639 \quad 0{\cdot}049$
n	521	526
X	$+0{\cdot}063 \pm 0{\cdot}044$	$+0{\cdot}134 \pm 0{\cdot}021$
Y	$+1{\cdot}194 \quad 0{\cdot}120$	$-0{\cdot}005 \quad 0{\cdot}055$
Z	$-0{\cdot}294 \quad 0{\cdot}143$	$-0{\cdot}625 \quad 0{\cdot}067$
A	$87^\circ{\cdot}0 \quad 2^\circ{\cdot}1$	$357^\circ{\cdot}8 \quad 24^\circ{\cdot}3$
D	$-13^\circ{\cdot}8 \quad 6^\circ{\cdot}5$	$-77^\circ{\cdot}9 \quad 1^\circ{\cdot}8$

The results are given in Table II, with the probable errors. The corresponding equatorial coordinates are also given to facilitate comparison with results from other types of stars. Table III gives a comparison of the present results with those obtained from the galactic zone of type A5–M stars of the previous paper (**4**).

TABLE III

	Drift I		Drift II	
	A5–M	B	A5–M	B
A	$94^\circ{\cdot}1$	$87^\circ{\cdot}0$	$305^\circ{\cdot}2$	$357^\circ{\cdot}8$
D	$-10^\circ{\cdot}6$	$-13^\circ{\cdot}8$	$-70^\circ{\cdot}9$	$-77^\circ{\cdot}9$

Bearing in mind the probable errors involved, the results indicate satisfactory accordance. The right ascension of the Drift II apex for the B-type stars is somewhat high—the angular distance between the two Drift II apices is 15°.

The important feature of the solution, however, is not the actual position of the Drift II apex, but the fact that it is determinable. The analysis for the separate regions, as exhibited in Table I and in Figs. 1 and 2, shows that a single-drift hypothesis is insufficient to explain the observed distribution, and gives

the constants describing a second drift, in each separate region, necessary to produce accordance. The solution given in Table II indicates that the second drifts determined from the separate regions can be interpreted as the regional symptoms of a drift which is common to all the regions. In other words, the B-type stars show similar drift-characteristics to the other types of stars.

5. From the values of L, B and hW as given in Table II it is possible to calculate the theoretical values of hV_c and θ_c in each region. These are shown in Table IV, together with the residuals $hV_c - hV$ and $\theta_c - \theta$. Considering the paucity of the data, the residuals are not unduly large, except for region 5, where $\theta_c - \theta_1$ is 49°. Reference to Fig. 1 shows the difficulty of determining θ_1 in this region. As expected, large residuals occur in hV_1 in regions 8 and 9 (which were excluded from the solution). The directions θ_1 in these regions, however, are normal—an indication that, as suggested in Section 3, the abnormal population has some characteristics similar to those of Drift I. The Drift II residuals are quite satisfactory. It is to be noted that this is true even in regions 8 and 9, where the difficulties of determination of θ_2 and hV_2 are much greater on account of the apparent preponderance of Drift I stars.

The convergence of the directions of the drifts, as determined from each region, towards the appropriate apices, is best indicated by calculating the angular distance β of the apex from the great circles defined by the directions. Values of β are shown in Table IV, together with the distances λ of each region from the drift apices.

TABLE IV

Drift I

Region	θ_c	$\theta_c - \theta_1$	β_1	λ_1	hV_c	$hV_c - hV_1$
	°	°	°	°		
1	124·7	+ 9·7	2·8	163·1	0·36	−0·39
2	109·0	−26·0	16·7	139·1	0·81	−0·39
3	106·7	−13·3	12·5	110·4	1·15	+0·05
4	109·7	+ 9·7	9·5	78·5	1·21	+0·16
5	119·2	+49·2	35·4	49·9	0·94	−0·16
6	176·6	+ 6·6	2·8	24·8	0·52	+0·12
7	244·2	+19·2	16·2	58·3	1·05	−0·25
8	252·4	+ 9·9	9·9	91·0	1·23	−0·97
9	254·1	− 3·4	2·9	122·4	1·04	−1·26
10	251·5	−28·5	7·8	163·4	0·35	−0·15

Drift II

Region	θ_c	$\theta_c - \theta_2$	β_2	λ_2	hV_c	$hV_c - hV_2$
	°	°	°	°		
1	230·7	−29·3	27·5	109·0	0·60	−0·05
2	224·2	+14·2	11·3	127·2	0·51	+0·06
3	201·1	− 8·9	5·3	143·2	0·38	−0·22
4	156·5	−13·5	8·0	143·6	0·38	−0·02
5	135·3	−14·7	12·0	124·8	0·52	−0·18
6	129·7	+ 9·7	9·7	93·2	0·64	−0·16
7	149·4	−20·6	16·9	56·0	0·53	+0·13
8	181·8	+11·8	8·7	47·8	0·47	−0·03
9	211·2	+11·2	9·5	57·6	0·54	−0·36
10	228·4	− 1·6	1·6	88·4	0·64	+0·19

6. The linear components x_v, y_v, z_v of the motion of Drift I relative to Drift II are shown in Table V, which also contains the galactic longitude l_v and the galactic latitude b_v of the vertex of star-streaming and the relative space-velocity

Ω of the drifts. The most noticeable feature of these results is the unexpectedly close agreement of the vertex position obtained here with the values which are normally found in such investigations, namely, (343°, −2°). Considering the probable errors involved, the closeness of the agreement must be regarded as fortuitous. But the result removes any shadow of doubt that the B-type stars exhibit the phenomenon of star-streaming.

Table V also gives the characteristics of the solar motion relative to the B-type stars. The weights of stars in the two drifts (omitting regions 8 and 9) are 521 and 526. The ratio of these is so close to unity that equality was assumed in the solution for the solar motion. The results are not notably different from those obtained in other investigations.

TABLE V

The vertex of star-streaming and the solar motion

	Vertex		Solar motion	
x_V	+1·193	± 0·139	l_0	28°·7
y_V	−0·358	0·127	b_0	+31°·1
z_V	−0·034	0·096	hU_0	0·757
l_V	343°·3	5°·9	A_0	260°·7
b_V	−1°·6	4°·4	D_0	+37°·3
Ω	1·247	0·138	n_1/n_2	0·99

University Observatory,
Glasgow, W.2:
1954 *March* 29.

References

(1) A. S. Eddington, *Stellar Movements and the Structure of the Universe*, pp. 35, 38, Macmillan and Co., 1914.
(2) A. S. Eddington, *M.N.*, **71**, 4, 1910.
(3) Benjamin Boss, *General Catalogue of* 33 342 *Stars*, Carnegie Institute of Washington, Publication 468, 1937.
(4) T. R. Tannahill, *M.N.*, **112**, 3, 1952.
(5) John Ohlsson, *Annals of the Observatory of Lund*, **3**, 1932.

THE CONSTANTS OF THE STAR-STREAMS AND OF THE VELOCITY ELLIPSOID FROM THE CAPE PHOTOGRAPHIC PROPER MOTIONS OF 19 839 STARS

D. G. Ewart

(Communicated by the Director, University Observatory, Glasgow)

(Received 1954 August 23)

Summary

The proper motions of the *Cape Catalogue of* 20 554 *Faint Stars*, 1939, have been analysed on the two-stream and the ellipsoidal hypotheses. A total of 19 839 stars of spectral classes later than B8 has been used in the discussion.

The results agree well with those from the analysis of the proper motions of the *Cape Zone Catalogue*, 1900, and confirm to some extent the variation with spectral class determined in that investigation.

There is a slight decrease in the longitude of the major axis of the velocity ellipsoid for the faint stars compared with the brighter stars of the *Zone Catalogue*, 1900. A vertex deviation of some 15° still remains.

---

1. The proper motions which have been examined in the present work are those of the *Catalogue of 20 554 Faint Stars*, 1939, published by the Royal Observatory, Cape of Good Hope (**1**). The stars in this catalogue are all in the Cape Astrographic Zone and the catalogue is a sequel to an earlier volume (**2**), published in 1936, which contained the proper motions of the stars in the *Zone Catalogue of* 20 843 *Stars*, 1900 (**3**). The 1936 and 1939 volumes are hereafter referred to as the first and second volumes respectively.

The photographs used in the determination of the proper motions and the star positions were taken in three series—1892 to 1896, 1897 to 1905 (with a few exceptions) and 1923 to 1928, the last series being taken through the glass. The first volume contains all the stars brighter than magnitude 9·00 on the C.P.D. scale, including 8 560 standard stars observed with the 8-inch transit circle for the reduction of the plates. The second volume contains all the stars of magnitudes 9·1 to 9·5 on the C.P.D. scale and also lists 2 432 stars fainter than magnitude 9·5—1 120 not being in the C.P.D.—which showed total relative proper motions exceeding 5″/century. The two catalogues thus contain over 40 000 of the 127 877 C.P.D. stars in the zone, and are complete to at least magnitude 10·2 on the Cape Photographic Magnitude Scale.

The reductions from relative to absolute proper motions were made by applying three series of corrections. They were:—

(*a*) a curvature correction to reduce from rectangular coordinates to R.A. and Dec.,

(*b*) a correction due to the position of the star image on the plate and its magnitude, and

(*c*) a correction for the systematic motion of the reference stars due to solar motion and galactic rotation. For the latter correction Van Rhijn and Bok's (**4**) results were used, the mean magnitude of the reference stars being 11·2. The

measurements and reductions were performed initially under the direction of Sir Harold Spencer Jones and later under Dr J. Jackson.

2. The proper motions of the first volume have been analysed on the two-stream theory by Professor W. M. Smart and Dr T. R. Tannahill (**5, 6**) and on the ellipsoidal theory by Dr J. Jackson (**7**). Their results clearly demonstrated the presence of preferential motion and were in substantial agreement with the results of previous investigations of other catalogues. The value determined for the declination of the solar apex was, however, rather lower than that normally found.

In this investigation the proper motions of 19 839 stars in the second volume have been analysed both on the two-stream theory—by Eddington's trial and error method—and on the ellipsoidal hypothesis by Schwarzschild's automatic method. Stars of spectral type earlier than B8 have been omitted by reason of their restricted numbers and extreme galactic concentration, and binary stars have been treated as single stars. Variable stars have also been omitted. Included in the 19 839 stars are 1735 with unclassified spectra, these stars being mainly among the stars fainter than C.P.D. magnitude 9·5.

3. For the purpose of this investigation the zone was divided into 16 regions each of one and a half hour's width in R.A., and scatter diagrams were prepared. Details of the centres of the regions and the number of stars in each region are given in Table IV. From the scatter diagrams counts of the numbers of stars in successive 10° sectors of position angle were made. In preparing these counts the position angles of stars in the two outer half-hours of each region were corrected for convergency of the meridians. The counts thus obtained were then smoothed by taking running means of three successive sectors, hence yielding the final distribution counts. These counts are the subjects of the analyses. The methods of analysis are described in references (**5**) and (**7**).

In both methods of analysis the closeness of the agreement between the observed and calculated distributions of the stars in position angle depends on the smoothness of the observed distribution counts. In the Cape Astrographic Zone the smoothness of the corresponding curves depends mainly upon the number of stars involved, and consequently upon the galactic latitude. The effects of irregularities are reflected in the uncertain or anomalous values obtained for the various parameters. In the two-stream analysis the effect of the irregularities is thrown almost entirely into Drift II as an increased uncertainty in the determination of its local velocity and direction. It should be noted here that as much of the zone is near the Drift II apex, the determination of Drift II in any region is always much more uncertain than that of Drift I.

In the analysis by Schwarzschild's automatic method, the effect of irregularities in the distribution counts is mainly reflected in the determinations of the position angles of the major axis of the velocity ellipsoid and of the solar motion, and, to a lesser extent, in the derived values of the axis-ratio and projected solar velocity. If anything, the automatic method is more sensitive to irregularities than the drift analysis, as the five constants determined for each region in the latter method are not so interdependent. The irregularities may, however, be so distributed as to have no effect at all in the determinations of the parameters by either method. There does not appear to be any evidence in the present case to decide in favour of one or other of the methods of analysis, as, although in the two-stream analysis the investigator is frequently required to decide which, of two or more calculated curves, is the best representation of the observed distribution, the evaluation of

the ellipsoidal parameters can often be quite largely affected by a single irregularity in the observed distribution or a small error in the derived values of the two position angles θ_1 and θ_0.

4. In this investigation five groupings of the material have been employed and analysed by each method. The first solution was for all 19 839 stars. The other groupings were by spectral classes. As it was found in the analysis of the first volume that the behaviour of the A-type stars (spectral types B8–A5) was anomalous, they were not treated separately. An analysis of this group of stars would also be hampered by their extreme galactic concentration. The three groupings used were (1) A5–F5, (2) F8–G5 and (3) K0–M. The final grouping was of spectral types A5–M.

The complete results of the analysis are given in the appendix, Tables V to XVII, in which the symbols $\Delta\theta$ and ΔhV refer to the differences between the calculated and observed values of the respective position angles and drift velocities (i.e. $\Delta\theta = \theta_{calc} - \theta_{obs}$; $\Delta hV = hV_{calc} - hV_{obs}$). The other symbols are standard, e.g. Smart (**8**).

Tables V to IX list the details of the drift analyses for each region and group. The convergency of the great circles defined by the drift position angles is best shown by the angle β between the apex and the great circle defined by the position angle obtained for the region. It will be noticed that, although the values are satisfactorily small for Drift I, there is a greater degree of scatter for Drift II. The degree of convergency is less in each case than was the case for the first volume. This is a consequence of the curves in this investigation being less smooth than in Smart and Tannahill's investigation. This may have been caused by the effects of accidental errors in the small proper motions.

Tables X to XIV give the results of the analyses by Schwarzschild's automatic method. In this case the divergences between the calculated and observed position angles are generally much smaller and there is little doubt about the degree of convergency.

In the case of the A5–F5 stars it was found necessary to omit 4 regions, their distribution counts being so irregular that no weight could be attached to their analyses.

Tables XV and XVI give the final results of the analyses by the two-stream method, and the derived positions of the vertex of star-streaming and the solar motion. The results of Smart and Tannahill's investigation of the first volume are given in brackets. Table XVII gives the values of the ellipsoidal constants and solar motion, Jackson's results being given in brackets for comparison.

Finally in Table XVIII the results of the two methods of analysis are compared for the vertex and the solar motion.

5. It can be seen from these tables that the positions of the drift apices and velocities of each group differ little from the values obtained from the first volume. When the probable errors of the determinations are considered then it can be seen that the differences are so small that we may take the sets of results as being identical for Drift I and almost so for Drift II. The increase of hW_1 with advancing spectral type noted by Smart and Tannahill (**6**) is not so clearly evident in this case, but may still be present when the larger probable errors are considered.

In Table I below the drift constants for each volume are compared with those obtained by Tannahill (**9**) from his analysis of the Boss G.C. It will be observed that the results are again in good agreement, the main difference being

TABLE I

Comparisons of Drift Constants

	All Stars			A5–F5			F8–G5			Ko–M			A5–M		
A_1	88°·0	90°·5		91°·0	90°·0	91°·1	90°·7	90°·0	92°·9	91°·1	91°·5	96°·0	90°·8	89°·5	93°·4
D_1	− 8°·5	− 7°·3		− 7°·5	−10°·8	− 8°·9	− 5°·1	− 8°·9	−10°·3	− 3°·9	− 8°·8	−10°·8	− 9°·7	− 9°·8	− 9°·9
hW_1	1·463	1·498		1·692	1·576	1·770	1·539	1·615	1·564	1·446	1·385	1·385	1·545	1·454	1·500
A_2	303°·6	289°·0		322°·2	321°·7	301°·0	288°·4	286°·5	273°·5	295°·2	256°·0	265°·8	304°·9	279°·5	274°·4
D_2	−75°·0	−79°·0		−69°·4	−80°·0	−63°·4	−77°·7	−74°·1	−71°·0	−80°·4	−71°·6	−74°·4	−76°·2	−76°·3	−70°·1
hW_2	0·650	0·614		0·661	0·592	0·735	0·686	0·694	0·889	0·595	0·616	0·770	0·649	0·604	0·797
	(*a*)	(*b*)	(*c*)	(*a*)	(*b*)	(*c*)	(*a*)	(*b*)	(*c*)	(*a*)	(*b*)	(*c*)	(*a*)	(*b*)	(*c*)

(*a*) *Cape—Smart and Tannahill.* (*b*) *Present Work.* (*c*) *G.C.—Tannahill.*

TABLE II

Comparison of Vertices and Solar Motion—from Drift Analysis

	All Stars			A5–F5			F8–G5			Ko–M			A5–M		
G	343°·2	343°·4		344°·5	347°·8	348°·6	340°·2	343°·0	341°·7	340°·6	343°·0	342°·4	342°·0	344°·2	343°·1
g	+ 0°·5	+ 0°·1		+ 2°·8	+ 1°·5	− 1°·2	−1°·2	− 0°·1	− 2°·0	− 1°·4	+ 2°·6	− 3°·4	− 1°·8	+ 2°·0	− 1°·7
k	1·638	1·648		1·873	1·639	2·075	1·756	1·697	1·912	1·606	1·601	1·638	1·747	1·618	1·816
A_0	265°·1	269°·4		265°·3	268°·3	266°·0	268°·9	268°·6	272°·8	269°·5	273°·2	277°·8	267°·5	268°·8	273°·2
D_0	+26°·1	+25°·4		+25°·6	+22°·4	+28°·1	+29°·2	+25°·5	+37°·4	+25°·3	+27°·0	+40°·3	+27°·3	+25°·9	+35°·4
hU_0	0·879	0·800		0·934	1·047	0·948	0·817	0·972	0·883	0·780	0·808	0·770	0·838	0·891	0·834
N_1/N_2	1·410	1·708		1·173	1·781	1·22	1·038	1·473	1·18	1·080	1·398	1·02	1·102	1·497	1·19
	(*a*)	(*b*)	(*c*)	(*a*)	(*b*)	(*c*)	(*a*)	(*b*)	(*c*)	(*a*)	(*b*)	(*c*)	(*a*)	(*b*)	(*c*)

(*a*) *Smart and Tannahill—Cape.* (*b*) *Present Work.* (*c*) *Tannahill—G.C.*

TABLE III

Comparison of Ellipsoid Constants and Solar Motion

	All Stars			A5–F5			F8–G5			Ko–M			A5–M		
G	343°·6	340°·0		348°·1	345°·8	342°·6	342°·1	342°·0		340°·3	337°·8	335°·6		341°·8	337°
g	+ 2°·1	+ 0°·8			− 6°·0	− 6°·7		+ 0°·6			− 0°·4	− 5°·1		− 0°·3	− 6°
K/H	0·62	0·602		0·55	0·676	0·574	0·56	0·554		0·65	0·606	0·67		0·601	0·62
A_0	266°·9	271°·5		266°·0	266°·9	263°·5	269°·9	271°·2		272°·3	275°·4	277°·6		269°·5	273°·1
D_0	+28°·3	+25°·0		+23°·2	+19°·8	+28°·3	+31°·6	+30°·9		+31°·8	+24°·2	+31°·2		+29°·5	+32°·5
hU_0	0·94	0·948		1·05	1·056	0·92	0·89	0·950		0·82	0·831	0·66		0·819	0·78
	(*a*)	(*b*)	(*c*)	(*a*)	(*b*)	(*c*)	(*a*)	(*b*)	(*c*)	(*a*)	(*b*)	(*c*)	(*a*)	(*b*)	(*c*)

(*a*) *Cape—Jackson.* (*b*) *Present Paper.* (*c*) *G.C.—Delhaye.*

in the higher values of hW_2 given by the G.C. This, however, was to be anticipated as the G.C. covers the whole sky and not a zone near the Drift II apex.

In Table II the values for the vertex of star-streaming and the solar motion are compared. The deviation of the vertex is clearly shown, the positions of the vertex from each analysis being in close agreement. As a result of the higher values of hW_2 given by the G.C., the G.C. values of the relative speeds of the drifts (k) are higher than those obtained from the Cape data.

For the solar apex, a slight decrease in the right ascension and declination of the apex with advancing spectral class is noted from each set of results. For the right ascension the three sets of data for each group agree well. The low value of the declination of the solar apex noted by Smart and Tannahill and by Jackson is still evident. It must, however, be recognized that the Cape declinations will have a probable error of about 5° (as shown by the ellipsoidal results).

An outstanding feature of the table is the high values of N_1/N_2 obtained in this investigation. The smallest value obtained in this investigation is 1·4 for the Ko-M group, whereas the other investigations average 1·05. This is probably a result of the uncertainties in the determinations of Drift II.

In Table III the constants of the velocity ellipsoid are compared with Jackson's results for the first volume and with Delhaye's (**10**) analysis of the G.C. It should be noted, however, that the grouping used by Delhaye is rather different from that employed in this paper. His groups are B8–A5, Fo–F9, Ko–K2, and were further divided into regions of high or low galactic latitude. The figures given above are thus approximate means of his results.

There is some slight indication of a decrease in the longitude of the major axis for the faint stars of the second volume compared with the brighter stars of the first volume. This is not certain as it is not fully evident in the results from the drift analysis. There is no doubt that the deviation of the vertex from the centre of the galaxy remains.

6. In conclusion, the following points are to be noted:

(1) The results for the analysis of the proper motions of the second volume are in complete agreement with those obtained by Smart and Tannahill and Jackson from the first volume. The uncertainties are somewhat greater, possibly as a result of the effects of accidental errors on the small proper motions.

(2) The increase in hW_1 with advancing spectral type noted by Smart and Tannahill from the first volume is not fully confirmed. It may well have been masked by the larger probable errors involved.

(3) A decrease in the right ascension and declination of the solar apex with advancing spectral type is indicated.

(4) Abnormally high values of N_1/N_2 are obtained. These may be spurious, being probably due to uncertainties in the determination of Drift II.

(5) A slight decrease in the longitude of the major axis of the velocity ellipsoid for the faint stars compared to the bright stars of the first volume is suggested by the results.

Finally I wish to tender my thanks to the Department of Scientific and Industrial Research for the award of a maintenance grant during the tenure of which the investigation was performed.

University Observatory,
Glasgow, W.2:
1954 *August* 14.

References

(1) *Catalogue of* 20 554 *Faint Stars*, 1939, Royal Observatory, Cape of Good Hope.
(2) *Proper Motions of Stars in the Zone Catalogue of* 20 843 *Stars*, 1936, Royal Observatory, Cape of Good Hope.
(3) *Zone Catalogue of* 20 843 *Stars*, 1900, Royal Observatory, Cape of Good Hope.
(4) P. J. van Rhijn and B. J. Bok, *Groningen Publ.*, No. 45, 1931.
(5) W. M. Smart and T. R. Tannahill, *M.N.*, **100,** 30, 1939.
(6) W. M. Smart and T. R. Tannahill, *M.N.*, **100,** 688, 1939.
(7) J. Jackson, ref. (2), Intro. p. xxx.
(8) W. M. Smart, *Stellar Dynamics*, Cambridge, 1938.
(9) T. R. Tannahill, *M.N.*, **112,** 3, 1952.
(10) J. Delhaye, *Bull. Astron.*, Tome 16, p. 1, 1951.

APPENDIX

TABLE IV

Centres of Regions and Numbers of Stars

Region	R.A. h m	Number of Stars: All	A5–F5	F8–G5	Kc–M	A5–M
1	0 45	422	39	173	79	291
2	2 15	394	38	122	84	244
3	3 45	525	73	160	128	361
4	5 15	630	122	237	164	523
5	6 45	1175	251	297	293	841
6	8 15	2137	435	302	345	1082
7	9 45	2437	494	455	431	1380
8	11 15	1604	324	469	381	1174
9	12 45	1526	271	488	407	1166
10	14 15	1519	275	466	375	1116
11	15 45	2308	379	484	428	1291
12	17 15	2419	353	441	464	1258
13	18 45	955	151	315	265	731
14	20 15	627	89	264	196	549
15	21 45	600	61	264	207	532
16	23 15	561	50	231	158	439
	Totals	19 839	3405	5168	4405	12 978

TABLE V

Analysis of the Drift Curves—All Stars

R.	Drift I: hV_1	θ_1	n_1	λ_1	$\Delta\theta_1$	ΔhV_1	Drift II: hV_2	θ_2	n_2	λ_2	$\Delta\theta_2$	ΔhV_2
		°		°	°			°		°	°	
1	1·35	85	206	77·3	+ 2·3	+0·11	0·65	210	216	43·9	−14·6	−0·22
2	1·0	70	284⅔	61·9	+ 0·1	+0·32	0·90	215	129⅓	47·9	−21·0	−0·44
3	1·0	40	253⅔	48·5	+ 8·2	+0·12	0·60	175	271⅓	51·3	+15·8	−0·12
4	1·0	20	253⅔	39·8	− 1·6	−0·04	0·25	180	376⅔	53·7	+ 6·6	0·25
5	1·0	340	600⅓	39·6	+ 3·2	−0·04	0·30	230	574⅔	54·8	−48·5	0·20
6	1·2	305	1354⅓	48·0	+ 8·0	−0·09	0·20	210	782⅔	54·6	−33·4	0·30
7	1·5	290	1601⅓	61·3	+ 0·8	−0·19	0·45	210	835⅔	53·0	−38·2	0·04
8	1·6	275	1075	76·6	− 1·8	−0·14	0·50	170	529	50·2	− 2·1	−0·03
9	1·5	260	1006⅔	92·2	− 2·8	0	0·35	160	519⅓	46·5	+ 5·3	0·10
10	1·4	240	1124	106·7	0	0·04	0·6	150	395	42·4	+14·6	−0·19
11	1·5	222½	1555⅓	118·7	− 3·0	−0·19	0·5	170	752⅔	38·4	− 3·7	−0·12
12	1·5	197½	1715⅔	125·9	− 3·1	−0·29	0·5	155	703⅓	35·2	+17·1	−0·15
13	1·3	175	598	126·0	− 8·2	−0·09	0·3	200	357	33·6	−22·4	0·04
14	1·0	157½	350⅓	119·2	−16·0	0·31	0·3	180	276⅔	34·0	+ 5·0	0·04
15	1·4	115	307	107·3	+ 5·8	0·03	0·6	215	293	36·2	−24·0	−0·24
16	1·5	100	247	92·9	+ 3·5	0	0·5	200	314	39·8	− 5·4	−0·11

$\Delta\theta_1 = (\theta_1)_{calc} - (\theta_1)_{obs}$. $\Delta hV_1 = (hV_1)_{calc} - (hV_1)_{obs}$.

TABLE VI

Analysis of the Drift Curves—Sp. Type A5–F5

	Drift I						Drift II					
R.	hV_1	θ_1	n_1	λ_1	$\Delta\theta_1$	ΔhV_1	hV_2	θ_2	n_2	λ_2	$\Delta\theta_2$	ΔhV_2
		°		°	°			°		°	°	
4	0·7	0	87⅔	36·3	17·9	0·23	0·7	215	34⅓	49·4	−23·2	−0·25
5	1·1	335	122⅔	36·3	7·1	−0·17	0·5	240	128⅓	52·1	−51·8	−0·03
6	1·1	305	317	45·3	4·8	0·02	0·2	180	118	53·8	3·8	0·28
7	1·6	287½	343	59·0	0·5	−0·25	0·5	200	151	54·2	−21·0	−0·02
8	1·7	270	201⅓	74·5	0·1	−0·18	0·5	180	122⅔	53·3	− 5·6	−0·03
9	1·4	255	190	90·0	− 0·9	0·18	0·5	165	81	51·2	5·2	−0·04
10	1·5	245	171⅔	104·3	− 3·3	0·03	0·7	200	103⅓	48·1	−32·8	−0·26
11	1·5	220	233⅓	115·8	− 2·7	−0·08	0·4	175	145⅔	44·3	− 9·4	0·01
12	1·9	195	209	122·5	− 2·4	−0·57	0·55	150	144	40·5	16·2	−0·17
13	1·4	170	85⅓	122·5	− 2·6	−0·07	0·4	175	65⅔	37·1	− 5·8	−0·04
14	1·0	150	51⅔	115·8	− 7·3	0·42	0·4	240	37⅓	34·8	−65·4	−0·06
15	1·2	120	39⅔	104·3	− 1·7	0·33	0·8	240	21⅓	34·3	−58·6	−0·47

TABLE VII

F8–G5

	Drift I						Drift II					
R.	hV_1	θ_1	n_1	λ_1	$\Delta\theta_1$	ΔhV_1	hV_2	θ_2	n_2	λ_2	$\Delta\theta_2$	ΔhV_2
		°		°	°			°		°	°	
1	1·1	90	89⅔	75·8	2·2	0·47	0·5	200	83⅓	45·0	2·7	−0·01
2	0·9	60	73⅓	66·8	10·9	0·58	0·8	230	48⅔	50·8	−30·2	−0·26
3	0·8	30	94⅔	46·9	18·8	0·30	0·9	190	65⅓	55·5	4·8	−0·33
4	0·9	20	113⅓	38·1	− 2·7	0·10	0·5	160	123⅔	58·7	28·6	0·09
5	1·1	335	153⅓	38·1	7·7	−0·10	0·4	210	143⅔	60·1	−28·3	0·20
6	1·2	305	164⅔	46·9	6·2	−0·02	0·4	190	137⅓	59·5	−15·4	0·20
7	1·7	295	222⅓	66·8	− 5·9	−0·22	0·45	195	232⅔	57·2	−27·0	0·13
8	1·6	276½	298⅔	75·8	− 4·0	−0·03	0·55	160	170⅓	53·1	2·4	0·01
9	1·5	257½	305⅓	90·1	− 2·1	0·11	0·4	185	182⅓	47·8	−26·6	0·11
10	1·6	237½	308⅔	105·8	1·1	−0·03	0·6	140	157⅓	41·8	17·0	−0·14
11	1·5	225	336⅓	117·5	− 6·8	−0·07	0·7	160	147⅔	35·8	− 1·1	−0·29
12	1·5	195	286	124·4	− 2·0	−0·17	0·5	160	155	30·9	5·6	−0·14
13	1·4	175	175⅓	124·4	− 8·0	−0·07	0·4	200	139⅔	28·4	−23·0	−0·07
14	1·1	160	175⅓	117·5	−18·2	0·33	0·1	190	88⅔	29·3	− 0·5	0·24
15	1·3	115	152⅓	105·8	6·4	0·27	0·7	230	111⅔	33·3	−31·4	−0·32
16	1·2	110	129	90·1	−17·8	0·41	0·6	220	102	38·9	−17·3	−0·16

TABLE VIII

K0–M

	Drift I						Drift II					
R.	hV_1	θ_1	n_1	λ_1	$\Delta\theta_1$	ΔhV_1	hV_2	θ_2	n_2	λ_2	ΔhV_2	$\Delta\theta_2$
		°		°	°			°		°		°
1	0·9	90	44⅓	76·9	− 0·8	−0·45	0·9	220	34⅔	54·1	−19·4	−0·40
2	0·9	60	52⅓	61·5	−12·0	−0·32	0·8	220	31⅔	58·9	−25·6	−0·27
3	0·9	40	65	47·7	10·4	−0·12	0·5	165	63	61·8	22·0	−0·04
4	1·1	20	66⅔	38·6	− 0·5	−0·24	0·3	170	97⅓	62·6	9·3	0·25
5	0·8	335	166⅓	37·9	9·2	−0·05	0·3	255	126⅔	61·2	−83·2	0·24
6	1·1	305	209	46·2	8·0	−0·10	0·5	190	136	57·9	−26·0	0·02
7	1·5	290	257⅓	59·5	0·5	−0·31	0·3	190	173⅔	52·7	−22·0	0·19
8	1·3	275	285	74·8	− 4·7	0·04	0·6	160	96	46·3	− 5·8	−0·15
9	1·6	262½	258⅔	90·4	− 5·3	−0·21	0·5	170	148⅓	39·3	−16·8	−0·11
10	1·5	242½	242⅓	105·0	− 2·6	−0·16	0·4	180	132⅔	32·5	−23·2	−0·07
11	1·5	222½	256⅓	117·0	− 2·7	−0·27	0·4	180	171⅔	27·5	−13·4	−0·12
12	1·5	195	254	124·2	0·3	−0·35	0·4	230	210	25·8	−48·9	−0·13
13	1·5	185	108⅔	124·8	−16·7	−0·36	0·3	180	156⅓	28·5	16·4	−0·01
14	0·9	150	113⅓	118·9	− 6·8	0·41	0·5	230	82⅔	34·1	−25·4	−0·15
15	1·2	120	91⅓	106·8	2·5	0·13	0·5	220	115⅔	41·0	−13·2	−0·10
16	1·1	100	97⅔	92·4	5·2	0·28	0·8	235	60⅓	48·0	−29·9	−0·34

TABLE IX

A5–M

	Drift I						Drift II				
R.	hV_1	θ_1	n_1	λ_1	$\Delta\theta_1$	ΔhV_1	hV_2	θ_2	n_2	λ_2	$\Delta\theta_2$	ΔhV_2
		°		°	°			°		°		
1	1·2	85	118⅓	74·9	3·4	0·20	0·4	200	172⅔	46·3	− 0·9	0·05
2	0·9	57½	157⅓	59·5	13·5	0·35	0·8	220	86⅔	51·1	−23·9	−0·32
3	0·7	40	224⅓	45·9	8·8	0·34	0·7	190	136⅔	54·8	1·5	−0·19
4	0·9	20	263⅔	37·2	− 2·3	−0·02	0·4	185	259⅓	57·2	− 0·7	0·12
5	1·0	335	467	37·5	5·6	−0·12	0·4	220	374	57·8	−40·4	0·13
6	1·2	310	649	46·4	0·1	−0·15	0·5	210	433	56·9	−36·7	0·02
7	1·5	290	846⅓	60·2	− 1·9	−0·24	0·4	190	533⅔	54·3	−22·2	0·11
8	1·5	272½	772	75·6	− 1·7	−0·09	0·5	160	402	50·4	3·2	−0·02
9	1·5	257½	777⅔	90·1	− 2·7	−0·05	0·5	180	388⅓	45·5	−19·1	−0·06
10	1·5	242½	709	105·4	− 4·8	−0·10	0·5	175	407	40·9	−11·1	−0·09
11	1·6	221¼	796	117·0	− 4·0	−0·30	0·3	180	495	35·2	−11·5	0·06
12	1·5	195	773	123·7	− 1·4	−0·29	0·5	185	485	31·7	−10·7	−0·17
13	1·5	175	377⅓	123·5	− 9·0	−0·30	0·3	205	353⅔	30·6	−24·2	0·02
14	1·1	155	338⅔	116·6	−13·3	0·20	0·3	240	210⅓	32·1	−49·5	0·03
15	1·3	115	280	104·8	6·5	0·11	0·6	220	252	36·0	−22·9	−0·23
16	1·2	102½	231⅓	90·0	1·9	0·25	0·5	220	207⅔	41·0	−20·3	−0·09

TABLE X

Ellipsoid Analysis—All Stars

R.	k/h	θ_0	Sh	θ_1	$\Delta\theta_0$	$\Delta\theta_1$
		°		°	°	°
1	0·570	67·1	0·536	292·7	2·7	−11·0
2	0·581	48·6	0·523	263·6	4·6	2·5
3	0·654	22·1	0·382	257·4	11·9	−11·4
4	0·708	12·0	0·314	208·1	− 0·4	2·5
5	0·683	344·6	0·449	140·4	0·7	15·6
6	0·703	324·4	0·805	118·4	0·8	− 0·8
7	0·599	306·3	1·022	100·8	− 0·2	− 4·7
8	0·551	290·1	1·087	86·0	− 0·4	− 5·8
9	0·656	276·0	1·072	71·9	− 3·0	− 6·3
10	0·667	265·0	1·116	54·4	− 7·7	− 4·3
11	0·668	237·1	1·090	35·0	− 1·9	− 2·6
12	0·807	204·4	1·154	12·8	− 3·3	− 0·6
13	0·816	170·8	0·957	357·7	−13·4	− 7·0
14	0·799	132·2	0·660	343·0	− 8·3	−12·9
15	0·649	92·2	0·699	321·3	9·8	− 9·2
16	0·598	83·9	0·680	304·7	1·4	− 8·4

TABLE XI

Ellipsoid Analysis—A5–F5

R.	k/h	θ_0	Sh	θ_1	$\Delta\theta_0$	$\Delta\theta_1$
		°		°	°	°
4	0·745	19·1	0·385	178·9	2·5	18·4
5	0·700	0·5	0·490	132·0	− 3·3	8·9
6	0·751	318·9	0·740	119·2	14·4	− 0·9
7	0·532	306·2	1·098	98·8	6·3	− 1·2
8	0·631	291·3	1·115	82·8	3·7	− 1·4
9	0·624	275·0	0·956	69·7	4·1	− 3·5
10	0·667	281·3	1·015	55·0	−18·3	− 5·4
11	0·555	240·6	1·094	29·8	2·9	2·0
12	0·882	197·2	1·465	10·3	+18·2	− 1·8
13	0·909	177·4	0·909	349·9	− 2·2	− 4·6
14	0·816	135·3	0·595	329·3	2·0	− 5·2
15	0·944	105·5	0·843	306·7	6·1	− 1·0

TABLE XII

Ellipsoid Analysis—F8–G5

R.	k/h	θ_0	Sh	θ_1	$\Delta\theta_0$	$\Delta\theta_1$
		°		°	°	°
1	0·707	65·0	0·529	290·6	6·8	− 4·0
2	0·459	50·4	0·442	256·2	4·6	16·0
3	0·588	19·7	0·292	244·5	16·1	9·0
4	0·725	8·9	0·250	220·0	4·2	− 2·5
5	0·646	346·1	0·388	140·6	2·4	8·3
6	0·587	325·0	0·518	105·0	0·6	4·2
7	0·526	312·1	0·852	95·0	− 6·1	− 5·4
8	0·497	294·8	1·000	80·9	− 5·5	− 5·9
9	0·575	277·1	1·084	69·4	− 3·4	− 8·2
10	0·631	264·1	0·874	50·4	− 7·3	− 4·0
11	0·637	234·1	1·307	36·0	0·9	− 6·3
12	0·719	204·1	1·317	11·7	− 1·8	− 0·7
13	0·617	161·3	1·046	0·8	− 0·9	− 9·6
14	0·726	150·0	0·745	341·3	−23·2	− 9·0
15	0·575	88·8	0·731	319·7	16·7	− 4·4
16	0·732	88·2	0·671	310·8	− 0·8	− 6·4

TABLE XIII

Ellipsoid Analysis—K0–M

R.	k/h	θ_0	Sh	θ_1	$\Delta\theta_0$	$\Delta\theta_1$
		°		°	°	°
1	0·534	67·5	0·431	320·0	0·5	−37·9
2	0·619	53·9	0·444	248·2	− 2·2	18·3
3	0·649	13·5	0·444	261·0	19·4	−14·1
4	0·657	17·7	0·322	213·2	− 6·6	2·4
5	0·536	334·2	0·483	150·0	13·7	16·6
6	0·638	327·5	0·949	122·9	− 1·5	3·1
7	0·599	302·5	0·891	103·3	6·0	− 1·2
8	0·593	289·2	0·932	88·4	2·1	− 3·4
9	0·650	276·7	1·086	74·8	− 0·7	− 4·7
10	0·677	261·8	0·962	61·4	− 2·4	− 5·8
11	0·785	238·2	1·064	39·0	− 0·8	− 2·1
12	0·848	222·5	1·116	17·7	−20·2	− 1·3
13	0·798	176·8	0·736	3·9	−21·0	− 9·7
14	0·783	124·0	0·641	348·3	− 3·0	−15·8
15	0·713	104·0	0·605	326·4	− 2·7	−12·8
16	0·538	86·7	0·493	308·1	− 3·4	−10·9

TABLE XIV

Ellipsoid Analysis—A5–M

R.	k/h	θ_0	Sh	θ_1	$\Delta\theta_0$	$\Delta\theta_1$
		°		°	°	°
1	0·670	69·5	0·443	294·3	2·3	−10·1
2	0·608	49·0	0·511	242·0	6·3	27·4
3	0·685	22·4	0·317	250·8	13·7	− 1·3
4	0·721	13·6	0·324	205·0	0·2	6·0
5	0·688	347·4	0·504	137·5	2·1	9·0
6	0·655	323·6	0·727	115·0	3·0	− 5·6
7	0·575	307·6	0·968	99·3	− 0·5	− 7·8
8	0·574	292·8	1·036	85·0	− 2·5	− 9·8
9	0·510	276·8	1·062	71·0	− 2·1	− 9·9
10	0·662	266·5	1·041	51·1	− 8·5	− 5·1
11	0·688	237·7	1·073	35·0	− 1·2	− 6·1
12	0·810	204·0	1·165	13·4	0	− 3·7
13	0·798	167·7	0·888	359·2	− 6·3	− 9·7
14	0·798	138·0	0·693	341·2	−10·9	−10·9
15	0·659	93·8	0·689	320·4	−10·7	− 6·3
16	0·587	86·7	0·591	308·1	− 0·7	− 9·9

TABLE XV

Drift Constants

Drift I

	All Stars	A5–F5	F8–G5	K0–M	A5–M
X_1	-0.013 ± 0.053	-0.000 ± 0.072	0.001 ± 0.074	-0.036 ± 0.078	0.013 ± 0.068
	(0.052 0.035)	(−0.028 0.054)	(−0.019 0.042)	(−0.029 0.052)	(−0.022 0.045)
Y_1	1.486 0.053	1.548 0.074	1.449 0.074	1.369 0.078	1.433 0.068
	(1.446 0.032)	(1.677 0.041)	(1.533 0.038)	(1.442 0.047)	(1.538 0.041)
Z_1	−0.190 0.054	−0.296 0.092	−0.226 0.076	−0.212 0.080	−0.246 0.069
	(−0.217 0.044)	(−0.220 0.067)	(−0.136 0.053)	(−0.099 0.064)	(−0.144 0.056)
A_1	90°.5 2°.0	90°.0 2°.6	90°.0 3°.0	91°.5 3°.3	89°.5 2°.7
	(88°.0 1°.4)	(91°.0 1°.8)	(90°.7 1°.6)	(91°.1 2°.1)	(90°.8 1°.7)
D_1	− 7°.3 2°.1	−10°.8 4°.5	− 8°.9 2°.4	− 8°.8 3°.3	− 9°.7 2°.7
	(− 8°.5 0°.6)	(− 7°.5 2°.3)	(− 5°.1 2°.0)	(− 3°.9 2°.5)	(− 5°.3 2°.1)
hW_1	1.498 0.053	1.576 0.074	1.615 0.068	1.385 0.078	1.454 0.067
	(1.463 0.035)	(1.692 0.042)	(1.539 0.038)	(1.446 0.046)	(1.545 0.041)
N_1	12 513	2052⅓	3078⅓	2568⅓	7781
	(10 745)	(1760)	(2015)	(2191)	(6002)

Drift II

	All Stars	A5–F5	F8–G5	K0–M	A5–M
X_2	0.037 ± 0.067	0.081 ± 0.083	0.056 ± 0.070	-0.047 ± 0.079	0.024 ± 0.058
	(0.093 0.029)	(0.182 0.033)	(0.046 0.028)	(0.040 0.037)	(0.092 0.024)
Y_2	−0.108 0.067	−0.064 0.086	−0.189 0.070	−0.188 0.079	−0.145 0.058
	(−0.140 0.026)	(−0.141 0.030)	(−0.139 0.025)	(−0.086 0.033)	(−0.131 0.022)
Z_2	−0.603 0.068	−0.583 0.107	−0.666 0.071	−0.585 0.081	−0.604 0.058
	(−0.628 0.036)	(−0.619 0.040)	(−0.670 0.034)	(−0.587 0.046)	(−0.649 0.030)
A_2	289°.0 33°.3	321°.7 40°	286°.5 20°.5	256°.0 23°.4	279°.5 22°.4
	(303°.6 9°.5)	(322°.2 7°.7)	(288°.4 10°.9)	(295°.2 21°.2)	(304°.9 8°.4)
D_2	− 79°.0 7°.1	− 80°.0 19°.2	− 74°.1 5°.9	− 71°.6 7°.4	− 76°.3 5°.3
	(− 75°.0 2°.4)	(− 69°.4 2°.9)	(− 77°.7 2°.2)	(− 80°.4 3°.1)	(− 76°.2 2°.0)
hW_2	0.614 0.068	0.592 0.106	0.694 0.023	0.616 0.084	0.622 0.058
	(0.650 0.035)	(0.661 0.039)	(0.686 0.034)	(0.595 0.046)	(0.668 0.029)
N_2	7326	1152⅔	2089⅔	1836⅔	5197
	(7578)	(1503)	(1941)	(2030)	(5446)

Smart and Tannahill's results are given in brackets.

TABLE XVI

The Vertex of Star-Streaming and the Solar Motion

Soln.	All Stars	A5–F5	F8–G5	K0–M	A5–M
A_v	271°.8 ± 2°.3	272°.9 ± 3°.9	271°.9 ± 3°.6	269°.6 ± 4°.1	270°.4 ± 3°.2
	(271°.5 1°.6)	(270°.6 2°.0)	(272°.2 1°.7)	(272°.6 2°.4)	(273°.8 1°.8)
D_v	−14°.5 1°.4	−10°.1 3°.1	−15°.0 3°.5	−13°.5 4°.0	−12°.8 3°.4
	(−14°.5 2°.0)	(−12°.3 2°.5)	(−18°.2 2°.2)	(−17°.7 3°.0)	(−16°.8 2°.2)
G_v	343°.4	347°.8	343°.0	343°.2	344°.2
	(343°.2)	(344°.5)	(340°.2)	(340°.6)	(342°.0)
g_v	+0°.1	+1°.5	−0°.1	+2°.6	+2°.0
	(+0°.5)	(+2°.8)	(−1°.2)	(−1°.4)	(−1°.8)
k	1.648 ± 0.041	1.639 ± 0.044	1.697 ± 0.075	1.601 ± 0.084	1.618 ± 0.100
	(1.638 0.043)	(1.873 0.052)	(1.756 0.049)	(1.606 0.060)	(1.747 0.048)
A_0	269°.6	268°.3	268°.6	273°.2	268°.8
	(265°.1)	(265°.3)	(268°.9)	(269°.5)	(267°.5)
D_0	+25°.4	+22°.4	+25°.5	27°.8	+25°.9
	(+26°.1)	(+25°.6)	(+29°.2)	(+25°.3)	(+27°.3)
hU_0	0.800	1.047	0.972	0.808	0.891
	(0.879)	(0.934)	(0.817)	(0.780)	(0.838)
N_1/N_2	1.708	1.781	1.473	1.398	1.497
	(1.410)	(1.173)	(1.038)	(1.080)	(1.102)

Smart and Tannahill's results are given in brackets.

TABLE XVII

Ellipsoidal Constants and Solar Motion

Soln.	All Stars	A5–F5	F8–G5	K0–M	A5–M
A	271°·6 ± 2°·0 (270°·2)	278°·7 ± 4°·3 (276°·6)	270°·7 ± 3°·6 (272°·6)	269°·6 ± 2°·6 (268°·5)	271°·6 ± 2°·6
D	−17°·2 ± 2°·0 (−13°·4)	−15°·4 ± 5°·2 (−11°·7)	−15°·5 ± 3°·5 (−16°·4)	−19°·7 ± 2°·6 (−16°·2)	−16°·2 ± 2°·5
G	340°·0 (343°·6)	345°·8 (348°·1)	342°·0 (342°·1)	337°·8 (340°·3)	341°·8
g	+0°·8 (+2°·1)	−6°·0	+0°·6	−0°·4	−0°·3
K/H	0·602 ± 0·036 (0·625)	0·676 ± 0·072 (0·552)	0·554 ± 0·075 (0·56)	0·606 ± 0·046 (0·65)	0·601 ± 0·046
A_0	271°·5 ± 4°·2 (266°·9)	266°·9 ± 3°·5 (266°·0)	271°·2 ± 4°·4 (269°·9)	275°·4 ± 5°·5 (272°·3)	269°·5 ± 4°·6
D_0	+25°·0 ± 3°·9 (+28°·3)	+19°·8 ± 4°·1 (+23°·2)	+30°·9 ± 3°·8 (+31°·6)	+24°·2 ± 5°·2 (+31°·8)	+29°·5 ± 4°·2
hU_0	0·948 ± 0·064 (0·94)	1·056 ± 0·064 (1·05)	0·950 ± 0·063 (0·89)	0·831 ± 0·074 (0·82)	0·819 ± 0·065

Jackson's results are given in brackets.

TABLE XVIII

Comparison of Ellipsoid and Two-Stream Positions of Vertex and Solar Motion

	G		g		A_0		D_0		hU_0	
Sol.	T.S.	Ell.	T.S.	Ell.	T.S.	Ell.	T.S.	Ell.	T.S.	Ell.
All Stars	343°·4 P.E. ∼± 2°	340°·0	+0°·1	+0°·8	269°·6	271°·5 ± 4°·2	+25°·4	+25°·0 ± 3°·9	0·800	0·948 ± 0·06
A5–F5	347°·8	345°·8 ± 4°	+1°·5	−6°·0	268°·3	266°·9 ± 3°·5	+22°·4	+19°·8 ± 4°·1	1·047	1·056 ± 0·06
F8–G5	343°·0	342°·0 ± 4°	−0°·1	0°·6	268°·6	271°·2 ± 4°·4	+25°·5	+30°·9 ± 3°·8	0·972	0·950 ± 0·06
K0–M	343°·2	337°·8 ± 3°	+2°·6	−0°·4	273°·2	275°·4 ± 5°·5	+27°·0	+24°·2 ± 5°·2	0·808	0·831 ± 0·07
A5–M	344°·2	341°·8 ± 3°	+2°·0	−0°·3	260°·8	269°·5 ± 4°·6	+25°·5	+29°·5 ± 4°·2	0·891	0·819 ± 0·07

REMARKS ON THE REVISION OF FK3 AND ITS RELATION TO N30

A. Kopff

(Received 1954 September 29)

Summary

In the first part of the paper the principles adopted for the revision of FK3 are explained. About 57 catalogues with epochs between 1918 and 1950 are to be used, including both those with independent instrumental systems and those tied by differential observations to the system of a fundamental catalogue. For the improvement of the position of each individual star in the system of FK3 all the catalogues are used; the method of correcting position and proper motion is that given by Boss in the P.G.C. For the correction of the system FK3 itself only the independent catalogues can be used.

The second part gives a comparison between FK3 and N30, shown by the tables at the end of the paper. Using the system of the G.C. as a basis of comparison, it is found that there are some systematic differences in the N30 system between those stars which are in the FK3 catalogue and those which are not, particularly in two zones of declination. The differences are shown in Tables I–IV. A satisfactory explanation of this difference cannot be given.

The revision of FK3

1. The many new star catalogues which have been published since 1930 have made it desirable to revise the catalogue FK3. The mean epoch of the Auwers stars in the FK3 is about 1900; that of the additional stars is somewhat later. The need to undertake this revision was confirmed in 1952 by the I.A.U. in Rome; moreover, for various reasons, an increase in the number of stars in the fundamental system is required. Recommendation No. 18 of Commission 4 is concerned with this matter. In the meantime the desire for an increase in the number of fundamental stars—which was particularly emphasized by geodesists—has been met by the compilation of a supplementary catalogue (FK3 Supp) for which positions and proper motions have been given (**1**).

2. In response to a circular letter of 1952 December (**2**), various observatories have forwarded observations not so far published or have promised to forward them within a very short time. About 57 newly observed catalogues are available for the revision of FK3. The revision was commenced in the middle of 1953.

3. The first survey of the expected correction of FK3 results from a comparison with the catalogue of Standard Stars by Morgan, called N30 (**3**), about which details are given later. For the part of the sky observed by the observatories in the northern hemisphere it is noticed that individual corrections of the single stars within the system of FK3 are small. But in the southern hemisphere the number of catalogues available for the compilation of FK3 was rather small, so that now the individual differences are appreciable.

4. The main task is, however, the systematic correction of FK3. The N30 catalogue shows some large systematic differences from FK3 ; but it is not possible to obtain valid information about the necessary correction of FK3

by comparing FK3 with N30. Though the catalogue N30 is to a great part free from systematic errors at its mean epoch 1930, this does not apply to the catalogue positions for the epoch 1950 (compare p. 480). These positions are derived from the 1930 positions by the use of proper motions which are based only on the systematically improved positions of the G.C. at the time of its mean epoch. The proper motions of the G.C. were completely left out of account; this has already been mentioned previously (**4**).

The systematic revision of the G.C. at its mean epoch, however, has not been carried through adequately. The corrections in R.A. of the G.C. were obtained without regard to the declination and are given in the form of a Fourier series (Cat. N30, p. XVI). According to a letter from Morgan, corrections of the right ascensions, depending on Dec., were taken into consideration only south of $-30°$. For the declinations there are small deviations from the Fourier series north of $+30°$ and south of $-30°$. In contrast, when compiling FK3 the relations of the catalogues were determined by graphical methods, owing to the very complicated and irregular nature of the catalogue differences. Thus the change of $\Delta\alpha_\alpha$ with Dec. was completely taken into account after subtracting the derived $\Delta\alpha_\delta$ (**5**). In the same way the values $\Delta\delta_\alpha$ also showed a dependence on Dec., which had to be applied (**6**). This procedure is being used again in the present revision.

Moreover, when FK3 was compiled, none of the catalogues which were observed before 1845 were used, because they contain many systematic errors. On the other hand, the proper motions of G.C. were considerably influenced by the catalogues of these epochs before 1845.

5. For the revision of FK3, the catalogue N30 cannot be used at all, as strictly speaking it is not a fundamental catalogue on account of its special composition and character. This was previously pointed out in 1950 at the Conference on Astronomical Constants in Paris (**7**).

There are particularly two parts of the sky where it is necessary to carry out systematic corrections of FK3. One is in the extreme northern sky. When compiling FK3 the discussions of Kahrstedt (**8**) in particular showed that in the north polar region there were strong marked discordances between the individual instrumental systems; in this region the system of FK3 was largely based on the instrumental system of Pulkovo. Secondly the southern part of the FK3 system (south of $-30°$) needs a more extensive systematic revision. The number of newly observed catalogues which can be used is, however, very small, and is even smaller than those used when FK3 itself was compiled. It is therefore most important to increase the number of meridian circles in the southern hemisphere.

6. The revision of FK3 will be carried out, as was the case with the compilation of FK3, in two steps: it begins with the determination of the individual corrections within the system FK3; then the correction of the system itself will be deduced separately. The discussion will, in the first place, be concerned with the corrections depending on the declinations; the corrected residuals will then be discussed for the dependence on R.A. Only those catalogues which have been observed on an independent system can be used for the systematic correction of FK3. The other catalogues are tied in a differential way to an existing fundamental system and they can only be used for the individual correction; it would not be logical to relate such observed catalogues to a common preliminary corrected system and to combine them with the absolute catalogues.

The method to be used for the revision of FK3 differs from the procedure which was used when FK3 was compiled. According to a method which was already proposed by Boss (**9**), it is intended to correct the positions and the proper motions of the fundamental catalogue within its own system. The mean errors given in FK3 for the position at the mean epoch and for the proper motion of each star provide the basis of the method. This has already been pointed out at the colloquium in Paris (**7**). This procedure was also used by Nowacki to correct the position and proper motion of 61 Cygni (**10**). The correction of the system itself has then to follow.

For uniformity the equinox of G.C. and N30 is adopted as the equinox of the revised FK3, though the old value could be used in every respect (compare FK3, part I, Appendix, p. 106).

The revision of FK3, commenced in the middle of 1953, should be completed in 1958. Immediately afterwards the final formation of FK3 Supp will follow.

The further necessary extension of FK3 is mentioned in the last part of Recommendation 18 ; the catalogue FK3 is to be supplemented by a fundamental catalogue of faint stars. It should thus be possible on the one hand to fix in a precise manner the system of the fainter stars of the old catalogues ; and on the other hand to provide a reliable basis for the establishment of a true fundamental system with the help of observations of faint extragalactic nebulae.

The relation between FK3 and N30

7. In the following a comparison between FK3 and N30, carried through by Nowacki, is given in the same form as for the reduction of G.C. to FK3 (**11**). A comparison between the positions and proper motions of FK3 and the standard catalogue N30 has already been made by Morgan (**3**, p. XXI) and in more detail by Nowacki (**4**). These two comparisons differ considerably in the method of their derivation. Morgan gives the difference between the catalogue positions and proper motions according to R.A. and Dec. in one table. Nowacki first determined the systematic differences between the catalogues depending on Dec. ($\Delta\alpha_\delta$, $\Delta\mu_\delta$, $\Delta\delta_\delta$, $\Delta\mu'_\delta$), following the method formerly used by the Astronomisches Rechen-Institut. After correcting for these differences, the residuals were analysed according to R.A. ($\Delta\alpha_\alpha$, $\Delta\mu_\alpha$, $\Delta\delta_\alpha$, $\Delta\mu'_\alpha$). The dependence of these variations on the declination become obvious by this method. The results of the comparisons are given at the end of this paper.

8. The other investigations, carried out by Nowacki concerning the relations between FK3 and N30, are only mentioned briefly ; a more elaborate publication will appear in the *Veröffentlichungen des Astronomischen Rechen-Instituts zu Heidelberg*. In these discussions it was necessary to include the G.C. in its unrevised form. It should be noted that the Standard Catalogue N30 is given for the equinox of 1950, and is therefore influenced to a very great extent by the adopted proper motions which are based on the G.C. positions.

The relation (N30—G.C.) was derived anew as a difference between the relation (FK3—N30) obtained in the investigation (**4**) and the (FK3—G.C.) formerly derived (**12**). These values (N30—G.C.), derived as a control, are based only on the stars of FK3. They are compared with $(\text{N30—G.C.})_M$, derived from the tables of Morgan (**3**, p. XIX and **13**), which were based on all N30 stars listed in G.C. These two comparisons should agree. The differences in R.A. and Dec., arranged according to Dec., i.e.

$$\Delta = [(\text{FK3—G.C.}) - (\text{FK3—N30})] \textit{ minus } (\text{N30—G.C.})_M \qquad (1)$$

are given in Fig. 1 only for the proper motions. It can be seen from it that on the whole the agreement is satisfactory.

9. There are, however, both in R.A. and Dec. regions with large differences. For the R.A. there are the regions at $+50°$ to $+70°$ and $-40°$ to $-60°$. In these parts the differences formed for the FK3 stars alone diverge appreciably from the differences formed for all N30 stars. This was the reason for a more special investigation of these areas. The following data are confined to the positions and proper motions in R.A. within the two areas mentioned above.

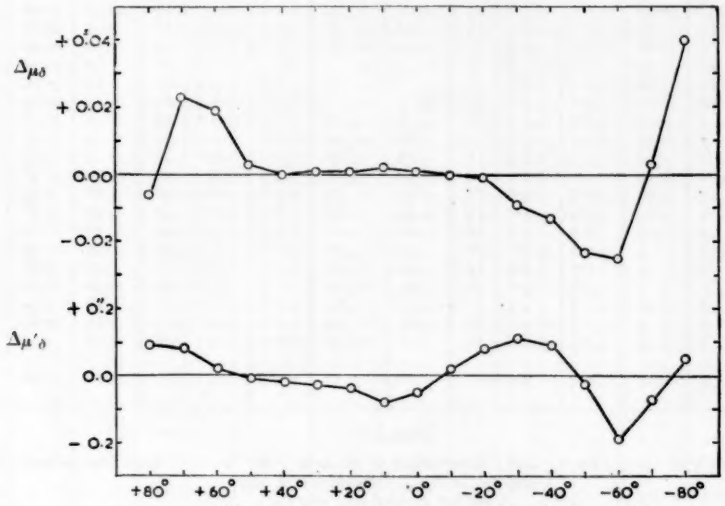

FIG. 1.—*Differences* $\Delta\mu_\delta$ *and* $\Delta\mu'_\delta$ *(compare formula* (1)*, p.* 480*).*

From the individual values $\Delta\alpha$ and $\Delta\mu$, listed for each star in the catalogue N30, the mean values for the two areas have been formed anew first for the FK3 stars and then for the other stars of catalogue N30. The means were calculated in two ways: at first for individual Dec. zones of 3° breadth for all R.A.'s for both areas, and secondly in R.A. for two hours each extending over all declinations of these areas. In both cases overlapping means of the consecutive values were formed. Finally the differences of these mean values for the FK3 stars and the non-FK3 stars were formed. The results are shown in Tables I–IV. The differences in R.A. and the proper motions in R.A. between the two groups of stars, which can be seen quite clearly from Fig. 1, are given in these four tables.

The tables give the overlapping means $\Delta\alpha$, $\Delta\mu$ (centennial) and their differences; the mean epochs and the number n of stars of these means are also given. For the last column of each table, values

$$\Delta\alpha_{(30)} = \Delta\alpha_{50} - \frac{\Delta\mu}{100}(1950.0 - \text{Ep. N30}) \qquad (2)$$

were calculated at first for FK3 stars and non-FK3 stars separately; these values are not given here separately, but the last column $\Delta\alpha_{(30)}$ in Tables I–IV contains the differences of the values.

TABLE I

Means of (N30—G.C.) for α_{50} and μ (centennial) in the area $+50°$ to $+70°$ with Dec. as argument (compare for $\Delta\alpha_{(30)}$ formula (2), p. 481)
Unit for $\Delta\alpha$ and $\Delta\mu$: 0s·001

δ	FK3 stars					non-FK3 stars					FK3 stars minus non-FK3 stars		
	$\Delta\alpha_{50}$	$\Delta\mu$	mean epoch G.C.	mean epoch N30	n	$\Delta\alpha_{50}$	$\Delta\mu$	mean epoch G.C.	mean epoch N30	n	$\Delta\alpha_{50}$	$\Delta\mu$	$\Delta\alpha_{(30)}$
°			1900+	1930+				1900+	1930+				
+50·5	− 3	− 7	−1·8	+3·9	24	−13	− 31	+1·8	+2·3	61	+10	+24	+ 5
+51·5	− 7	−18	−1·1	+3·8	19	−13	− 34	+2·8	+3·6	68	+ 6	+16	+ 4
+52·5	−10	−21	−1·7	+3·7	19	−13	− 36	+4·1	+3·3	58	+ 3	+15	0
+53·5	− 8	−16	+0·1	+4·3	20	−10	− 26	+4·1	+3·2	55	+ 2	+10	+ 1
+54·5	−10	−17	−0·6	+4·0	20	− 5	− 9	+3·2	+3·5	50	− 5	− 8	− 3
+55·5	−10	−19	−0·3	+3·9	23	0	0	+3·7	+3·4	60	−10	−19	− 7
+56·5	−10	−22	0·0	+3·8	25	+ 1	+ 1	+3·0	+3·8	65	−11	−23	− 7
+57·5	− 4	−15	−0·2	+3·8	23	− 2	− 7	+3·2	+3·6	65	− 2	− 8	− 1
+58·5	− 5	−15	+0·1	+3·7	21	−12	− 26	+3·5	+3·8	61	+ 7	+11	+ 5
+59·5	− 8	−17	−0·5	+3·5	20	−15	− 32	+4·1	+3·6	47	+ 7	+15	+ 5
+60·5	−11	−19	0·0	+3·6	18	−30	− 67	+5·1	+3·3	47	+19	+48	+11
+61·5	− 7	−18	−0·6	+3·6	19	−35	− 77	+5·8	+2·9	41	+28	+59	+18
+62·5	− 3	−14	−0·4	+3·4	17	−43	−102	+6·0	+2·6	47	+40	+88	+25
+63·5	− 4	−15	0·0	+3·4	19	−42	−100	+5·3	+3·0	40	+38	+85	+24
+64·5	− 3	− 4	+1·4	+3·7	18	−42	− 98	+3·6	+3·3	39	+39	+94	+23
+65·5	− 3	− 1	+1·7	+3·9	15	−42	− 87	+3·0	+3·9	28	+39	+86	+25
+66·5	0	+ 2	+2·3	+4·1	18	−35	− 74	+2·6	+4·1	35	+35	+76	+23
+67·5	− 8	−12	+2·3	+4·1	17	−30	− 65	+2·6	+4·7	28	+22	+53	+14
+68·5	− 2	+ 5	+2·4	+4·4	19	−26	− 59	+2·6	+4·2	35	+24	+64	+14
+69·5	− 2	+ 9	+0·3	+4·6	15	+ 8	+ 16	+2·6	+4·1	28	−10	− 7	− 8
Mean	− 6	−11	0·0	+3·9		−16	− 37	+3·5	+3·3		+10	+26	+ 6

TABLE II

Means of (N30—G.C.) for α_{50} and μ (centennial) in the area $-40°$ to $-60°$ with Dec. as argument (compare for $\Delta\alpha_{(30)}$ formula (2), p. 481)
Unit for $\Delta\alpha$ and $\Delta\mu$: 0s·001

δ	FK3 stars					non-FK3 stars					FK3 stars minus non-FK3 stars		
	$\Delta\alpha_{50}$	$\Delta\mu$	mean epoch G.C.	mean epoch N30	n	$\Delta\alpha_{50}$	$\Delta\mu$	mean epoch G.C.	mean epoch N30	n	$\Delta\alpha_{50}$	$\Delta\mu$	$\Delta\alpha_{(30)}$
°			1900+	1930+				1900+	1930+				
−40·5	+16	+ 38	+7·0	+1·4	27	+23	+ 52	+ 7·7	+3·0	76	− 7	−14	− 5
−41·5	+18	+ 44	+7·3	+1·7	37	+24	+ 54	+ 7·3	+3·3	70	− 6	−10	− 5
−42·5	+21	+ 53	+6·9	+1·8	37	+22	+ 49	+ 7·0	+3·5	57	− 1	+ 4	− 3
−43·5	+23	+ 56	+6·7	+2·1	31	+31	+ 74	+ 7·6	+3·5	49	− 8	−18	− 5
−44·5	+25	+ 60	+6·7	+2·4	25	+33	+ 76	+ 8·1	+3·4	49	− 8	−16	− 6
−45·5	+23	+ 52	+6·9	+2·8	24	+39	+ 90	+ 7·7	+3·4	57	−16	−38	−10
−46·5	+21	+ 41	+6·4	+2·3	31	+35	+ 82	+ 7·4	+3·6	54	−14	−41	− 8
−47·5	+23	+ 48	+6·2	+2·5	25	+37	+ 89	+ 7·1	+3·4	57	−14	−41	− 8
−48·5	+27	+ 58	+6·4	+2·0	23	+36	+ 91	+ 7·6	+3·3	51	− 9	−33	− 4
−49·5	+39	+100	+7·9	+1·0	17	+44	+110	+ 7·9	+3·1	53	− 5	−10	− 5
−50·5	+41	+ 97	+7·5	+0·6	19	+55	+131	+ 8·3	+2·7	60	−14	−34	−10
−51·5	+46	+110	+7·6	+0·5	23	+51	+126	+ 8·6	+2·5	65	− 5	−16	− 4
−52·5	+52	+120	+7·4	+0·4	24	+56	+136	+ 8·8	+2·3	55	− 4	−16	− 4
−53·5	+42	+101	+7·5	+0·3	26	+55	+137	+ 9·0	+2·7	45	−13	−36	−10
−54·5	+40	+ 92	+7·5	−0·1	21	+68	+165	+ 8·9	+2·6	41	−28	−73	−18
−55·5	+39	+ 95	+6·8	+0·1	23	+56	+142	+ 8·9	+2·6	43	−17	−47	−12
−56·5	+49	+111	+6·7	+0·1	21	+53	+138	+10·1	+2·3	42	− 4	−27	− 1
−57·5	+54	+126	+7·2	+0·2	23	+45	+117	+10·0	+2·2	43	+ 9	+ 9	+ 5
−58·5	+45	+104	+6·7	−0·2	18	+52	+131	+10·0	+2·2	46	− 7	−27	− 4
−59·5	+42	+107	+6·5	−0·1	20	+53	+132	+ 9·5	+2·2	41	−11	−25	− 8
Mean	+32	+ 75	+6·9	+1·1		+41	+100	+ 8·3	+2·9		− 9	−25	− 6

TABLE III

Means of (N30—G.C.) for α_{50} and μ (centennial) in the area +50° to +70° with R.A. as argument (compare for $\Delta\alpha_{(30)}$ formula (2), p. 481)

Unit for $\Delta\alpha$ and $\Delta\mu$: 0^s·001

α	FK3 stars					non-FK3 stars					FK3 stars minus non-FK3 stars		
	$\Delta\alpha_{50}$	$\Delta\mu$	mean epoch		n	$\Delta\alpha_{50}$	$\Delta\mu$	mean epoch		n	$\Delta\alpha_{50}$	$\Delta\mu$	$\Delta\alpha_{(30)}$
			G.C.	N30				G.C.	N30				
h			1900+	1930+				1900+	1930+				
0·0	+ 6	−10	−0·5	+3·4	10	−22	− 80	+2·6	+3·2	30	+28	+70	+16
1·0	+ 4	−11	−1·6	+4·0	14	+ 7	− 2	+3·6	+3·6	33	− 3	− 9	− 1
2·0	+ 6	0	+1·1	+4·1	13	+10	+ 14	+4·5	+4·2	32	− 4	−14	− 2
3·0	+ 2	+ 5	+3·6	+3·6	10	+ 2	+ 1	+4·2	+4·3	27	0	+ 4	− 1
4·0	− 4	+ 2	+2·5	+4·1	11	0	+ 5	+5·7	+3·9	24	− 4	− 3	− 3
5·0	−13	− 9	+0·5	+4·6	10	−19	− 28	+5·5	+3·8	25	+ 6	+19	+ 3
6·0	−13	+ 1	+2·4	+4·5	9	−36	− 59	+3·7	+3·8	27	+23	+60	+14
7·0	− 7	+ 8	+3·7	+3·9	9	−37	− 53	+3·0	+3·5	26	+30	+61	+20
8·0	−14	− 8	+2·8	+3·8	9	−29	− 35	+3·2	+3·8	26	+15	+27	+10
9·0	− 5	+13	+0·7	+3·6	10	−25	− 32	+3·6	+3·8	29	+20	+45	+13
10·0	+15	+50	0·0	+4·2	12	− 4	+ 7	+4·6	+4·0	28	+19	+43	+12
11·0	+15	+45	−0·5	+4·3	13	− 1	+ 10	+3·6	+4·0	24	+16	+35	+11
12·0	0	+ 9	−0·8	+3·9	12	−14	− 24	+3·2	+3·1	25	+14	+33	+ 9
13·0	− 6	− 4	+0·5	+3·7	9	−13	− 23	+3·3	+2·7	23	+ 7	+19	+ 4
14·0	−13	−21	+0·5	+3·2	9	−22	− 43	+1·8	+3·1	22	+ 9	+22	+ 6
15·0	−24	−45	+0·8	+3·5	11	−33	− 73	+3·8	+3·0	24	+ 9	+28	+ 4
16·0	−32	−66	+1·2	+3·9	10	−40	− 91	+3·5	+3·3	25	+ 8	+25	+ 4
17·0	−27	−57	−2·0	+3·4	13	−33	− 80	+4·3	+3·1	22	+ 6	+23	+ 2
18·0	−21	−47	−2·4	+3·5	12	−27	− 77	+6·2	+2·2	21	+ 6	+30	0
19·0	− 6	−22	−1·7	+4·2	9	−17	− 50	+1·6	+3·0	25	+11	+28	+ 7
20·0	− 2	−21	−2·0	+3·8	10	−18	− 53	+1·0	+3·9	29	+16	+32	+11
21·0	− 9	−43	−0·5	+3·8	9	−24	− 74	+2·3	+4·0	36	+15	+31	+10
22·0	− 3	−35	−1·2	+3·8	11	−24	− 79	+3·5	+3·4	32	+21	+44	+14
23·0	+ 6	−15	+0·8	+3·5	11	−31	−104	+4·5	+3·2	27	+37	+89	+21
24·0	+ 6	−10	−0·5	+3·4	10	−22	− 80	+2·6	+3·2	30	+28	+70	+16
Mean	− 6	−11	+0·2	+3·8		−18	− 42	+3·6	+3·5		+12	+31	+ 7

10. At present it is not possible to give sufficient reason for the fact that, in both areas mentioned above, the FK3 stars systematically differ from the other stars of catalogue N30. It must, however, be mentioned that the FK3 stars are to a large extent identical with the standard stars of Lewis Boss (**14**). So it is possible that in the uncorrected G.C. the standard stars differ systematically from the other stars. This conjecture is supported by the following circumstance. For the $\Delta\alpha$ the differences in Tables I–IV for the epoch 1950 are much greater than for epoch 1930. The figures for 1950 have been influenced by proper motions, but those for 1930 have not; the proper motions, however, are based on the positions of G.C., so that systematic differences between different groups of stars in G.C. will influence the catalogue N30 for the epoch of 1950 through the proper motions adopted in N30.

It is also possible that the systematic deviation of FK3 stars from the other stars is the result of the additional correction applied to G.C. for 1900, before the derivation of the proper motions of N30. The corrections applied to the positions of G.C. for 1900 were valid only for the mean epoch of 1900. In deducing the proper motions of the individual stars, the exact difference of epochs for each star was used ; but as the epochs of the standard stars, which in general correspond to the FK3 stars, deviate to some extent from the other epochs, it is quite possible that the difference found in N30 has been caused by the insufficient additional systematic correction of G.C.

TABLE IV

Means of (N30—G.C.) for α_{50} and μ (centennial) in the area $-40°$ to $-60°$ with R.A. as argument (compare for $\Delta\alpha_{(30)}$ formula (2), p. 481)
Unit for $\Delta\alpha$ and $\Delta\mu$: 0s·001

α	FK3 stars					non-FK3 stars					FK3 stars minus non-FK3 stars		
	$\Delta\alpha_{50}$	$\Delta\mu$	mean epoch G.C.	mean epoch N30	n	$\Delta\alpha_{50}$	$\Delta\mu$	mean epoch G.C.	mean epoch N30	n	$\Delta\alpha_{50}$	$\Delta\mu$	$\Delta\alpha_{(30)}$
h			1900+	1930+				1900+	1930+				
0·0	+55	+ 97	+6·9	+1·5	15	+62	+115	+8·0	+2·8	30	− 7	−18	− 5
1·0	+39	+ 58	+5·4	+1·5	15	+58	+108	+8·1	+2·8	32	−19	−50	−12
2·0	+39	+ 57	+5·5	+1·8	13	+61	+116	+7·9	+2·8	31	−22	−59	−12
3·0	+31	+ 53	+7·7	+1·8	14	+51	+ 98	+7·2	+2·9	26	−20	−45	−13
4·0	+21	+ 37	+7·7	+1·1	13	+36	+ 72	+7·7	+3·3	31	−15	−35	−10
5·0	+23	+ 53	+7·9	+1·1	14	+20	+ 45	+8·3	+3·1	31	+ 3	+ 8	+ 1
6·0	+24	+ 62	+6·8	+0·7	14	+13	+ 40	+7·9	+2·8	30	+11	+22	+ 6
7·0	+15	+ 50	+5·8	+0·4	13	+19	+ 64	+8·7	+2·6	30	− 4	−14	− 3
8·0	+13	+ 48	+6·6	+0·8	15	+16	+ 60	+8·6	+2·6	31	− 3	−12	− 2
9·0	+10	+ 41	+5·7	+0·2	14	+11	+ 46	+7·6	+2·7	34	− 1	− 5	− 1
10·0	− 2	+ 14	+6·6	+0·6	13	+22	+ 72	+7·9	+2·7	33	−24	−58	−15
11·0	+10	+ 47	+8·4	+2·1	12	+34	+104	+9·2	+2·7	31	−24	−57	−14
12·0	+24	+ 85	+7·7	+1·5	13	+41	+127	+8·9	+2·9	30	−17	−42	−11
13·0	+26	+ 94	+7·5	+0·8	14	+45	+139	+8·1	+3·1	29	−19	−45	−13
14·0	+23	+ 88	+7·5	+1·6	15	+44	+142	+8·9	+2·8	26	−21	−54	−13
15·0	+20	+ 77	+7·5	+2·0	15	+37	+119	+8·5	+2·8	25	−17	−42	−11
16·0	+42	+123	+7·7	+1·2	14	+38	+115	+8·6	+3·1	30	+ 4	+ 8	+ 1
17·0	+42	+112	+6·5	0·0	13	+50	+141	+9·4	+3·0	34	− 8	−29	− 6
18·0	+41	+102	+7·0	+0·1	13	+58	+149	+8·8	+2·5	27	−17	−47	−11
19·0	+54	+123	+7·3	+1·7	13	+58	+133	+8·5	+3·1	27	− 4	−10	− 3
20·0	+50	+ 96	+6·3	+2·0	14	+56	+119	+8·7	+3·5	25	− 6	−23	− 3
21·0	+45	+ 74	+7·3	+1·4	16	+61	+115	+7·2	+3·4	20	−16	−41	−10
22·0	+56	+ 95	+6·9	+1·1	13	+71	+134	+7·4	+3·3	28	−15	−39	−10
23·0	+74	+137	+6·5	+1·0	12	+73	+138	+7·7	+3·0	33	+ 1	− 1	− 2
24·0	+55	+ 97	+6·9	+1·5	15	+62	+115	+8·0	+2·8	30	− 7	−18	− 5
Mean	+32	+ 76	+6·9	+1·2		+43	+103	+8·2	+2·9		−11	−27	− 7

A further possible explanation for the difference between the FK3 stars and the others may be found in the method of formation of N30. Tables I–IV show that the values $\Delta\alpha_{50}$ and $\Delta\alpha_{(30)}$ are of the same general character, both according to Dec. and to R.A. But the values are smaller for $\Delta\alpha_{(30)}$ than for $\Delta\alpha_{50}$. As the compilation of N30 was based on differences from the G.C., systematic differences which might be present in G.C. between the standard and the other stars could therefore reappear in the catalogue N30.

It is possible that these different causes were working together when N30 was compiled At present it can only be pointed out that N30 does not possess a fully homogenous system, especially in the two regions mentioned above.

11. In the following Tables V–XI the reduction of the N30 system to FK3 is given in the sense (FK3—N30), in the same manner as the reduction (FK3—G.C.) was formerly given (**11**).

The tables contain the values $\Delta\alpha_\delta$, $\Delta\delta_\delta$ and then the $\Delta\alpha_\alpha$, $\Delta\delta_\alpha$ for zones of 30° breadth for the epochs 1900 and 1930 to 1970. The values of $\Delta\alpha_\alpha$ in the north and south polar caps are multiplied by $\cos\delta$; the values $\Delta\alpha_\delta$ are on the contrary not reduced to the equator. For smaller zones in Dec. the values of Nowacki for $\Delta\alpha_\alpha$, $\Delta\delta_\alpha$ and the proper motions must be used (**4**). Corrections for magnitude equation are not given, because the values are absolutely insignificant.

TABLE V

FK3—N30

δ	$\Delta\alpha_\delta$ Unit: 0ˢ·001						$\Delta\delta_\delta$ Unit: 0″·01					
	1900	1930	1940	1950	1960	1970	1900	1930	1940	1950	1960	1970
+90°	0	0	0	0	0	0	+ 5	− 2	− 4	− 6	− 8	−10
+87	−19	− 8	− 4	0	+ 4	+ 8	+ 3	− 2	− 4	− 6	− 8	−10
+86	−21	− 9	− 4	0	+ 4	+ 9	+ 1	− 2	− 4	− 5	− 6	− 8
84	−29	− 18	− 14	− 10	− 6	− 2	+ 2	0	0	− 1	− 2	− 2
82	−36	− 32	− 30	− 29	− 28	− 26	0	0	0	0	0	0
80	−35	− 45	− 48	− 52	− 55	− 59	+ 1	+ 1	0	0	0	− 1
+78	−29	− 46	− 52	− 58	− 64	− 70	+ 4	+ 1	0	− 1	− 2	− 3
+76	−25	− 42	− 48	− 54	− 60	− 66	+ 6	+ 2	0	− 1	− 2	− 4
74	−22	− 39	− 45	− 51	− 57	− 63	+ 9	+ 6	+ 4	+ 3	+ 2	0
72	−13	− 32	− 38	− 45	− 51	− 58	+ 4	+ 5	+ 6	+ 6	+ 6	+ 7
70	− 9	− 30	− 37	− 44	− 51	− 58	+ 3	+ 4	+ 4	+ 5	+ 5	+ 6
+65	−12	− 31	− 37	− 43	− 49	− 55	+ 5	+ 3	+ 3	+ 2	+ 1	+ 1
+60	−16	− 27	− 30	− 34	− 38	− 41	+ 4	+ 2	+ 1	0	− 1	− 2
55	−16	− 22	− 24	− 26	− 28	− 30	+ 2	+ 1	0	0	0	− 1
50	−10	− 12	− 12	− 13	− 14	− 14	+ 1	+ 1	+ 2	+ 2	+ 2	+ 3
45	− 8	− 10	− 11	− 12	− 13	− 14	− 2	+ 2	+ 3	+ 4	+ 5	+ 6
+40	− 8	− 12	− 14	− 15	− 16	− 18	0	0	0	0	0	0
+35	−11	− 13	− 13	− 14	− 15	− 15	+ 1	0	− 1	− 1	− 1	− 2
30	−10	− 10	− 10	− 10	− 10	− 10	− 1	− 1	− 2	− 2	− 2	− 3
25	−10	− 8	− 8	− 7	− 6	− 6	0	+ 2	+ 2	+ 3	+ 4	+ 4
20	−10	− 11	− 11	− 12	− 12	− 13	− 1	+ 1	+ 1	+ 2	+ 3	+ 3
+15	− 9	− 9	− 10	− 10	− 10	− 11	− 2	− 1	0	0	0	+ 1
+10	− 9	− 10	− 10	− 10	− 10	− 10	+ 1	+ 2	+ 3	+ 3	+ 3	+ 4
+ 5	− 9	− 9	− 10	− 10	− 10	− 11	+ 1	+ 2	+ 2	+ 3	+ 3	+ 4
0	− 8	− 10	− 11	− 12	− 13	− 14	+ 1	+ 0	+ 7	+ 9	+11	+12
− 5	− 7	− 10	− 11	− 12	− 13	− 14	+ 1	+ 5	+ 7	+ 8	+ 9	+11
−10	− 6	− 10	− 12	− 13	− 14	− 16	0	0	0	0	0	0
−15	− 8	− 11	− 12	− 13	− 14	− 15	+ 1	+ 1	+ 1	+ 1	+ 1	+ 1
20	−10	− 9	− 9	− 9	− 9	− 9	− 2	− 2	− 1	− 1	− 1	0
25	−10	− 8	− 7	− 6	− 5	− 4	− 2	0	0	+ 1	+ 2	+ 2
30	−13	− 14	− 14	− 14	− 14	− 14	+ 6	+ 8	+ 9	+10	+11	+12
−35	−17	− 22	− 24	− 26	− 28	− 30	+10	+11	+11	+11	+11	+11
−40	−18	− 28	− 31	− 34	− 37	− 40	+11	+ 9	+ 8	+ 7	+ 6	+ 5
45	−12	− 25	− 30	− 34	− 38	− 43	+ 6	+ 5	+ 4	+ 4	+ 3	+ 3
50	− 6	− 27	− 34	− 41	− 48	− 55	+ 4	+ 5	+ 5	+ 6	+ 6	+ 7
55	− 6	− 32	− 41	− 50	− 59	− 68	+ 2	+11	+15	+18	+21	+25
−60	− 4	− 33	− 42	− 52	− 62	− 71	+ 1	+15	+19	+24	+29	+33
−65	0	− 23	− 30	− 38	− 46	− 53	− 2	+10	+14	+18	+22	+26
70	+ 6	− 3	− 6	− 9	− 12	− 15	− 2	+ 4	+ 6	+ 8	+10	+12
72	0	+ 2	+ 2	+ 3	+ 4	+ 4	− 4	+ 1	+ 2	+ 4	+ 6	+ 7
74	− 5	+ 2	+ 4	+ 7	+ 9	+ 12	− 5	0	+ 2	+ 4	+ 6	+ 8
−76	− 5	− 12	− 14	− 17	− 19	− 22	− 8	+ 6	+11	+16	+21	+26
−78	−10	− 61	− 79	− 96	−113	−131	− 3	+12	+18	+23	+28	+34
80	−17	− 97	−123	−150	−176	−203	− 2	+14	+19	+24	+29	+34
82	− 7	−115	−151	−187	−223	−259	+ 1	+12	+16	+20	+24	+28
84	−19	−134	−173	−211	−249	−288	− 1	+ 6	+ 8	+10	+12	+14
−86	+43	+ 17	+ 9	0	− 9	− 17	+ 2	+ 2	+ 3	+ 3	+ 3	+ 4
−87	+38	+ 61	+ 68	+ 76	+ 84	+ 91	+ 4	0	− 2	− 3	− 4	− 6
−90	0	0	0	0	0	0	+ 4	− 2	− 4	− 6	− 8	−10

Table VI

FK3—N30 (+90° to +60°)

α	$\Delta\alpha_\alpha \cos\delta$ Unit: 0.ˢ001						$\Delta\delta_\alpha$ Unit: 0.″01					
	1900	1930	1940	1950	1960	1970	1900	1930	1940	1950	1960	1970
h												
0	− 2	− 5	− 5	− 6	− 7	− 7	− 4	+ 4	+ 7	+10	+13	+16
1	− 1	− 3	− 3	− 4	− 5	− 5	− 3	− 1	0	+ 1	+ 2	+ 3
2	0	− 2	− 3	− 4	− 5	− 6	− 2	− 3	− 3	− 3	− 3	− 3
3	+ 3	+ 1	0	− 1	− 2	− 3	0	− 2	− 3	− 4	− 5	− 6
4	+ 3	+ 1	+ 1	0	− 1	− 1	− 2	− 2	− 1	− 1	− 1	0
5	+ 4	0	− 1	− 3	− 4	− 6	− 3	0	+ 1	+ 2	+ 3	+ 4
6	+ 4	− 1	− 3	− 5	− 7	− 9	0	+ 3	+ 4	+ 5	+ 6	+ 7
7	+ 6	− 2	− 5	− 8	−11	−14	+ 1	+ 7	+ 8	+10	+12	+13
8	+ 4	− 6	− 9	−13	−16	−20	0	+ 3	+ 3	+ 4	+ 5	+ 5
9	+ 2	− 6	− 8	−11	−14	−16	0	− 2	− 3	− 4	− 5	− 6
10	+ 3	− 5	− 8	−11	−14	−17	0	− 6	− 9	−11	−13	−16
11	+ 2	− 4	− 6	− 8	−10	−12	+ 3	− 4	− 6	− 8	−10	−12
12	+ 2	0	0	− 1	− 2	− 2	+ 2	− 1	− 3	− 4	− 5	− 7
13	+ 1	+ 3	+ 3	+ 4	+ 5	+ 5	+ 4	− 3	− 5	− 7	− 9	−11
14	− 2	+ 3	+ 4	+ 6	+ 8	+ 9	+ 2	− 4	− 6	− 8	−10	−12
15	− 4	+ 2	+ 4	+ 6	+ 8	+10	+ 2	0	− 1	− 2	− 3	− 4
16	− 4	+ 1	+ 2	+ 4	+ 6	+ 7	+ 3	+ 2	+ 1	+ 1	0	0
17	− 4	+ 2	+ 4	+ 6	+ 8	+10	+ 2	− 1	− 2	− 3	− 4	− 5
18	− 3	+ 2	+ 4	+ 6	+ 8	+10	+ 3	0	− 1	− 2	− 3	− 4
19	− 4	+ 3	+ 5	+ 7	+ 9	+11	+ 5	+ 1	0	− 1	− 2	− 3
20	− 3	+ 6	+ 9	+12	+15	+18	+ 3	+ 6	+ 7	+ 8	+ 9	+10
21	− 3	+ 5	+ 7	+10	+13	+15	0	+ 6	+ 7	+ 9	+11	+12
22	− 4	+ 3	+ 5	+ 7	+ 9	+11	− 4	+ 4	+ 6	+ 9	+12	+14
23	− 2	0	0	+ 1	+ 2	+ 2	− 6	+ 5	+ 8	+12	+15	+19
24	− 2	− 5	− 5	− 6	− 7	− 7	− 4	+ 4	+ 7	+10	+13	+16

Table VII

FK3—N30 (+60° to +30°)

α	$\Delta\alpha_\alpha$ Unit: 0.ˢ001						$\Delta\delta_\alpha$ Unit: 0.″01					
	1900	1930	1940	1950	1960	1970	1900	1930	1940	1950	1960	1970
h												
0	− 3	+ 1	+ 3	+ 4	+ 5	+ 7	− 4	+ 1	+ 3	+ 5	+ 7	+ 9
1	− 4	− 2	− 2	− 1	0	0	− 5	− 1	0	+ 1	+ 2	+ 3
2	− 3	− 3	− 3	− 3	− 3	− 3	− 5	− 2	− 1	0	+ 1	+ 2
3	− 1	+ 2	+ 3	+ 4	+ 5	+ 6	− 1	+ 1	+ 1	+ 2	+ 3	+ 3
4	− 2	+ 1	+ 2	+ 3	+ 4	+ 5	− 1	− 3	− 3	− 4	− 4	− 5
5	− 1	− 2	− 2	− 2	− 2	− 2	− 1	− 2	− 2	− 2	− 2	− 2
6	− 1	− 3	− 4	− 5	− 6	− 7	0	0	+ 1	+ 1	+ 1	+ 2
7	0	− 5	− 7	− 9	−11	−13	− 1	− 2	− 3	− 3	− 3	− 4
8	0	− 8	−11	−14	−17	−20	− 3	− 4	− 5	− 5	− 5	− 6
9	+ 3	− 9	−13	−17	−21	−25	− 2	− 3	− 4	− 4	− 4	− 5
10	+ 4	− 6	− 9	−12	−15	−18	− 1	− 3	− 3	− 4	− 5	− 5
11	+ 3	− 4	− 6	− 9	−11	−14	+ 2	− 3	− 4	− 6	− 8	− 9
12	+ 3	− 2	− 3	− 5	− 7	− 8	+ 3	+ 2	+ 1	+ 1	+ 1	0
13	+ 2	+ 1	+ 1	+ 1	+ 1	+ 1	+ 3	+ 6	+ 7	+ 8	+ 9	+10
14	0	0	0	0	0	0	+ 4	+ 6	+ 6	+ 7	+ 7	+ 8
15	− 2	0	+ 1	+ 2	+ 3	+ 4	+ 4	+ 2	+ 2	+ 1	0	0
16	− 4	+ 1	+ 2	+ 4	+ 6	+ 7	+ 3	+ 1	0	− 1	− 2	− 3
17	− 1	+ 3	+ 5	+ 6	+ 7	+ 9	+ 4	+ 3	+ 2	+ 2	+ 2	+ 1
18	+ 1	+ 6	+ 7	+ 9	+10	+12	+ 3	+ 1	+ 1	0	− 1	− 1
19	+ 2	+ 3	+ 4	+ 4	+ 4	+ 5	+ 1	− 1	− 1	− 2	− 3	− 3
20	+ 3	+ 4	+ 4	+ 4	+ 4	+ 4	0	− 1	− 1	− 2	− 2	− 3
21	+ 1	+ 9	+11	+14	+16	+19	+ 1	0	0	0	0	0
22	0	+ 9	+12	+15	+18	+21	0	+ 1	+ 2	+ 2	+ 2	+ 3
23	0	+ 5	+ 7	+ 9	+11	+13	− 2	+ 1	+ 2	+ 3	+ 4	+ 5
24	− 3	+ 1	+ 3	+ 4	+ 5	+ 7	− 4	+ 1	+ 3	+ 5	+ 7	+ 9

Table VIII

FK3—N30 (−30° to 0°)

α	$\Delta\alpha_\alpha$ Unit: $0^{s}.001$						$\Delta\delta_\alpha$ Unit: $0''.01$					
	1900	1930	1940	1950	1960	1970	1900	1930	1940	1950	1960	1970
h												
0	− 2	+ 1	+ 2	+ 3	+ 4	+ 5	− 1	+ 4	+ 6	+ 8	+10	+12
1	0	− 1	− 1	− 1	− 1	− 1	− 3	− 2	− 1	− 1	− 1	0
2	+ 2	0	− 1	− 2	− 3	− 4	− 2	− 3	− 3	− 3	− 3	− 3
3	+ 3	+ 1	+ 1	0	− 1	− 1	− 2	− 2	− 2	− 2	− 2	− 2
4	+ 2	+ 3	+ 4	+ 4	+ 4	+ 5	0	0	0	0	0	0
5	0	+ 3	+ 4	+ 5	+ 6	+ 7	0	− 1	− 1	− 1	− 1	− 1
6	+ 1	+ 2	+ 3	+ 3	+ 3	+ 4	− 2	− 5	− 6	− 7	− 8	− 9
7	+ 2	0	− 1	− 2	− 3	− 4	0	− 1	− 1	− 1	− 1	− 1
8	+ 2	0	0	− 1	− 2	− 2	0	− 1	− 1	− 1	− 1	− 1
9	+ 2	+ 1	0	0	0	− 1	0	− 2	− 2	− 3	− 4	− 4
10	+ 1	− 1	− 1	− 2	− 3	− 3	0	− 1	− 1	− 2	− 2	− 3
11	0	0	+ 1	+ 1	+ 1	+ 2	0	0	− 1	− 1	− 1	− 2
12	0	0	+ 1	+ 1	+ 1	+ 2	+ 2	+ 1	+ 1	+ 1	+ 1	+ 1
13	0	0	0	0	0	0	+ 5	+ 2	+ 1	0	− 1	− 2
14	− 4	+ 1	+ 3	+ 5	+ 7	+ 9	+ 3	+ 1	+ 1	0	− 1	− 1
15	− 6	+ 2	+ 4	+ 7	+10	+12	+ 1	0	0	− 1	− 1	− 2
16	− 3	+ 1	+ 2	+ 4	+ 5	+ 7	0	+ 1	+ 2	+ 2	+ 2	+ 3
17	+ 1	− 2	− 3	− 4	− 5	− 6	0	+ 1	+ 1	+ 1	+ 1	+ 1
18	+ 3	− 2	− 4	− 6	− 8	−10	0	− 2	− 3	− 4	− 5	− 6
19	+ 2	− 2	− 3	− 5	− 6	− 8	0	0	0	0	0	0
20	+ 2	− 2	− 3	− 4	− 5	− 6	− 2	0	+ 1	+ 2	+ 3	+ 4
21	+ 2	0	− 1	− 2	− 3	− 4	0	0	+ 1	+ 1	+ 1	+ 2
22	+ 1	0	0	0	0	0	+ 1	+ 1	0	0	0	− 1
23	− 2	+ 1	+ 2	+ 3	+ 4	+ 5	0	+ 4	+ 5	+ 7	+ 8	+10
24	− 2	+ 1	+ 2	+ 3	+ 4	+ 5	− 1	+ 4	+ 6	+ 8	+10	+12

Table IX

FK3—N30 (0° to −30°)

α	$\Delta\alpha_\alpha$ Unit: $0^{s}.001$						$\Delta\delta_\alpha$ Unit: $0''.01$					
	1900	1930	1940	1950	1960	1970	1900	1930	1940	1950	1960	1970
h												
0	0	+ 1	+ 1	+ 2	+ 2	+ 3	+ 1	+ 6	+ 7	+ 9	+10	+12
1	− 1	+ 2	+ 3	+ 4	+ 5	+ 6	− 1	+ 5	+ 7	+ 9	+11	+13
2	0	+ 3	+ 4	+ 5	+ 6	+ 7	− 4	+ 4	+ 7	+10	+13	+16
3	+ 1	+ 1	+ 1	+ 1	+ 1	+ 1	− 2	+ 5	+ 8	+10	+12	+15
4	+ 2	+ 4	+ 4	+ 5	+ 6	+ 6	0	+ 6	+ 7	+ 9	+11	+12
5	− 1	+ 6	+ 8	+11	+13	+16	+ 1	+ 4	+ 5	+ 6	+ 7	+ 8
6	− 1	+ 4	+ 6	+ 8	+10	+12	− 1	+ 1	+ 1	+ 2	+ 3	+ 3
7	+ 1	+ 1	0	0	0	− 1	0	− 1	− 2	− 2	− 2	− 3
8	0	− 1	− 2	− 2	− 2	− 3	+ 5	0	− 1	− 3	− 5	− 6
9	− 1	0	+ 1	+ 1	+ 1	+ 2	+ 3	− 2	− 4	− 6	− 8	−10
10	0	+ 2	+ 3	+ 4	+ 5	+ 6	+ 1	− 2	− 3	− 4	− 5	− 6
11	− 1	+ 2	+ 3	+ 4	+ 5	+ 6	0	− 2	− 3	− 4	− 5	− 6
12	− 2	− 2	− 1	− 1	− 1	0	+ 2	− 3	− 5	− 7	− 9	−11
13	− 3	− 2	− 1	− 1	0	0	0	− 7	− 9	−12	−14	−17
14	− 5	− 1	0	+ 1	+ 2	+ 3	0	− 5	− 6	− 8	− 9	−11
15	− 6	− 2	0	+ 1	+ 2	+ 4	0	− 4	− 5	− 7	− 8	−10
16	− 5	− 2	0	+ 1	+ 2	+ 4	0	− 5	− 6	− 8	− 0	−11
17	− 3	− 3	− 3	− 3	− 3	− 3	− 1	− 5	− 6	− 7	− 8	− 9
18	+ 2	− 5	− 7	− 9	−11	−13	− 1	− 6	− 7	− 9	−10	−12
19	+ 4	− 4	− 6	− 9	−12	−14	− 2	− 3	− 3	− 3	− 3	− 3
20	+ 4	− 4	− 6	− 9	−12	−14	− 2	0	0	+ 1	+ 2	+ 2
21	+ 3	− 4	− 7	− 9	−11	−14	− 2	+ 1	+ 3	+ 4	+ 5	+ 7
22	+ 1	− 1	− 1	− 2	− 3	− 4	− 2	+ 3	+ 4	+ 6	+ 8	+ 9
23	+ 1	+ 1	+ 1	+ 1	+ 1	+ 1	− 1	+ 4	+ 5	+ 7	+ 9	+10
24	0	+ 1	+ 1	+ 2	+ 2	+ 3	+ 1	+ 6	+ 7	+ 9	+10	+12

TABLE X

FK3—N30 (−30° to −60°)

α	$\Delta\alpha_\alpha$ Unit : $0^s.001$						$\Delta\delta_\alpha$ Unit : $0''.01$					
	1900	1930	1940	1950	1960	1970	1900	1930	1940	1950	1960	1970
h												
0	+ 2	− 1	− 3	− 4	− 5	− 7	0	+11	+14	+18	+22	+25
1	− 4	+ 1	+ 2	+ 4	+ 6	+ 7	+ 1	+12	+16	+20	+24	+28
2	− 3	− 1	0	+ 1	+ 2	+ 3	+ 1	+ 7	+ 9	+11	+13	+15
3	+ 2	0	0	− 1	− 2	− 2	+ 1	+10	+13	+16	+19	+22
4	− 1	− 3	− 3	− 4	− 5	− 5	+ 1	+ 8	+11	+13	+15	+18
5	− 4	− 4	− 4	− 4	− 4	− 4	+ 1	0	0	0	0	0
6	− 3	− 4	− 4	− 4	− 4	− 4	− 1	+ 1	+ 1	+ 2	+ 3	+ 3
7	− 3	− 4	− 5	− 5	− 5	− 6	− 1	+ 3	+ 5	+ 6	+ 7	+ 9
8	− 3	0	+ 1	+ 2	+ 3	+ 4	− 1	+ 6	+ 8	+10	+12	+14
9	− 6	+ 5	+ 8	+12	+16	+19	− 3	+ 8	+12	+16	+20	+24
10	− 6	+ 8	+13	+18	+23	+28	− 7	+ 6	+10	+14	+18	+22
11	0	+ 9	+12	+15	+18	+21	− 5	+ 1	+ 3	+ 5	+ 7	+ 9
12	0	+ 4	+ 5	+ 7	+ 8	+10	− 2	0	+ 1	+ 2	+ 3	+ 4
13	+ 2	+ 1	0	0	0	− 1	0	− 1	− 1	− 1	− 1	− 1
14	+ 3	+ 1	0	− 1	− 2	− 3	+ 2	− 8	−11	−15	−18	−22
15	+ 3	+ 4	+ 4	+ 4	+ 4	+ 4	+ 7	− 9	−14	−19	−24	−29
16	+ 3	0	− 1	− 2	− 3	− 4	+ 9	− 9	−15	−21	−27	−33
17	− 1	+ 1	+ 1	+ 2	+ 3	+ 3	+ 7	− 8	−13	−18	−23	−28
18	+ 2	+ 1	+ 1	+ 1	+ 1	+ 1	+ 3	− 7	−10	−14	−17	−21
19	+ 7	− 7	−11	−16	−21	−25	+ 4	− 7	−11	−15	−19	−23
20	+ 4	− 8	−13	−17	−21	−26	+ 1	− 1	− 2	− 3	− 4	− 5
21	+ 2	− 3	− 4	− 6	− 8	− 9	− 1	− 1	− 1	− 1	− 1	− 1
22	+ 2	− 2	− 3	− 4	− 5	− 6	− 1	+ 1	+ 1	+ 2	+ 3	+ 3
23	+ 5	− 5	− 8	−11	−14	−17	− 3	+ 5	+ 7	+10	+13	+15
24	+ 2	− 1	− 3	− 4	− 5	− 7	0	+11	+14	+18	+22	+25

TABLE XI

FK3—N30 (−60° to −90°)

α	$\Delta\alpha_\alpha \cos\delta$ Unit : $0^s.001$						$\Delta\delta_\alpha$ Unit : $0''.01$					
	1900	1930	1940	1950	1960	1970	1900	1930	1940	1950	1960	1970
h												
0	+ 4	+ 5	+ 5	+ 5	+ 5	+ 5	0	+ 3	+ 4	+ 5	+ 6	+ 7
1	+ 4	0	− 1	− 2	− 3	− 4	− 2	+18	+25	+32	+39	+46
2	+ 6	− 2	− 5	− 8	−11	−14	− 1	+18	+25	+31	+37	+44
3	+ 6	− 1	− 4	− 6	− 8	−11	0	+ 5	+ 7	+ 9	+11	+13
4	+ 4	+ 1	0	− 1	− 2	− 3	− 1	− 1	− 1	− 1	− 1	− 1
5	+ 1	+ 1	0	0	0	− 1	− 1	− 3	− 3	− 4	− 5	− 5
6	+ 2	− 3	− 4	− 6	− 8	− 9	0	0	− 1	− 1	− 1	− 2
7	+ 1	− 5	− 7	− 9	−11	−13	+ 2	+ 2	+ 1	+ 1	+ 1	0
8	− 3	− 1	− 1	0	+ 1	+ 1	+ 4	0	− 2	− 3	− 4	− 6
9	− 6	+ 7	+11	+16	+20	+25	+ 3	+ 6	+ 6	+ 7	+ 8	+ 8
10	− 7	+ 4	+ 7	+11	+15	+18	0	+10	+13	+17	+21	+24
11	− 7	− 1	+ 2	+ 4	+ 6	+ 9	− 2	+ 7	+10	+13	+16	+19
12	+ 6	+11	+12	+14	+16	+17	−11	− 8	− 7	− 6	− 5	− 4
13	+11	+15	+16	+17	+18	+19	− 9	− 9	− 9	− 9	− 9	− 9
14	− 3	0	+ 1	+ 2	+ 3	+ 4	+ 3	+ 1	0	− 1	− 2	− 3
15	− 5	− 3	− 2	− 1	0	+ 1	0	− 7	− 9	−11	−13	−15
16	− 5	− 3	− 3	− 2	− 1	− 1	− 4	−10	−12	−14	−16	−18
17	− 3	+ 1	+ 3	+ 4	+ 5	+ 7	− 7	− 9	−10	−11	−12	−13
18	+ 4	+ 6	+ 6	+ 7	+ 7	+ 8	− 8	−12	−14	−15	−16	−18
19	+ 6	+ 3	+ 2	+ 1	0	− 1	− 5	−18	−22	−26	−30	−34
20	+ 5	0	− 2	− 4	− 6	− 8	+ 1	− 9	−12	−15	−18	−21
21	+ 3	− 2	− 4	− 6	− 8	−10	+ 5	− 6	− 9	−13	−17	−20
22	+ 7	+ 3	+ 2	+ 1	0	− 1	+ 3	− 4	− 6	− 9	−12	−14
23	+ 8	+ 5	+ 4	+ 3	+ 2	+ 1	0	− 3	− 5	− 6	− 7	− 9
24	+ 4	+ 5	+ 5	+ 5	+ 5	+ 5	0	+ 3	+ 4	+ 5	+ 6	+ 7

I am deeply grateful to the Astronomer Royal, Sir Harold Spencer Jones, for his help in translating this paper into English. I also thank Mr Sadler for his assistance.

Astronomisches Rechen-Institut,
Heidelberg :
1954 *September* 24.

References

(1) A. Kopff, *Astronomisch-Geodätisches Jahrbuch* 1954 ; *ibid.*, 1956.
(2) A. Kopff, Circular letter, Dec. 1952 ; *Astron. J.*, **58,** 207, 1953 ; *Astron. Nachr.*, **281,** 139, 1953.
(3) H. R. Morgan, *Astron. Papers, American Ephemeris and Nautical Almanac*, Vol. XIII, Part III, 1952.
(4) H. Nowacki, *Nachrichtenblatt der Astronomischen Zentralstelle*, **7,** 21, 1953.
(5) A. Kahrstedt, *Astron. Nachr.*, **228,** 57, 1926.
(6) A. Kopff, *Astron. Nachr.*, **225,** 273, 1925.
(7) Colloques Intern. XXV, *Constantes Fondam. de l'Astronomie*, 5. Séance, Paris, 1950.
(8) A. Kahrstedt, *Astron. Nachr.*, **235,** 369, 1929.
(9) L. Boss, *P.G.C.*, p. XXXIII, 1910 ; B. Boss, *G.C.*, Vol. I, p. 49, 1937.
(10) H. Nowacki, *Veröffentl. Astron. Rechen-Inst. zu Heidelberg*, Nr. 4, 1952.
(11) A. Kopff, *Abh. Preuss. Akad. der Wiss.*, Jahrgang 1939. *Math-naturw. Klasse*, Nr. 18.
(12) A. Kopff, *Astron. Nachr.*, **269,** 160, 1939.
(13) H. R. Morgan, *Astron. J.*, **56,** 97, 1951.
(14) L. Boss, *P.G.C.*, p. XI, 1910 ; *List of* 1059 *Standard Stars for* 1910, Albany, N.Y., 1909.

PHOTOGRAPHIC OBSERVATIONS OF MONOCHROMATIC MAGNITUDE AT SIX WAVE-LENGTHS

R. v. d. R. Woolley, S. C. B. Gascoigne and A. de Vaucouleurs

(Received 1954 March 9)

Summary

Relative monochromatic magnitudes for 85 bright southern stars have been determined by photographic photometry at the following six wave-lengths: λλ 4050, 4250, 4550, 4945, 5980, 6360. The relative energy distribution is examined as a function of spectral type. Comparisons are made with the results of other observers and it appears that while the standard of accuracy achieved for colours is good, there is evidence for a possible error of about 2 per cent in the magnitude scale.

---

1. *Introduction and observational.*—Observations of monochromatic magnitude, by Hogg and Hall (**1**), and of colour gradient, by Gascoigne (**2**), have been made on Mt Stromlo in recent years and have already been described. Both these sets of observations were relative. It had been planned for some time to make them absolute, by fixing their zero-points with respect to an accurately calibrated terrestrial source. As a convenient way of doing this, the slitless spectrograph with which both programmes (**1**) and (**2**) had been carried out was removed from the Reynolds reflector and mounted separately on the polar axis belonging to the Farnham refractor. Here it became effectively an objective prism telescope of four inches aperture, and could be directed equally well at a star or at a standard lamp set up in the Observatory grounds. Some observations of relative magnitude and gradient, originally of a preliminary nature, were made with this equipment. As these showed features of interest, this part of the programme was expanded to include all the southern stars brighter than about the third magnitude, and forms the subject matter of the present paper. The comparisons with the standard lamp will be described in a sequel.

A smaller angle prism was substituted for the original 45° prism in the spectrograph. This gave a dispersion of 290 A/mm at $H\gamma$, adequate for the purpose in hand, and which, with the plates used (mostly Kodak O-F), enabled a spectrum of a third magnitude star to be obtained in 60 seconds. Spectra were widened $\frac{1}{2}$ mm by rocking a diagonal mirror as described in (**2**). The calibration of each plate was effected by spinning in turn in front of the prism a number of sectors, concentric with the circular telescope aperture. A set of these was made in $\frac{1}{2}$ magnitude steps from 0 to 4 magnitudes.

Dr Hogg kindly checked the sector attenuations, by attaching to the spectrograph the photomultiplier he had used in (**1**), and measuring with it the apparent brightness of the standard lamp (a suitable steady light source) as seen through each of the sectors in turn. The values determined photoelectrically agreed in

all cases with those computed geometrically to within a few thousandths of a magnitude.

To calibrate a plate at least one and often two bright stars were given a considerable range of sectors. Three exposures were usually made on remaining stars, if necessary through different sectors to enable suitable densities to be recorded at each wave-length. Each plate accommodated about 40 spectra, and on a good night four or more plates could be secured. Atmospheric absorption was determined each night, by observing stars as they rose or set through a considerable range of air mass. In all, 130 plates were secured on 66 nights, and of these, 110 were measured. The remaining plates were omitted, usually because of unsatisfactory absorption on the night on which they were taken.

Mean measurements of absorption are shown in Table I, which includes also the standard deviations on individual nights and earlier determinations. The agreement between the present values and those determined previously on Mount Stromlo (**1, 9**) is noteworthy.

TABLE I

Determinations of absorption (*unit :* 0·01 *mag/sec z*)

	λ4050	λ4250	λ4550	λ4945	λ5980	λ6360
Mean absorption	37	32	26	21	15	12·6
Standard deviation	±4·3	±4·0	±3·4	±3·6	±2·8	±2·4
Hogg and Hall (**1**)			25·4 (east)			
			28·1 (west)			
Sun and Sirius (**9**)			λ4510	λ4945	λ5550	λ6209
			26	21	17	13

Plates were measured in the projection photometer described in (**2**), with a slit of projected width 0·08 mm, and at the following wave-lengths: λλ 4050, 4250, 4550, 4945, 5980, 6360. The bandwidth accepted thus ranged from about 20 angstroms in the blue to about 50 in the red. The regions were chosen to avoid absorption lines as far as possible, but this cannot of course be done completely, and our magnitudes refer to the integrated spectrum and not the continuum "between the lines". λ 4550 was the wave-length at which Hogg and Hall made their measurements. It was hoped also to have a set of magnitudes at about λ 5450, the photovisual effective wave-length, but the plates used had either rapidly varying or low sensitivity in this region, and it was therefore not suitable for measurement.

2. *The reductions.*—The observations were reduced by selecting as standards the thirteen stars in Table II (δ Velr and α Virg were occasionally used as secondary standards). These were intercompared frequently and least-squares solutions made of their relative magnitudes at each of the six wave-lengths. The zero-point of m_{4550} was chosen so as to make the mean magnitudes of the standard stars agree with Hogg and Hall's magnitudes; the zeros of the other five magnitudes were then fixed so as to make the mean gradient agree with Gascoigne's gradients. Details are shown in Table III. The zero of these gradients should, like Gascoigne's, be close to that of the Greenwich gradients (**3**). A comparison of the twelve stars in common shows that we average about 0·028 bluer than Greenwich. If we omit four stars in Orion for which there is some evidence that the Greenwich gradients are anomalously red, this figure is reduced to 0·015. Similarly a comparison of the seventy stars in common with Gascoigne shows that we average 0·015 bluer. While one would like to see this figure reduced, it can nevertheless be regarded as satisfactorily small.

TABLE II

The standard stars

	m_F	m_{HH}	$m_F - m_{HH}$	G_F	G_R	$G_F - G_R$
α Erid	0·296	0·274	0·022	−0·225	−0·236	0·011
γ Orio	1·429	1·434	− ·005	−0·272	−0·285	− ·013
ε C Maj	1·307	1·295	·012	−0·277	−0·278	·001
β Cari	1·599	1·596	·003	0·024	0·017	·007
α Leon	1·224	1·238	− ·014	−0·092	−0·118	·026
γ Cent	2·023	2·038	− ·015	−0·022	−0·016	− ·006
β Cent	0·410	0·402	·008	−0·327	−0·332	·005
α Ophi	2·087	2·096	− ·009	0·290	0·305	− ·015
ε Sgtr	1·730	1·742	− ·012	0·011	0·036	− ·025
α Aqil	0·820	0·834	− ·014	0·410	0·416	− ·006
α Pavo	1·731	1·718	·013	−0·239	−0·249	·010
α Grus	1·587	1·585	·002	−0·196	−0·180	− ·016
α PscA	1·117	1·108	·009	0·119	0·107	·012

m_F and m_{HH} are the magnitudes at λ 4550 determined on the Farnham refractor and by Hogg and Hall (**1**) respectively. G_F and G_R are gradients determined on the Farnham and on the Reynolds reflector (**2**).

3. *Results.*—The results for the 85 stars * on the programme are set out in Table III. These consist of the six magnitudes, together with the gradients computed from them. Spectral types were taken from Yerkes lists, or from some unpublished work of Miss Woods. There was some difficulty in deciding on a suitable measure of colour for the later type stars. As is well known, magnitude differences between these and early type stars do not plot linearly against $1/\lambda$, the later types exhibiting a deficiency in the violet. However, over the limited range λ 4550–λ 6360 the relation appears reasonably linear (see Section 4), and gradients for stars later than F5 were therefore computed from these four wave-lengths only.

From internal evidence the accuracy at each wave-length for the standard stars is better than 0·01 mag. For the programme stars it averages 0·02 or 0·03 mag. Red stars tend to be less accurate, possibly because of their rapid variation of photographic density with wave-length.

4. *Relative energy distribution.*—The material in Table III enables us to examine the variation of relative energy distribution as a function of spectral type. Of previous work in this field (**4, 5**), ours is most nearly like that of Kienle, Strassl and Wempe (**6**). To reduce observational error we represented each spectral type by the means of the following groups of stars:

B0 : ε C Maj B1 II, β Cent B1 II, ι Orio O9 V, ε Orio B0 I.
B5 : α Pavo B3 IV, α Erid B5 IV, α Grus B5 V, α Leon B8 V.
A0 : ε Sgtr B9 IV, α Pegs B9 V, β Cari A0 III, α Cent A0 III.
A5 : α Psc A A3 V, α Ophi A5 III, α Aqil A7 V.
F0 I : α Cari F0 Ia, α Leps F0 Ib, ι Cari F0 Ib.
F0 V : α Hydi F0 V, α Circ F0 V, β Tr Au F2 V.
F9 I : δ C Maj F8 Ia, β Aqar G0 Ib.
G1 V : η Boot G0 IV, β Hydi G1 IV, α Cent G2 V.
G5 III : β Corv G5 II, μ Velr G5 III, β Ceti G8 III.
K0 III : β Gemi K0 II, θ Cent K0 III–IV, ε Scor K2 III.

* The following bright stars were omitted : θ Cari, which is in a cluster; γ Velr, a double star only partly resolved on our plates; α Crux, omitted inadvertently.

TABLE III

Collected results

Star	R.A. h m	Spec.	λ4050	λ4250	λ4550	λ4945	λ5980	λ6360	*G*
γ Pegs	00 11	B2 V	2·56	2·58	2·62	2·69	2·81	2·86	−0·32
β Hydi	00 23	G1 IV	3·57	3·51	3·12	2·86	2·48	2·34	1·08
β Ceti	00 41	G8 III	3·48	3·48	2·69	2·27	1·61	1·51	1·73
γ Erid	01 36	B5 IV	0·26	0·28	0·30	0·38	0·42	0·50	−0·23
γ Hydi	01 57	Fo V	3·12	3·06	2·97	2·86	2·61	2·55	0·60
β Erid	05 05	A3 V	2·85	2·77	2·74	2·72	2·64	2·56	0·25
β Orio	05 12	B8 Ia	0·20	0·18	0·16	0·12	0·10	0·16	0·06
γ Orio	05 22	B2 IV	1·38	1·38	1·43	1·46	1·57	1·64	−0·27
β Leps	05 26	G2 II	3·92	3·78	3·30	2·90	2·48	2·33	1·34
δ Orio	05 30	O9·5 III	1·99	1·94	2·00	2·00	2·10	2·17	−0·20
α Leps	05 30	Fo Ib	2·81	2·74	2·68	2·56	2·39	2·33	0·49
ι Orio	05 33	O9 V	2·46	2·48	2·55	2·60	2·64	2·72	−0·25
ε Orio	05 34	Bo I	1·53	1·53	1·54	1·56	1·70	1·72	−0·22
α Colm	05 38	B8 Ve	2·41	2·41	2·44	2·47	2·52	2·48	−0·10
ζ Orio	05 38	O9·5 III	1·52	1·49	1·56	1·58	1·76	1·68	−0·24
κ Orio	05 45	Bo II	1·81	1·84	1·92	1·89	2·01	2·04	−0·23
β C Maj	06 20	B1 II	1·72	1·75	1·77	1·85	2·01	2·01	−0·33
α Cari	06 23	Fo Ia	−0·49	−0·51	−0·59	−0·68	−0·80	−0·82	0·35
α C Maj	06 43	A1 V	−1·44	−1·44	−1·43	−1·43	−1·42	−1·37	−0·05
ε C Maj	06 57	B1 II	1·26	1·25	1·31	1·34	1·48	1·50	−0·28
δ C Maj	07 06	F8 Ia	2·75	2·55	2·29	1·89	1·53	1·44	1·18
η C Maj	07 22	B5 I	2·32	2·30	2·33	2·32	2·31	2·24	0·05
α C Min	07 37	F5 IV	0·91	0·83	0·63	0·43	0·12	0·09	0·88
β Gemi	07 42	Ko III	2·55	2·33	1·85	1·30	0·62	0·58	1·89
ζ Pupp	08 02	O5	1·89	1·94	2·01	2·03	2·20	2·18	−0·32
ρ Pupp	08 05	F6 II	3·29	3·11	3·02	2·81	2·55	2·39	0·87
ε Cari	08 22	Ko, B	...	...	2·97	2·34	1·40	1·06	2·72
δ Velr	08 43	Ao V	1·89	1·87	1·83	1·84	1·85	1·76	0·09
β Cari	09 13	Ao III	1·59	1·58	1·60	1·58	1·58	1·56	0·02
ι Cari	09 16	Fo Ib	2·34	2·33	2·29	2·13	2·04	1·99	0·38
κ Velr	09 21	B2 IV	2·22	2·25	2·25	2·33	2·45	2·40	−0·23
α Hyda	09 25	K3 III	...	...	2·85	2·26	1·48	1·16	2·38
α Leon	10 06	B8 V	1·18	1·18	1·22	1·24	1·26	1·27	−0·10
μ Velr	10 45	G5 III	3·89	3·71	3·25	2·78	2·31	2·14	1·53
λ Cent	11 34	B9 III	2·93	2·94	2·94	2·93	2·92	2·85	0·06
β Leon	11 47	A3 V	2·10	2·07	2·04	2·02	1·97	1·95	0·14
δ Cent	12 06	B2 Ve	2·39	2·41	2·39	2·44	2·46	2·42	−0·05
δ Cruc	12 10	B2 IV	2·42	2·48	2·56	2·63	2·77	2·66	−0·30
γ Corv	12 13	B8·5 III	2·35	2·38	2·42	2·46	2·47	2·44	−0·10
γ Cruc	12 28	M3 II	3·71	3·43	2·62	2·30	0·80	0·41	3·38

TABLE III (*cont.*)

Star	R.A. h m	Spec.	λ4050	λ4250	λ4550	λ4945	λ5980	λ6360	*G*
β Corv	12 32	G5 II	3·82	3·69	3·14	2·77	2·27	2·10	1·46
α Musc	12 34	B3 IV	2·32	2·36	2·41	2·43	2·62	2·56	−0·29
γ Cent	12 39	Ao III	1·97	2·01	2·02	2·05	2·02	2·01	−0·03
β Cruc	12 45	Bo III	0·91	0·94	1·05	1·11	1·22	1·24	−0·35
α Virg	13 23	B1 III	0·68	0·73	0·76	0·85	0·94	0·95	−0·29
ε Cent	13 37	B1 IV	1·91	1·93	1·99	2·14	2·24	2·24	−0·37
ζ Cent	13 52	B1 IV	2·14	2·16	2·24	2·37	2·49	2·44	−0·37
η Boot	13 52	Go IV	3·32	3·20	2·89	2·73	2·36	2·15	1·05
β Cent	14 00	B1 II	0·32	0·37	0·41	0·51	0·61	0·63	−0·33
θ Cent	14 04	Ko III–IV	3·39	3·27	2·65	2·21	1·63	1·49	1·66
α Boot	14 13	K2 p	1·73	1·48	0·76	0·27	−0·48	−0·70	2·11
α Cent	14 36	G2 V	0·74	0·56	0·13	−0·09	−0·60	−0·67	1·22
α Circ	14 38	Fo V Sr	3·27	3·18	3·12	3·07	2·83	2·89	0·41
α Lupi	14 39	B2 II	2·02	2·06	2·06	2·20	2·28	2·24	−0·26
α Libr	14 48	A3 met	2·78	2·75	2·72	2·76	2·57	2·53	0·25
β Lupi	14 55	B2 V	2·35	2·40	2·37	2·51	2·65	2·53	−0·26
γ Tr Au	15 14	Ao V Eu	2·72	2·74	2·74	2·77	2·69	2·64	0·08
β Libr	15 14	B8 V	2·38	2·40	2·39	2·50	2·49	2·42	−0·08
γ Lupi	15 32	B3 V	2·48	2·47	2·51	2·56	2·79	2·66	−0·28
α Cor B	15 33	Ao V	2·02	2·06	2·07	2·05	2·09	2·06	−0·04
β Tr Au	15 51	F2 V	3·13	3·10	2·98	2·82	2·62	2·49	0·65
π Scor	15 56	B2 IV	2·60	2·64	2·64	2·68	2·86	2·81	−0·26
δ Scor	15 57	Bo IV	2·10	2·11	2·19	2·22	2·24	2·22	−0·13
σ Scor	16 18	B1 III	2·98	2·97	2·89	2·80	2·73	2·61	0·42
τ Scor	16 33	Bo V	2·47	2·56	2·61	2·64	2·83	2·82	−0·36
α Scor	16 26	M1 Ib	...	...	2·31	1·44	0·33	−0·04	3·34
ζ Ophi	16 34	O9.5 V	2·52	2·55	2·51	2·44	2·43	2·40	0·14
α Tr Au	16 43	K2 III	...	...	2·90	...	1·30	1·24	2·60
ε Scor	16 47	K2 III	3·94	3·62	2·97	2·49	1·80	1·64	1·95
υ Scor	17 27	B2 IV	2·35	2·40	2·45	2·49	2·64	2·62	−0·30
α Arae	17 28	B3 Ve	2·72	2·78	2·76	2·79	2·96	2·87	−0·20
λ Scor	17 30	B2 IV	1·26	1·30	1·38	1·40	1·56	1·55	−0·31
α Ophi	17 32	A5 III	2·16	2·13	2·09	2·01	1·93	1·87	0·28
θ Scor	17 34	Fo I–II	2·29	2·20	2·05	1·83	1·58	1·51	0·81
κ Scor	17 39	B2 IV	2·09	2·14	2·19	2·21	2·33	2·35	−0·26
ε Sgtr	18 21	B9 IV	1·70	1·72	1·73	1·71	1·72	1·70	0·00
σ Sgtr	18 52	B3 V	1·82	1·86	1·89	1·93	2·07	2·02	−0·29
ζ Sgtr	18 59	A2 IV	2·58	2·56	2·59	2·46	2·50	2·44	0·13
α Aqil	19 48	A7 V	0·94	0·90	0·82	0·77	0·59	0·55	0·41
α Pavo	20 22	B3 IV	1·65	1·69	1·73	1·75	1·88	1·88	−0·23
β Aqar	21 29	Go Ib	3·87	3·76	3·35	2·83	2·46	2·35	1·24
δ Capr	21 44	A5 met	3·17	3·11	2·98	2·87	2·67	2·61	0·57
α Grus	22 05	B5 V	1·54	1·57	1·59	1·63	1·72	1·73	−0·20
α Psc A	22 55	A3 V	1·18	1·16	1·12	1·10	1·06	1·07	0·12
α Pegs	23 02	B9 V	2·38	2·36	2·40	2·32	2·40	2·37	−0·01

From the observed magnitudes we subtract those computed from the mean gradient for each group, on the assumption of a linear relation between m_λ and $1/\lambda$. For later types the gradient was computed from the four longest wavelengths only. Residuals in the sense O–C are shown in Table IV and also plotted in Fig. 1. The change in the character of the residuals for types later than F5 is well shown. It will be noticed that with these later types departures from linearity are more marked for giants than for dwarfs.

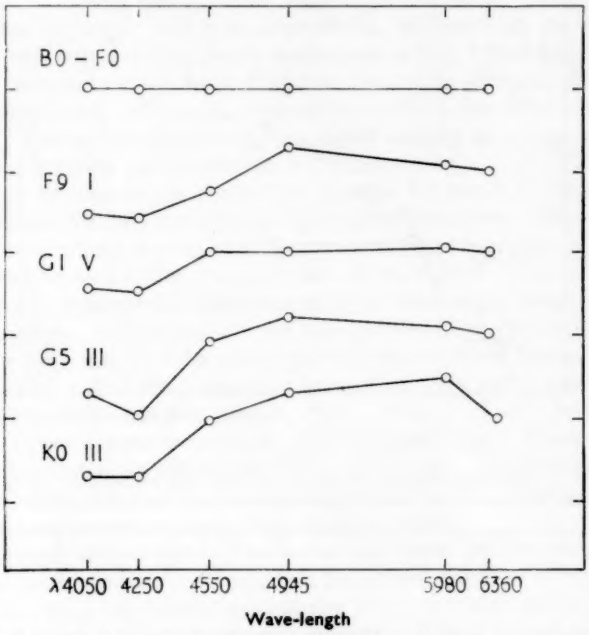

FIG. 1.—*Relative energy distribution. The vertical spacers are 0·4 mag. apart.*

TABLE IV

Residuals in the sense O–C in 0·01 mag.

	λ4050	λ4250	λ4550	λ4945	λ5980	λ6360
B0	1	0	− 0·5	− 0·6	0·5	− 0·6
B5	0	0	0	0	0	0·5
A0	− 1	0	2	− 1	1	− 1
A5	0	0	0	0	0	0
F0 I	− 1	1	2	− 2	0	1
F0 V	− 1	0	1	1	− 1	0
F9 I	22	24	10	−13	− 3	0
G1 V	18	20	1	1	− 2	0
G5 III	28	38	4	− 8	− 3	0
K0 III	28	29	1	−13	−19	0

5. *Colour comparisons.*—Most comparisons so far made between gradient and colour indices have shown a good deal of scatter (3). This may be attributed on the one hand to observational errors, and on the other to effects of absolute magnitude, interstellar reddening, unrecognized variables, binaries of different spectral types and peculiar objects such as Wolf-Rayet stars. If however the

comparison is confined to nearby, i.e. unreddened, main sequence stars, there should be a strictly functional (though not necessarily either linear or one-to-one) relation between two measures of colour, even if they refer to widely different

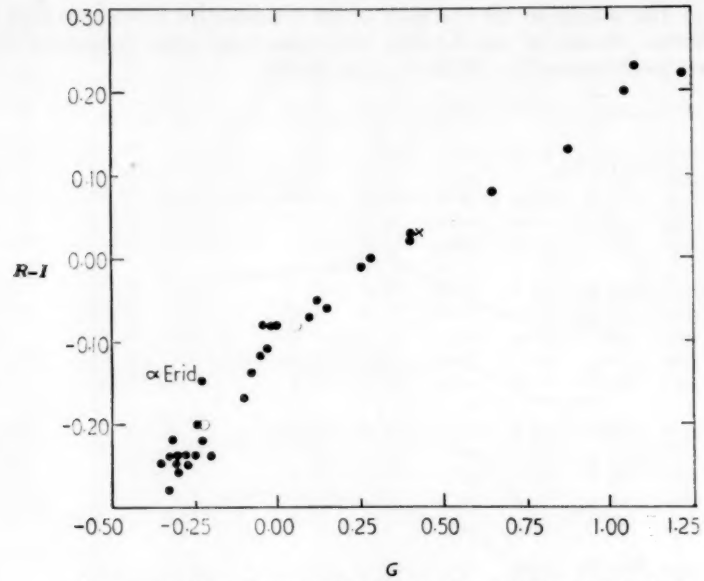

FIG. 2.—*Gradients plotted against Kron's infra-red photoelectric colours. Open circles are supergiants, crosses space-reddened stars, filled circles main sequence.*

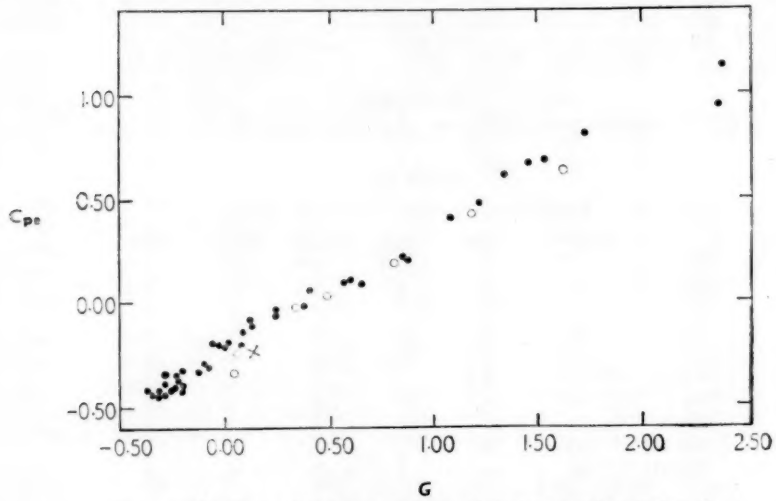

FIG. 3.—*Gradients plotted against Cape photoelectric colour indices* C_{pe}.

regions of the spectrum. The same considerations should apply to comparisons between monochromatic and heterochromatic magnitudes.

In Fig. 2 our gradients are plotted against infra-red photoelectric colour indices measured by Kron and his collaborators (**7**), and in Fig. 3 against

"blue–yellow" photoelectric colours measured at the Cape (**8**). In these figures high-luminosity stars are distinguished by open circles, space-reddened stars by crosses and main sequence stars by filled circles. The correlations are good. In fact mean errors of $\pm 0{\cdot}02$ in the gradients, and of $\pm 0{\cdot}01$ in the infra-red colours, are large enough to account for almost all the scatter. Exceptions are α Erid and β Hydi. A similar situation exists in the comparison with the Cape. Here α C Maj, α Circ and perhaps β Hydi stand off on one side, and β and γ Tr Au on the other. α C Maj and γ Tr Au, with Cape colours of $-0{\cdot}19$ and $-0{\cdot}20$, and gradients of $-0{\cdot}05$ and $0{\cdot}08$ respectively, represent an extreme case of scatter. (The vertical scale is much more open in Fig. 2 than in Fig. 3.) The anomalous infra-red colour for α Erid (see Fig. 2) is puzzling, as it has high weight on all systems. A possible explanation could be that it has a very late-type companion; but no variations in light or radial velocity have been reported for this star, and it seems unlikely that it is a binary.

There are 70 stars in the present programme for which gradients have also been determined on the Reynolds (**2**). The arithmetic mean difference between the two determinations is $0{\cdot}04$, with the following large residuals, all in the sense Farnham–Reynolds: α C Maj $+0{\cdot}11$, α Cari $+0{\cdot}10$, β Hydi $+0{\cdot}19$, β Libr $-0{\cdot}14$, κ Orio $-0{\cdot}14$. Where such differences exist the evidence is usually in favour of the current series. For instance, it had been pointed out in (**2**) that α C Maj and α Cari were both too blue for their spectral types; these anomalies are now largely removed. And the present gradients for κ Orio and β Libr agree much better with their photoelectric colours.

We have twelve stars in common with Greenwich (**3**). These include four in Orion, which we make about $0{\cdot}05$ bluer in the mean. Most modern observers agree in including these among the bluest stars in the sky. The mean difference for the other eight stars is about $0{\cdot}02$, which is small.

6. *Magnitude comparisons.*—The indications from the preceding discussion are that our gradients have reached a very satisfactory order of accuracy. When, however, our m_{4550} are plotted against the Hogg and Hall magnitudes a scale difference of about 2 per cent becomes evident. This is investigated in Fig. 4, where we plot as a function of magnitude

(*a*) $\boldsymbol{R} - m_{5980} - 0{\cdot}14\ G$.

(*b*) $m_{\mathrm{HH}} - m_{4550}$.

(*c*) $\mathrm{BPg} - \mathrm{C_{pe}} - m_{4945}$.

Here the $\boldsymbol{R}$ are Kron's red magnitudes, and BPg and $\mathrm{C_{pe}}$ colours and magnitudes taken from the Cape Mimeograms (**8**). Before heterochromatic magnitudes can be compared with monochromatic magnitudes in this way colour effects must be eliminated as far as possible. We do this by interpolating between the monochromatic magnitudes to the effective wave-length of the heterochromatic system (as was done by Hall, reference **4**, p. 234). This turned out to be necessary only in case (*a*), as the effective wave-length of $\mathrm{BPg} - \mathrm{C_{pe}}$ is very near λ 4945. In case (*a*) we have worked from m_{5980} rather than from m_{6360}, which was nearer the effective wave-length of $\boldsymbol{R}$ as there was less scatter with the shorter wave-length.

Fig. 4 indicates a well-defined scale error of about 2 per cent, in the sense that we have made the bright stars too faint. This difference between our photographic magnitude scale and the photoelectric ones (BPg is at least partly photoelectric) is disappointing; the weight of evidence undoubtedly supports the

latter, although we have been unable to detect any source of systematic error in the present series. It is perhaps worth noting that the mean difference $m_{HH} - m_{4550}$ is only 0·02.

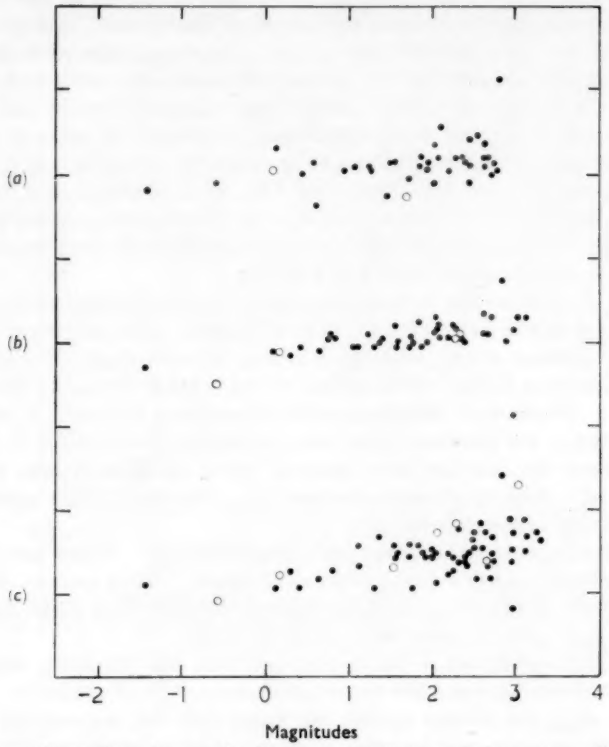

FIG. 4.—*Comparisons between the Farnham magnitudes and those measured by Kron (a), Hogg and Hall (b), and at the Cape (c), to test for possible scale error. Vertical spacers are 0·2 magnitudes apart.*

A new photographic programme on the Farnham telescope with some slight modifications of the present equipment will be put into operation in 1954. It is hoped that this will throw some light on the origin of the scale error.

Commonwealth Observatory,
Canberra :
1954 *March* 2.

References

(1) A. R. Hogg and Beryl Hall, *M.N.*, **111,** 325, 1951.
(2) S. C. B. Gascoigne, *M.N.*, **110,** 15, 1950.
(3) *Observations of Colour Temperatures of Stars*, Vol. II, Royal Observatory, Greenwich, 1952.
(4) J. S. Hall, *Ap. J.*, **95,** 231, 1942.
(5) J. Stebbins and A. E. Whitford, *Ap. J.*, **102,** 318, 1952.
(6) H. Kienle, H. Strassl and J. Wempe, *Z. Astrophys.*, **16,** 201, 1938=*Gott. Veroff* Nr. 50.
(7) Gerald E. Kron, Howard S. White and S. C. B. Gascoigne, *Ap. J.*, **118,** 502, 1953.
(8) *Cape Mimeogram* No. 1, 1953.
(9) R. v. d. R. Woolley and S. C. B. Gascoigne, *M.N.*, **108,** 491, 1948.

Addendum.—The observations mentioned in Section 6 of the paper have now been completed and reduced. The programme consisted of two bright stars (α C Ma and α Car), two faint stars (β Leo and γ Tr A) and a number of standard stars. The results are shown in Table V. The magnitudes at λ 4550 A were found by adopting Hogg and Hall's values for the standard stars, i.e. all except the four stars already mentioned. For example, the 1954 value given for β Cen was found by assuming HH values for all the other standard stars with which it was compared, and so on. Some stars were used a few times as standards (e.g. γ Ori and δ Vel) but have not been kept in Table V as the 1954 observations of the stars (considered as programme stars and not as standards) is of too low weight.

Table V shows the magnitudes found in 1954, together with the weight, the magnitude found in 1952, and the photoelectric magnitude according to Hogg and Hall. The next two columns show differences. The last three columns show the gradient found in 1954, the gradient found in 1952 and the differences. The 1954 gradients were found by least squares from magnitudes in six colours using the values shown in Table III as standards.

TABLE V

Results obtained in 1954

Star	Magnitude at λ 4550 A				Differences in hundredths of a magnitude		Gradients G		
	(1) Photographic 1954	wt.	(2) Photographic 1952	(3) Photoelectric Hogg & Hall	(1)–(2)	(1)–(3)	1954	1952	Difference
α Car	−0·62	35	−0·59	−0·69	−3	+7	0·32	0·35	−03
α C Ma	−1·47	27	−1·43	−1·49	−4	+2	−0·03	−0·05	+02
ϵ C Ma	1·29	17	1·31	1·30	−2	−1	−0·29	−0·28	−01
β Car	1·57	34	1·60	1·60	−3	−3	+0·05	+0·02	+03
α Leo	1·19	33	1·22	1·24	−3	−5	−0·13	−0·10	−03
β Leo	2·08	20	2·04	2·10	+4	−2	+0·21	+0·14	+07
α Vir	0·75	68	0·76	0·77	−1	−2	−0·33	−0·29	−04
β Cen	0·41	96	0·41	0·40	0	+1	−0·31	−0·33	+02
γ Tr A	2·81	30	2·74	2·80	+7	+1	+0·11	+0·08	+03
α Oph	2·10	17	2·09	2·10	+1	0	+0·30	+0·28	+02
ϵ Sgr	1·73	50	1·73	1·74	0	−1	+0·04	0·00	+04
α Aql	0·87	70	0·82	0·83	+5	+4	+0·43	+0·41	+02
α Ps A	1·11	33	1·12	1·11	−1	0	+0·09	+0·12	−03
	Root mean squares, unweighted				±3·3	±3·0			±0·033

The differences photographic 1954 minus photoelectric (Hogg and Hall) show a little correlation with magnitude, as is shown by the following least squares results:—

Including all stars $= +0^{m}\cdot016-(0\cdot014\pm0\cdot007$ s.e.$)m_{4550}$.

Excluding α Carinae $= +0^{m}\cdot006-(0\cdot007\pm0\cdot008$ s.e.$)m_{4550}$.

The differences also show a correlation with gradient, as follows:

Including all stars $= -0^{m}\cdot004+(0^{m}\cdot062\pm0^{m}\cdot023)G_{1952}$.

Excluding α Carinae $= -0^{m}\cdot005+(0^{m}\cdot043\pm0^{m}\cdot030)G_{1952}$.

Since α Carinae is both bright and (relative to the B stars) red, its large difference 1954 minus photoelectric supports either a scale effect or a colour effect. The general run of the 1952 differences suggests very strongly that the colour effect is not real, and the authors feel that the scale effect is not real either. In our view it is the Earth's atmosphere rather than photometric technique which limits the accuracy of magnitude comparisons over wide angles.

The agreement between the gradients determined in 1954 and 1952 is highly satisfactory.

Mr Gottlieb and Dr Heintz have assisted us by taking many of the 1954 plates.

ERRATA

M.N., **113**, No. 6:

S. Chandrasekhar, *Problems of stability in hydrodynamics and hydromagnetics* (George Darwin Lecture).

P. 672, the legend to Fig. 1 should read as follows:—

FIG. 1.—*The variation of the critical Rayleigh number, R_c, for the onset of convection as a function of $T(=4\Omega^2 d^4 \cos^2 \vartheta/\nu^2)$ for the three cases: (a) both bounding surfaces free, (b) both bounding surfaces rigid and (c) one bounding surface free and the other rigid; the abscissa in case (c) is* log $(16T)$.

P. 674, the legend to Fig. 2 should read as follows:—

FIG. 2.—*The variation of the critical Rayleigh number, R_c, for the onset of instability as a function of Q for the three cases* (i) *both bounding surfaces free (curve marked* I), (ii) *both bounding surfaces rigid (curve marked II) and* (iii) *one bounding surface free and the other rigid (curve marked* III): *the abscissa in case* (iii) *is* log $(4Q)$. *The points marked* I, II *and* III *on the R_c-axis are the limiting values for the three cases considered in the absence of a field.*

P. 678, line 2:—

For the Fifteenth International Congress, ***read*** the Fifth International Congress.

P. 721, equation (20) should read as follows:—

$$v_r^{\mu}\frac{(n-\frac{3}{2})}{(n+1)}\rho_0 g_0 = -\frac{L}{4\pi r^2}\left[\frac{\partial}{\partial r}\left\{\left(1+T_0\frac{\partial}{\partial T_0}\left(\ln\frac{T_0^3}{\kappa_0\rho_0}\right)\right)\left(\lambda-\tfrac{1}{2}\int_0^{\pi}\lambda\sin\theta\,d\theta\right)\right.\right.$$
$$\left.\left.+\frac{T_0}{T_0'}\frac{\partial}{\partial r}\left(\lambda-\tfrac{1}{2}\int_0^{\pi}\lambda\sin\theta\,d\theta\right)\right\}\right.$$
$$\left.+\frac{T_0}{T_0'}\frac{1}{r^2}\frac{1}{\sin\theta}\frac{\partial}{\partial\theta}\left(\sin\theta\frac{\partial\lambda}{\partial\theta}\right)\right],$$

P. 728, second paragraph, the following addition should be made:—

The dependence of A_2 on $(z'-z)$ near the edge of the star is in general more complicated than that given, but the conclusion concerning the feed-back currents holds.

P. 728, equation (51) should read:—

$$1{\cdot}52\times10^{-2}\left(\frac{M}{R}\right)\Big/m'q^2,$$

CONTENTS

PAGE

Meeting of 1954 March 12:
Fellows elected 385
Junior Members elected 385
Presents announced 385

Meeting of 1954 April 9:
Fellows elected 385
Associates elected 386
Presents announced 386

C. W. Allen, Whole-sky statistics of celestial objects 387

Antoni Przybylski, The maximum effect of convection in stellar atmospheres on the observed properties of stellar spectra. II 406

P. J. D. Gething, The collimation error of the Airy Transit Circle 415

Sir Harold Jeffreys, Second-order terms in the figure of Saturn 433

L. Mestel, The influence of stellar radiation on the rate of accretion .. 437

T. R. Tannahill, Star-streaming from the stars of spectral type B 460

D. G. Ewart, The constants of the star-streams and of the velocity ellipsoid from the Cape photographic proper motions of 19 839 stars 467

A. Kopff, Remarks on the revision of FK3 and its relation to N30 478

R. v. d. R. Woolley, S. C. B. Gascoigne and A. de Vaucouleurs, Photographic observations of monochromatic magnitude at six wave-lengths 490

Errata 500

Printed in London by Taylor & Francis, Ltd., 1955 March